ASSESSMENT OF THE RESPONSE OF LAND SURFACE TEMPERATURE TO LAND USE AND LAND COVER IN KANO METROPOLIS AND ITS SUBURBS

BY

SIMON, Susan Ojochide
MTech/SPS/2015/6065

WEST AFRICAN SERVICE CENTER ON CLIMATE CHANGE AND ADAPTED LAND USE (CC&ALU) FEDERAL UNIVERSITY OF TECHNOLOGY MINNA, NIGER STATE

MARCH, 2018

ASSESSMENT OF THE RESPONSE OF LAND SURFACE TEMPERATURE TO LAND USE AND LAND COVER IN KANO METROPOLIS AND ITS SUBURBS

BY

SIMON, Susan Ojochide
MTech/SPS/2015/6065

A THESIS SUBMITTED TO THE POSGRADUATE SCHOOL, FEDERALUNIVERSITY OF TECHNOLOGY, MINNA, NIGERIA, IN PARTIAL FULFILLMENT OF THE REQUIREMENT FOR THE AWARD OF THE DEGREE OF MASTER OF TECHNOLOGY (MTech) IN CLIMATE CHANGE AND ADAPTED LAND USE

MARCH, 2018

DECLARATION

I, hereby declare that this titled: "**Assessment of the Response of Land Surface Temperature to Land Use and Land Cover in Kano Metropolis and its Suburbs**" is collection of my original research work and it has not been presented for any other qualification anywhere. The study acknowledged information from both published and unpublished sources.

SIMON, Susan Ojochide ……...……...

MTech/SPS/2015/6065 SIGNATURE AND DATE

FEDERAL UNIVERSITY OF TECHNOLOGY,
MINNA, NIGERIA

CERTIFICATION

This thesis titled: "**Assessment of the Response of Land Surface Temperature to Land Use and Land Cover in Kano Metropolis and its Suburbs**" by: SIMON, Susan Ojochide **(**MTech/SPS/2015/6065) meets the regulations governing the award Degree of Master of Technology (MTech) of the Federal University of Technology, Minna and it is approved for its contribution to scientific knowledge and literary presentation.

Prof. A. A. Okhimamhe .....……
Major Supervisor Signature and Date

Prof. A. A. Okhimamhe ……
WASCAL Director Signature and Date

Prof. M. G. M. Kolo …….
Dean, Postgraduate School Signature and Date

DEDICATION

To Baba Na; my husband “Mr. Akor Joel Enemona”, for his support, prayers and sacrifices; I pray that our Lord Jesus Christ will keep you, sustain you and continue to bless the works of your hands (Amen). *“*The lord is my strength and shield; my heart trusts on him, and he helps me. my heart leaps for joy, and with my song I praise him Psalm 28:7”.

ACKNOWLEDGEMENTS

First, I will like to appreciate my father in heaven, the author and finisher of my faith for his eternal love, grace, protection and continuous open doors all through this study and in my life. May his name alone be highly exalted.

I will like to thank Prof. A. A. Okhimamhe the Director of WASCAL MRP, Minna and my supervisor for her timeless guidance, corrections, input and words of encouragement. I sincerely appreciate the conducive and enabling environment you provided for our studies and I pray you attain more height and receive grace to do more. My immense appreciation goes to Dr. Michael Thiel my co-supervisor, from Remote Sensing department at University of Würzburg, Germany for his technical support, suggestions and constructive comments. May God guide all your doings. I will not forget to appreciate Mr. Christian also at remote sensing department university of Würzburg for helping me correct the Landsat imageries used in this study.

I am grateful to my mentor Dr. (Mrs) Saratu.U. Ibrahim, it really an opportunity to have met you and be mentored by you. I want to thank you for all your advice and time when things seemed rough. To the entire WASCAL staffs (both academic and non-academic staffs), thank you for working tirelessly to make sure everything works out well. I wish you all more grace.

From a grateful heart I want to appreciate my parents Mr. and Mrs. Simon Amodu and Elder and Deaconess Clement S. Akor. I want to thank you for your love, calls, wishes, understanding and prayers. May God keep you all. To all my brothers (Daniel, Joseph, Samuel) and sisters (Eunice, Elizabeth, Peace and Deborah) thank you all for all your

calls, best wishes and prayers. It my prayer that God will lift you all higher than your imaginations.

Immerse gratitude goes to my classmates (David, Lucette, Sanusi, Charles, Fafa, Gildas, Paul, Peter and Sidibe) for their time listening ears, teamwork, watching each other's back, advice, gifts (wedding gifts), fun and jokes. May all our efforts and sleepless nights be crowned with success and may God make us recognizable instruments in our various countries. I will definitely miss you all.

To my friends, Gift Sunday and Victoria Friday, thank you for your physical and moral support and to everyone who in one way or the other contributed directly or indirectly to this work, I appreciate you and say thank you.

My sincere appreciation goes to the Federal Ministry of Education and Research (BMBF) and West Africa Science Centre on Climate Change and Adapted Land Use (WASCAL) for providing the scholarship and financial support for this program.

ABSTRACT

Kano State is faced with increasing air and surface temperature caused as a result of the continuous development activities, constructions and influx of people to the state. The study therefore analyses the development of land surface temperature (LST) on different land cover and land use categories and to determine the possible impact of the various class on LST. Landsat 8 Operational Land Imager and Thermal Infrared Sensor (OLI/TIR), multi-temporal remote sensing satellite data of 2015 and 2016 were used to retrieve LST and derive land use and land cover classification map using random forest machine learning algorithm and various land cover indices such as Normalised Difference Vegetation Index (NDVI), Normalised Difference Built Index (NDBI) and Modified Normalised Difference Water Index (MNDWI) were derived using R statistics software. These land cover indices were used to examine the landscape attributes, characteristics and to further understand the cause-effect relationship between LST and LULC using a Pearson's correlation analysis and simple linear regression model. LULC classification map showed that using several multi-temporal satellite imageries for classification to extract biophysical information provide a more accurate result with a kappa coefficient of 1.017 and 1.013 and overall accuracy of above 85% which showed an excellent agreement between the map and ground truth data. The retrieved LST pointed out that land surface temperature could be as high as 38^{o}C to 40^{o}C in hot seasons and as low as 22^{o}C to 25^{o}C in wet seasons. LST values were extracted for the different land cover and land use class and result revealed that there is a decreasing trend of LST all through the season from built up areas (such as residential, commercial and industrial) which recorded a higher LST to water bodies (such as lakes, ponds, streams and rivers) which showed a low LST value. The correlation analysis generated between LST and the three land cover indices showed that for all time steps MNDWI showed a negative correlation with LST (-0.313 to -0.686 and -0.208 to -0.786 in 2015 and 2016 respectively). Likewise, NDVI showed a higher negative correlation of between -0.127 to -0.436 and -0.137 to -0.389 in 2015 and 2016 respectively. While, NDBI revealed a high positive correlation with LST of between 0.491 to 0.804 and 0.666 to 0.839 in 2015 and 2016 respectively. Urban Heat Island (UHI) effect was described by determining hot and cold spots areas with the core of the study area characterised to be hotspot areas while the periphery and most notably the western part of the study area where irrigation fed agriculture are practiced characterised to be cold spot areas and this explains why there is a decreasing trend of surface temperature as one move from the core to the periphery. This study infer that vegetation plays a vital role in weakening LST and recommend that tree planting campaign should be carried out, landscaping should be done alongside road or bridge constructions, urban greening concept should be carried out by town planners and individuals to reduce the effect of UHI.

TABLE OF CONTENTS

Page

LIST OF TABLES

LIST OF FIGURES

LIST OF PLATES

LIST OF ABBREVIATIONS/GLOSSARIES

CLCLU	Change in Land Cover and Land Use
CRAN	Comprehensive R Archive Network
DN	Digital Number
DOS	Dark Object Subtraction
EPA	Environmental protection Agency
EHA	Electronic Health Africa
GDAL	Geospatial Data Abstraction Library
GIS	Geographic Information System
GPS	Global Positioning System
GUI	Graphic user Interface
IPCC	Intergovernmental Panel on Climate Change
Kc	Kappa Coefficient
Landsat TM	Landsat Thematic Mapper
Landsat ETM	Landsat Enhanced Thematic Mapper
LIDAR	Light Detection and Ranging
LGAs	Local Governmental Areas
LULC	Land Use Land Cover
LULCC	Land Use and Land Cover Change
LST	Land Surface Temperature
MNDWI	Modified Normalised Difference Water Index
MODIS	Moderate-resolution Imaging Spectro-radiometer
NASA	National Aeronautics and Space Administration
NBS	National Bureau Statistics

NCC	Natural Colour Composite
NDBI	Normalised Difference Vegetation Index
NDVI	Normalised Difference Built up Index
OA	Overall Accuracy
OLI/TIRS	Operational Land Imager/Thermal Infrared Sensor
PA	Producer Accuracy
QGIS	Quantum Geographic Information System
RADAR	Radio Detection and Ranging
RF	Random Forest
RGB	Red Green Blue
RS	Remote Sensing
SVF	Sky View Factor
SAR	Synthetic-Aperture Radar
SLRM	Simple Linear Regression Model
UA	User Accuracy
UHI	Urban Heat Island
USGS	United States Geological Survey
UTM	Universal Transverse Mercator
WASCAL	West Africa Science Service Centre for Climate Change and Adapted Land Use
WMO	World Meteorological Organisation

CHAPTER ONE

1.0 INTRODUCTION

1.1 Background to the Study

The earth is faced with lots of problems which have deterred the environment and anthropogenic activities is some of the major problems. Recently, human species have crossed an important threshold as over half of us presently live in cities (United Nation, 2007). “The urban footprint now doubles every 30 years and at this rate, it is projected that urban land use should approach 10% of the land surface by 2070 and continuous conversions of land use can be multiple if followed over a long time period” (Tayyebi, 2013). Urbanization influences the land use and land cover category of an environment by causing significant effect on it, due to the replacement of natural landscape such as vegetal cover, open soil, and stagnant water with buildings, roads and other urban features (Alavipanah *et al.,* 2015; Jiang *et al.,* 2015). Urbanization refers to the expansion of towns and its periphery as a result of growth in population that leads to vital alterations in land use and land cover mainly due to human actions. As a result of rapid growth in population and socio-economic development, urbanization is said to be an inevitable process. In view of this, Ayedun *et al.* (2011) found out that more than ten (10) cities and eight hundred and forty (840) urban centres are reordered to be over a million populated.

It is a well-recognised and accepted fact that local weather and climate have being affected by urbanization (Anjana, Shastri, and Joshi, 2014). Urbanization is revealed to be the main driver and most significant factor of land cover changes (Kalnay and Cai 2003; Chen *et al.,* 2006). In the same view, Bharath *et al.* (2013) and Shishegar (2013)

revealed that these changes can alter the local, regional and global climate of an area, looking at its radiative, aerodynamic and energy balance (Alexander and Mills, 2014).

Ayedun *et al*. (2011) revealed that in Nigeria, fifty years ago in the 20th century the country experienced unprecedented urbanization with a spectacular population growth rate in recent times. Over the last three decades, urban population in Nigeria had a growth rate close to 5.8 percent per annum and urban population that consist of about 48.2 percent of the total population in the country and projection has shown that by 2025 above 60 percent of the population will dwell in urban centres (Alkali, 2005). In Kano metropolis and its suburbs, urban growth has caused extreme stress to the environment by the alterations in different land use types. The State generally is still growing owing to the commercial activities exceling in the area and also as a result of other social, economic, physical and political developments going on (Ayila *et al*., 2014).

Kalnay and Cai (2003), revealed that urban expansion and land use changes cause decrease in diurnal temperature by half and changes from natural cover to impermeable cover such as concrete pavements, rooftops, blacktop (asphalt) are the main causes of increase in land surface temperature (LST). This is attributed to the fact that each land cover type has a unique quality in absorption and radiation of energy. For example, natural covers like vegetation has high albedo thus absorb less incoming solar energy and evaporate the little that was absorbed while impervious surfaces reradiated more solar energy because it absorbs more incident solar energy due to its low albedo (Patz *et al*., 2005).

Several decades ago the concept of urban heat island (UHI) was discovered when a significant difference in temperature in urban centres was noticed to be higher than its

suburbs (Oke, 1988; Kaya *et al.*, 2012). Landsat imageries can be used to determine the different land use and cover types, land cover indices and retrieve land surface temperature. The accessibility of remote sensing database of particular location for different time steps have intensified further studies on the different LULC and their relationships with LST. Therefore, with a difference in the land use type of any environment vegetated, barren or built up lands the response of land surface temperature will be different and felt in the study area.

1.2 Statement of the Research Problem

Land surface temperature increase has been a serious problem facing our cities today particularly in third world countries where development is the major priority and little attention is given to environmental issues. Alteration in land cover is the most significant component of global environment change particularly those changes caused by human activities (Fonji and Taff, 2014). As globalization and urbanization continue rapidly at different rate, cities will become the foremost actors in land cover dynamics thereby affecting the surface temperature of cities in different ways.

Several authors have stated that Urban Heat Island (UHI) is the most prominent effect of urbanization (Zhan *et al.*, 2013; Anjana *et al.*, 2014; Jalan and Sharma, 2014; Alavipanah *et al.*, 2015; Jiang *et al.*, 2015). They described UHI as a terminology used to describe a situation that occurs when a municipal area is significantly hotter than its suburbs. Urbanization and different land use types have drastically modified the interactions of urban surfaces with the atmosphere (Jalan and Sharma, 2014). The consequences of replacing vegetation with asphalt, concretes, different type of building structures has led to changes in surface temperature and this is also the reason why there is lower

temperature in rural areas than urban centres. Research have shown that, temperature on land is different from the one near and above water bodies and this signifies that water bodies have a positive effect on the local climate of the environment because of its cooling evaporative impact (Ishii *et al.*, 1991; Yang *et al*., 2015; Manteghi *et al*., 2015). Cool air moving say 400m from the water body to streets can be reheated by pavement or heat from the sun's radiation making cities hotter than their surrounding environment (Ishii *et al.,* 1991) and this has become a thing of concern.

In Nigeria, urbanization and growth of cities like Lagos, Ibadan, Port Harcourt and Kano are described as been sporadic and Nigeria in sub-Saharan Africa is said to have the most complex growth rate with a population of 140 million as at 2006 population census (National Bureau of Statistics, 2012). Nigeria like other developing countries is faced with challenges of urbanization mainly due to rural-urban migration and anthropogenic activities which has caused tremendous impact on the natural and human environment. Kano metropolis is highly commercialized and as a result there is constant movement of people from the rural areas to the metropolis. The city has witnessed recognised development and growth such as increasing market, road constructions or schools to mention a few due to the continuous influx of people. Land cover type in Kano suburbs is also noticed from field observations and satellite imagery to be changing fast as a result of conversion of forest/dense fields with shrubs and grasses to agricultural lands so as to meet up with the demand of the commercial market and its population. Buildings and roads are being constructed by the government not considering the effect it will have on the environment and putting down an alternative plan to combat these effects especially on the increasing land surface temperature.

Estimating land surface temperature (LST), is a component and the major step for analysing UHI (Liu and Zhang, 2011). Estimate from remote sensing techniques and GIS tools have shown that surface radiant temperature in Nigeria (Jimeta, Adamawa State) has increased by 9°C from 1986 to 2008 in the urbanized areas (Zemba *et al*., 2014). Recently, Mukhtar (2016) in his studies revealed that, there is an increase in the built-up area from 11.80% in 1985 to 26.20% in 2003 and high decrease in vegetation cover and bare surface. Further research revealed that in the last 19 years the built up area is increasing in size, and this have impact on the natural environment (Ayila *et al*., 2014).

Recent studies carried out by Mahmoud (2016) and Adeyeri *et al.* (2017), examined UHI effect by determining the connection between LULC, land cover indices and LST in Abuja. Their studies revealed that land surface temperature has been greatly influenced by the different land use and land cover in the environment. These studies showed that, there is profound pressure on infrastructures, establishment of more buildings, roads, market and increase demand for fuel. This means if the rate of urbanization is left uncontrolled, increase in surface temperature will be inevitable. Previous studies used satellite imageries of single time steps in different years to analyse the impact of LULC on LST and even predict into the future. Their result reflects particular sites and time in a year and not considering the different climatic zones, seasons and the time such satellite imageries were acquired, which could cause variation in the relationship between LST and different land cover. This means many studies have failed to consider collecting multi-temporal satellite imageries within a year to examine LULC and LST in order to get a more accurate model to understand this relationship before simulating into the future.

Many people in developing countries like Nigeria do not understand how urban growth and their activities can influence microclimate of their environment, let alone ways of handling the situation. Hence, this study has found out that the increase in land surface temperature is as a result of increase in urbanization activities and the presence of different land use types. With rapid urbanization and commercial activities in Kano metropolis over the years, it is believed that, urban problems which have being neglected will increase with time and space. Previous studies have failed to assess the effect of increasing urbanization on land surface temperature in Kano State. The temporal variation of land surface temperature has not been assessed and its response on the different existing land use and land cover types of the study area have not been examined. Therefore, multi-temporal Landsat 8 optical imageries of 2015 and 2016 was used to determine the present pattern of land use types of the study area in order to get a more accurate classification result rather than using a single time step imagery as seen in previous studies. Also assess the response of land surface temperature on these land use and land covers and determine if there is a temporal variation or constant.

1.3 Aim and Objectives

The study was aimed at examining the variation of land surface temperature over a year on the different land cover types in Kano metropolis and its suburbs. The following objectives where achieved:

i. Analyse the pattern of land use and land cover in Kano metropolis and its suburbs
ii. Perform temporal variation analysis of land surface temperature in the study area
iii. Examine the spatiotemporal variation of land surface temperature to different land use and land cover classes

iv. Determine the relationship between land cover indices and land surface temperature in the study area.

Therefore, the following research questions were set to guide the study:

i. What is the land use and land cover pattern in the study area?

ii. What is the temporal variation of land surface temperature in the study area?

iii. How does land surface temperature respond on different land use and land cover classes?

iv. What is the relationship between various land cover indices and land surface temperature over 2015 and 2016 in the study area?

1.4 Justification of the Study

Researches have been conducted on land cover pattern in several cities in Nigeria but little is known on the response of land surface temperature to this land cover pattern in Kano (Ahmed *et al*., 2013). Land use and land cover across Kano State are experiencing significant and rapid change. Hence the study area is not exempted from this, because land surface temperature will respond to this different land use and cover type. The connection between the different land use and cover type and land surface temperature in Kano metropolis and its suburbs have not been examined in order to determine the development of the LST over a year on the different land cover types. Accurate assessment of the response of most regions to global warming is difficult because of indispensable reliable temperature data. Temperature data are mostly collected from weather stations mostly located in or close to airports. For Kano metropolis, for instance, the closest weather station is very far, which means the data collected might not be

representative enough for the study area. Satellite imagery now serves as a substitute for these weather records as land surface temperature can presently be derived from them.

With rapid urbanization and commercial activities in Kano metropolis over the years, it is believed that, urban problems which have being neglected will increase with time and space. In many developing countries like Nigeria, many people do not understand how urban growth and their activities can influence microclimate of cities, let alone ways of handling the situation. The continuous use and high dependency on water for irrigation activities in cities have affected the volume of water in urban and rural areas and thus the evaporative effect of water will be affected and as such other indices like normalized difference water index was considered necessary. It is therefore necessary not to only know the dynamics of city growth in Nigeria and Kano metropolis in particular but to also know the response of land surface temperature on the different land use and land cover in Kano metropolis and its suburbs. Recent studies by Mahmoud *et al.* (2016) and Adeyeri *et al.* (2017) have proven this type of study to be useful for urban planning activities in Abuja, Nigeria. This research provides adequate information about the development of land surface temperature from satellite imagery of Kano metropolis and its suburb, and could serve as a primary resource for further environmental and climatology studies, useful for urban and suburb planning so as to maintain LST and reduce the impact high LST could have on the citizens.

1.5 Scope and Limitation of Study

This study was conducted to assess the development trend of land surface temperature and the response of land surface temperature on the different land use and land cover in Kano metropolis and its suburbs. The study area consists of 24 Local Government Areas

(LGAs). The research was divided into two (2) phase; collection of data and analysis phase and interpretation of result and possible recommendation phase. The data collection phase involved collection of primary data (ground truth data) and secondary data such as population data, administrative boundaries and shape files and Landsat 8 satellite imageries of the study area.

The second phase involved pre-processing of data, data analysis and presentation of findings. The duration of study was for six months; one month for field work, two months for data analysis and three months for seminar and presentation of results. The data used were secondary data and this means that any error associated with the data could be transferred to the study.

1.6 Description of the Study Area

The study area is Kano metropolis and its suburbs in Kano State, Nigeria which is situated between 10°25″N and 12°47″N latitudes, and 8°22″E and 9°00″E longitude (Figure 1.1). Kano metropolis has eight Local Government Areas (L.G.A.) namely; Kano Municipal, Nassarawa, Gwale, Dala, Tarauni, Fagge, Kumbotso and some parts of Ungogo (Ayila *et al*., 2014) and the selected suburbs has 16 L.G.A. which are Rimin Gado, Tofa, Dawakin Tofa, Minjibir, Gezawa, Warawa, Dawakin Kudu, Kura, Madobi, Garum Mallam, Bankure, Bebeji, Rano, Kibiya, Garko, and Tudun Wada. These areas were selected to cover a wide range of different types of LULC observed from imageries. Hence, the study area consists of 24 local government area (L.G.A.) (Figure 1.1) with a total population of 5,577,074. Kano State is the third largest city in Nigeria with a population of 9,401,288 behind Lagos and Ibadan, based on national population census of 2006 (Ayila *et al*., 2014; NBS, 2012). Kano is 481 metres above sea level and it is located between Kano and

Challawa rivers which meet to form Hadeja River. The city is bordered by Jigawa to the East, Katsina to the West, Kaduna, Jos and Bauchi to the South.

Generally, marketing and trading is the dominant economic activity in Kano State, thus the State is referred to as the Centre of Commerce in Nigeria (Ayila *et al*., 2014). The study area has two seasons: wet and dry seasons. Wet season is characterised by warm and humid air experienced from May to September while dry season is experienced from October to April and is characterised by dry continental wind which blows from the North. Air temperature in Kano State is as high as 39°C during the rainy season and an average of about 14°C in the dry season, with rainfall range between 0.0 to 980mm (WMO, 2016) and the sunshine hours longer in March and October (Mukhtar, 2016).

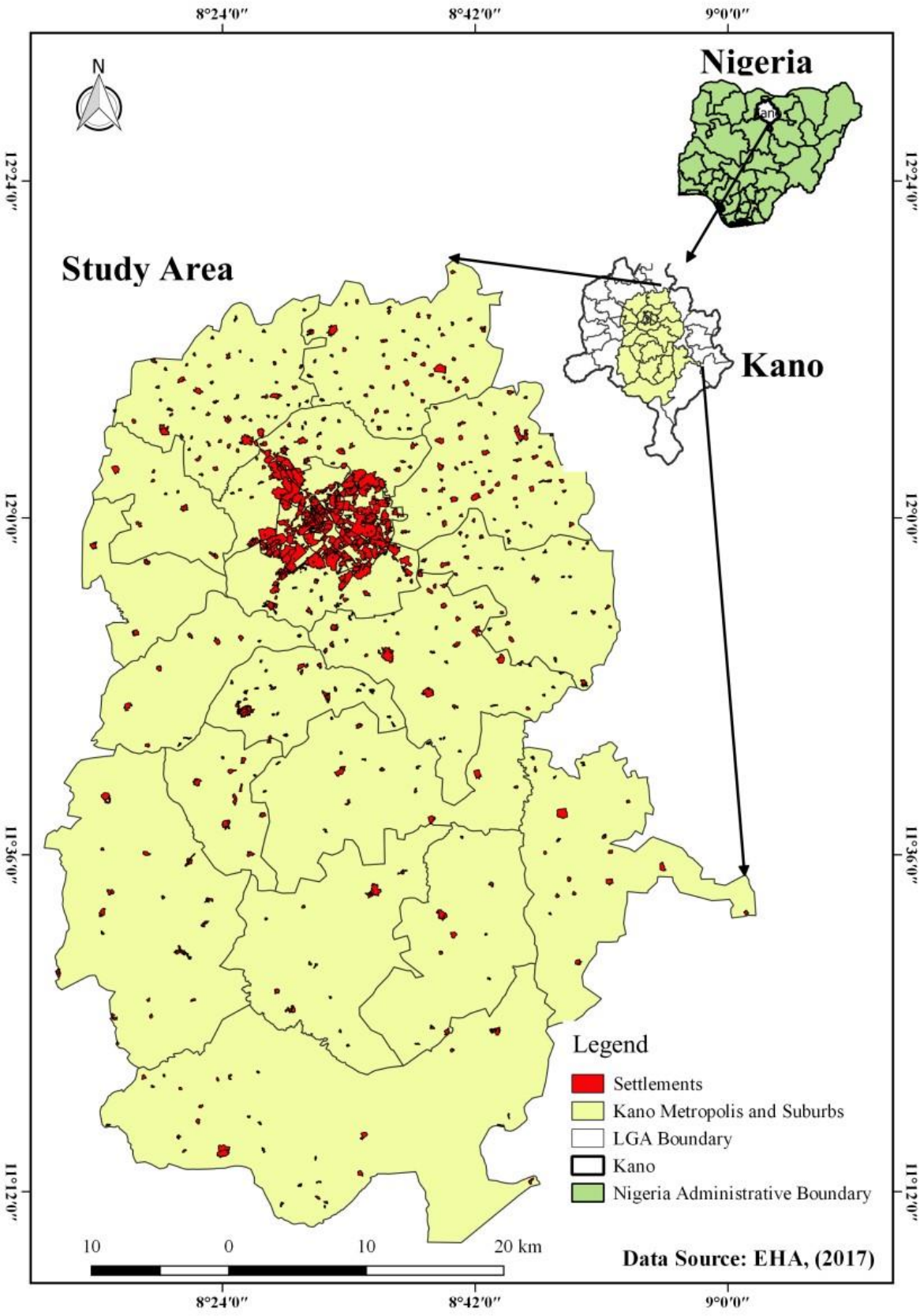

Figure 1. 1: Study area

1.6.1 Geology and soil

About four fifth of Kano is lie underlain by quartzite and identical upper Cambrian of Basement Complex rocks. The rocks in the study area have been exposed to weathering activities which have form rich clay soil and laterite outcrops found in Dala hills and Goron Dutse hills. Extreme south of the study area consists of a ring complex of well jointed younger granites. It consists plain lands of about 500m, highlands of about 1000m above sea level and landforms such as Rishi hills, sandy plains and alluvial channels.

Kano consist of all the three major categories of soil namely: azonal, intra-zonal and zonal. Zonal soils are mainly ferruginous soils which are formed from crystalline acid rock and covers the largest part of the State. Intra zonal soils are popularly known as fadama land or hydromorphic soils which are characterised to be wet, fertile and mostly found in river basins. While azonal soils are immature and infertile soils found in river beds or slopes. The soil texture, structure, chemical characteristics and character have been affected due to the continuous use of manure and fertilizers.

1.6.2 Climate and hydrology

Kano features a tropical savannah climate. World meteorological organisation (WMO, 2016) indicate that the city receives on average precipitation per year of about 980mm, and monthly mean total rainfall of around 320mm, with heavier rains from June to September. The rains last for three to five months. Kano is usually very hot all through the year, though cool temperatures are felt in December, January and February especially at night with an average low temperatures ranging from 14.2°C to 16.2 °C with mean temperature ranging from 25°C to 39°C as shown in Figure 1.2 (WMO, 2016).

The study area is notable for dry and cool weather characterised with dust (mid-November to February). This season is locally called “Kaka”; Bazara is another notable season called the hot and dry season (March mid-May) and at this period temperature could be as high as 39.1°C (WMO, 2016); Damina is another season called the warm and wet season (mid-May to September) and lastly is a season locally known as Rani. Rani is a warm dry season (October to mid-November) almost as hot as bazara season (Mukhtar, 2011). Water is essential for all systems of human settlements and irrigation activities. In order to improve portable water supply to towns and villages lakes such as Tiga, Bagauda and Mingibir were constructed (Danba *et al.*, 2015).

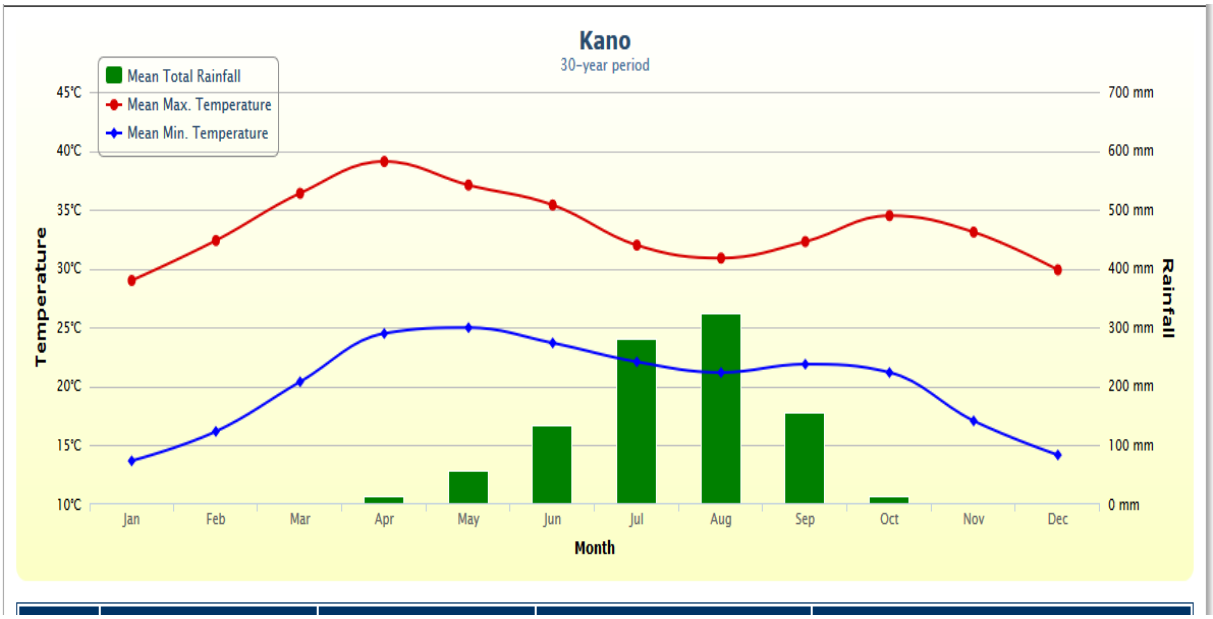

Figure 1. 2 Temperature and rainfall of Kano State (WMO, 2016)

1.6.3 Land use and vegetation

Mukhtar (2016) described the land use and vegetation type of Kano State as follows. To the south it consists of savannah wood and natural vegetation to the north. There is high cultivation of peanuts, onions, tobacco, wheat, sorghum, beans and maize because the

study area consist of high concentration of fertile sandy soil. The natural vegetation type is divided into three: Guinea savannah found in the extreme south, rich in biodiversity and luxurious tall trees; Sudan savannah (highly characterised with natural vegetation and sparse trees and) located 200 kilometres from Doguwa local government area and lastly is Sahel savannah found at the extreme North with sparse natural vegetation. Vegetables and varieties of tropical leafy foods, cereals, tubers can be sustained in the land and economic trees are known to be left on farmlands (Mukhtar, 2016).

1.6.4 Population and economy

Processed foods, textiles, cement, rolled steel, light trucks, furniture are produced in Kano city, thus the city is known as a manufacturing centre. It is known as a State of commerce in Nigeria with its large economy and a continuous increase in population. Kano State comprises of 44 Local Government Areas (LGAs) but this study is interested in 24 LGAs with a population of about 5,577,074 (NBS, 2012) as shown in Table 1.1.

Table 1. 1 Population of the study area as at 2006 population census

Local Government Areas	2006 Population
Dala	418,759
Dawakin kudu	225,497
Dawakin tofa	246,197
Fagge	200,095
Gwale	357,827
Kano municipal	371,243
Nassarawa	596,411
Ungogo	365,737
Tarauni	221,844
Kumbotso	294,391
Tofa	98,603
Mingibir	219,611
Gezawa	282,328
Warawa	131,858
Bebeji	191,916
Garun mallam	118,622
Bunkure	174,467
Tudun wada	228,658
Rano	148,276
Madobi	137,685
Kibiya	138,618
Kura	143,094
Garko	161,966
Rimin gado	103,371
Total	5,577,074

Source: National Bureau of Statistics (NBS), 2012.

CHAPTER TWO

2.0 LITERATURE REVIEW

2.1 Introduction

Ejaro and Abdullahi (2013) in their study on spatiotemporal analyses of land use and land cover changes in Suleja Local Government Area, Niger State, Nigeria, were of the view that a region consists of factors such as, resources, population, technology and institutions which are constantly in a state of dynamic equilibrium .It is therefore imperative to note that as population, technology and urbanisation changes in size and distribution, it causes changes in land surface temperature and this have impact on its immediate environment and surroundings. Research carried out by Kaya *et al.* (2012) stipulated that as population progression in cities increase, it leads to more construction of impervious land. This chapter describes some concepts and review related literatures on land cover, land use and land surface temperature.

2.2 Definition of Key Terms and Concepts

2.2.1 Urbanization

The word "urbanization" has been variously defined. According to Jiboye (2011) urbanization is the social transformation of the world that varies in the same proportion with the population living in the area, but the United Nations (2014), in its report categorised urbanisation based on population living in a particular place and highlighted that most of the urbanization processes occurred within the last six decades at an alarming rate. The report further maintained that urbanization is hinged on the three pillars of sustainable development which includes: environmental protection, social and economic

development. Similarly, United Nations-Habitat (2016) while studying the structural transformation in developing countries observed that urbanization is a global trend which has led to more than 50% of the world population moving to the city centres with a projected increase to about 60% in 2030. The report also emphasized that large proportion of this migration would take place in developing countries. The driving force for this massive migration to the urban areas is directly related to economic factors with more people being optimistic that movement into city hubs would provide better economic opportunities. Also, Jamei *et al.* (2016) and Faqe (2017), both indicated that, increase in population from net rural-urban migration, natural population growth and reclassification of small villages to towns are the major determinant of urban growth. Globally, since 2007, urban population has been on the increase, exceeding rural population and the trend has remained unchanged.

This process of urbanization has brought with it some unprecedented consequences. Braimoh and Onishi (2006) have shown that the major consequences of urbanization are the associated increase in the air, water and noise pollution, high energy consumption, accumulation of sediment, surface runoff, eutrophication of wetlands and decline in infiltration and increase in impervious surface due to the conversion of urban land covers which has resulted in high temperature. Balogun *et al.* (2011) in their findings found out that globally, agriculture and livestock raising, deforestation and lack of forest management, urban and suburban construction and development has directly altered land cover. In the world today all the vegetation has been tampered with, it is difficult to see any natural vegetation that has not be altered by man and their unlimited needs. In addition to the above findings, research by Balogun *et al*. (2011) formulated that annually, up to 400,000ha of vegetal cover is said to be lost.

Over the last 50 years, Nigeria as a country has witnessed an exceptional increase of urban centres (urbanization) coupled with a high population growth rate in those urban areas. Nigeria urban population is estimated to have grown at the rate of approximately 5.5 to 5.8 percent yearly (Alkali, 2005), with most of these urban centres being a result of oil discovery in the country. The discovery of oil in Nigeria brought with it massive infrastructural development in the areas of road constructions and the availability of automobiles (Olorunfemi, 2014). According to Ayedun *et al.* (2011), oil sector delivered over 90 percent of profits, rapid health/educational advancement and huge development in infrastructure before the end of the 1970s.

2.2.2 Land use and land cover dynamics

Land cover and land use are described in distinctive ways. Agarwal *et al.* (2002) described land use as the activities of man on land or the reason for human exploit that are directly or indirectly related to modifying land cover. Generally, land use and land cover types are always changing mainly because of the ever increasing human population and the rising process of urbanization. Mukhtar (2016) understudied land use and land cover change detection in Kano state using remote sensing and revealed that vegetation cover and bare surface have over the years continued to decrease while built up is continuously increasing.

Similarly, Lambin *et al*. (2003) reviewed the dynamics of land use and land cover change in tropical regions and observed that land use changes interact with climate driven land cover modifications factors and that the use to which a land is put is a function of some factors which work in tandem. They noted that some of the factors that drive land use change are resource scarcity, policy change or intervention, new market opportunities,

adjustment in societal organization and attitudes. The description of LULC change vary with the context of their use and are always changing. Lambin *et al.* (2003) described land-cover conversion as a shift of land from one cover to another while land-cover modifications involve alterations that change the attribute of the land cover without necessarily altering its total form.

Thus, land use can be categorised for instance as land used for agricultural production (including food production, rearing of animal), mining and logging while land cover could include forests, ranches, pasture, wetlands, roads, croplands and settlements (Ouedraogo *et al.,* 2010). Research over the years have argued that some of the many changes occurring in the environment today are the cumulative effects of land use and land cover changes (Lambin *et al.*, 2003).

Some of the critical areas of the environment known to be undergoing some changes as a result of changes in LULC include: climate, surface albedo and terrestrial ecosystem. The modifications or different land cover types particularly agricultural and urban growth, is best-known to have a direct impact on the pattern of climate change (contributing about 25 percent) patterns by increasing effect on land surface temperature and their indirect effects through the emission of greenhouse gases when vegetation are burned and cleared (Kalnay and Cai, 2003; IPCC, 2007). Thus, determination of modification in land cover is a difficult and pressing problem in environmental science research that need to be understood in order to know it drivers and its impact on local micro climate (Zhang *et al.*, 2016).

2.3 Review of Related Literatures

2.3.1 Image classification and accuracy assessment

There are many algorithms that can be used for land use and land cover image classification. Automated classification method such as supervised classification method requires collection of training samples for the algorithm to run while an unsupervised approach does not require any field point collections, the information on the raw images is used which however has some critical limitations (Bruzzone and Prieto, 2002). In recent time, machine learning algorithms like neural networks, random forest and support vector machine have become increasingly used. Random Forest (RF) classification is a learning algorithm that guess a class from sets of sample data by generating numerous decision trees and cumulate their outcomes (Farkuor *et al.*, 2014). RF creates huge arrays of classification tree by selecting the best split randomly from the original training data.

In addition, Forkour *et al*. (2015) revealed that random forest approach in this algorithm increases classification accuracy by decreasing the correlation between trees. The findings of Gómez *et al.* (2016) further reveals that the stregnth of random foret approach are; ability to determine the significance of a variable, perform vigorous data reduction, does not over-fit and produces an unbaised and higher accuracy and it weakness are; it contains an unknown decision rules and an intense input parameter computation are needed. In the same view a study carried out by Ma *et al.* (2017) found out that for a supervised object based classification Random Forest shows the best performance compared to fuzzy techniques which is seen to be limited to object-based framework.

Image accuracy assessment in principle helps to evaluate the LULC classification result. Which is also known as contingency table or confusion matrix. It contrasts the actual,

observed or true class of a sample from the fieldwork or image interpretation (Wegmann *et al.,* 2016). The contingency table consist of User Accuracy (UA), Producer Accuracy and kappa coefficient. UA gives information of error of commission and pixels assigned into a class that it truly belongs to while PA is the accuracy from the perspective of the map producer and are errors associated with omission (Mahmoud, 2016). When pixels belonging to a different class is classified into another class error of omission is committed.

Kappa coefficient is a statistical method that calculate the observed agreement between the ground reference and classification map and the agreement between the map that might be by chance (Congalton, 2001; Batisani and Yarnal, 2008). They characterize kappa coefficient into three agreement levels. The first level indicates that when Kc is > 0.75 there is a strong or excellent agreement, between 0.4 and 0.75 means it has a fair to good agreement and the last level indicates that value of Kc = 0.4 and Kc < 0.4 shows a poor agreement. Kc value ranges between 0 (complete disagreement or inaccurate) and 1 (complete agreement or accurate).

2.3.2 Determination of land cover index

Several studies (Chen *et al.,* 2006; Liu and Zhang, 2011; Essa *et al.,* 2012; Ahmed *et al.,* 2013; Kaspersen, *et al*., 2015; Li *et al.,* 2017) used different land cover indices to examine the correlation between LULC and LST. In order to achieve the second objective of this research, this study used different land cover indices namely: Normalized Difference Vegetation Index ((NDVI), which is widely used to predict agricultural production, fire regions, monitor drought and map out desert advancement and express the thickness of vegetation); secondly Normalized Difference Built-up Index ((NDBI), is subtle to built-

up area and are used to characterise the magnitude of built up areas); Thirdly, Modified Normalised Difference Water Index ((MNDWI) which shows the extraction of water against a background dominated by water). NDVI values varies from -1 to +1 (green covers value range from 0 to 1; cloud and water are normally less than zero, shrubs, grasslands and parks range from 0.2 to 0.3 and tropical and temperate rainforest have high values of about 0.6 to 0.8) (McFeeters, 1996; Wegmann *et al.,* 2016).

2.3.3 Factors influencing land surface temperature

The consistent increase in the environmental temperature and the factors responsible for them have been a topical issue in our world for a long while now. Land surface temperature (LST) plays a very significant role in many ecological processes and can provide primary information on the physical properties of urban surfaces and the climate. Different researchers have revealed different views and results on the factors responsible for the consistent increase in environmental temperature. In one of such studies, Bhatta (2010) reported that two factors are majorly responsible for this increase in the observed environmental temperature found in developed/built-up centres. The first factor noted was the dark surfaces such as roadways and rooftops. Dark surfaces according to his finding, usually absorb shortwave radiations and reradiate them as longwave radiations, causing about 28 to 39^{o}C increase in temperature which is usually higher than the surrounding.

Furthermore, Doick and Hutchings (2015) while studying the role of vegetation in curbing the problem of surface temperature reported that, non-vegetative cover is the second factor responsible for the increase in the environmental temperature. Their finding revealed that trees provide shades and cools the air through evapotranspiration but when

these trees are cut off for the purpose of building and construction of dark surfaces, these ecosystem services are lost.

Research carried out by Ifatimehin *et al.* (2010) in Lokoja revealed that, there is a significant variation in temperatures among the various LULC types with built area and vacant area having the highest land surface temperatures 59.5^{o}C and 58.5^{o}C respectively while cultivated land, natural vegetation and water bodies have the least with 26.5^{o}C, 28.5^{o}C and 34^{o}C. Similar another study revealed a direct relationship between the pattern of CLCLU and LST variations on the land use types (Weng *et al.,* 2004; Sobrino *et al.,* 2004; Ifatimehin *et al*., 2009). Ahmed *et al*. (2013) in their study titled; "Simulating Land Cover Changes and Their Impacts on Land Surface Temperature in Dhaka, Bangladesh" revealed that, about 56 to 87% of the study area will experience temperatures as high as 30°C in 2019 and 2029, if the trend of changes and loss of vegetation continues. In conclusion, Maduako *et al.* (2016) and Faqe, (2017) finalised that the main factor linked to rise in urban heat and local climatic warming is known as Land Surface Temperature (LST).

2.3.4 Effects of land use and land cover changes on land surface temperature

One of the most significant impact of land use land cover changes on land surface temperature is urban heat island. A process mainly caused by urbanization and has consequently resulted in Urban Heat Island (UHI). Urbanization and continuous change in land cover generally have direct and indirect impacts on land use transformation. Research on urban heat island (UHI) effect began many years (ICSC, 2011; Oke, 1982; Ifatimehin, *et al.,* 2009). Chandler (1952) cited by ICSC (2011), was the first to discover and measure UHI effect using his car attached with thermometer to traverse specific

routes of the city in order to record the temperature. He discovered that the measured temperature data plot created a distinctive concentric pattern.

UHI according to Doick and Hutchings (2015) is a phenomenon of varied increase in the temperature obtainable in the urban area compared to their rural surrounding and generally intensifies during hot periods and significantly affect human health and energy demands due to the need for cooling of the environment**.** It is a climatic phenomenon that is best described when cities/urban areas have higher temperature than in suburbs (Oke, 1988; Buyadi *et al.,* 2013). And occurs due to the conversion of vegetated lands into non vegetated urban surfaces as a result of the dynamics of urban growth, (Solecki *et al.,* 2005). Li and Zhao (2012) also attributed excess heat from human activity like from combustion engines and air conditions to UHI. Additionally, Bharath *et al.* (2013) in his review of "land surface temperature responses to land use land cover dynamics, observed that "Landscape dynamics involving LULC changes contributes to high land surface temperature".

To further buttress the role of LULC on land surface temperature, Adebayo and Zemba (2003), investigated the effects of LULC on the surface temperature in Lokoja using remote sensing and Geographic Information System (GIS) and reported that the surrounding environment to cities have cooler climate than the cities and attributed this variation to non-uniform distribution of thermal conductivities and heat capacities of objects across urban environment and their surroundings. Sailor (1995) cited by Zhan *et al.* (2013) argued that urban climate is most noted to be warmer and more polluted than rural counterpart due to city expansion. Contrary to the above, Kaya *et al.* (2012) revealed that, the urban heat island is majorly caused by the alteration of land covers through human development activities by using materials that retains heat and this can also be

attributed to increasing population because there will be continuous modification of land in the environment and this has a corresponding effect on land surface temperature.

Similarly, De Carolis (2012) assessed the vulnerability and mitigation strategies of urban heat island effect on Windsor, ON and revealed that apart from the infrastructural and surface properties in urban areas, that UHI can also be influenced by the geometry of urban structures which causes changes in the reflectance pattern. A phenomenon that has been described as "urban canyon effect" by Shishegar (2013) and Jamei *et al.* (2015). They also maintained that the amount and process of heat absorption are affected by the narrow arrangement of buildings in the urban areas.

Similarly, Morris *et al.* (2001) have shown that large buildings also block wind thereby causing reduction in wind speed and stopping the transfer of warm air. This inadvertently leads to multiple heat absorption of incident radiation by more than one surface thereby leading to high absorbed energy that could contribute to UHI (De Carolis, 2012).

In appraising the role of LULC dynamics and green roofs in influencing the temperature of urban centres, Solecki *et al.* (2003) in the New York Metropolitan Region Research Report, observed that the magnitude of UHI effect varies as a result of seasonal changes but occurs all through the year. UHI intensity can also be affected by a phenomena called Sky View Factor (SVF: “is the extent of visible area of the sky that can be viewed on the ground at a point”) (De Carolis, 2012). A finding which was exhaustively adopted by Rosenzweig *et al.* (2009), who noted that the phenomena of UHI are strongest at night and on summer days when the air is calm and clear. They concluded that in these periods, short-wave radiation tends to travel directly to the earth’s surface without obstruction.

Another cause of UHI is waste heat from industries, automobile combustions, high level of pollution and air conditioning (Sailor, 2011; Li and Zhao, 2012). Environmental protection agency (2008), outlined various sources of anthropogenic heat such as: "vehicular emission, warming, air conditioning system, heating appliances, industrial emission, agricultural emission and ventilation". However, De Carolis (2012), revealed that anthropogenic heat is believed to have small impact on UHI intensity when compared to other causes earlier mentioned and this is why many UHI mitigation strategies and recommendations do not include measures of reducing waste heat production.

Furthermore, EPA (2008) reveals that the formation of UHI can also be exerted on temporal effect that are caused by topography and geographic locations. In agreement with the above findings Rosenzweig *et al.* (2009) showed that "UHI effect is stronger on days that are characterised with less clouds and low wind speeds". The transfer of air can be hindered when wind speed declines and more frequent in urban centres because in such situations warm temperature will be conserved and maintained while in rural areas, wind speed is usually high and could result to cooling by convection (Morris *et al*., 2001).

In addition, different heat effect is experience in cities with mountains and hills because the meteorological conditions and the current pattern of wind produces a number of UHI effect on the leeward and windward sides therefore Urban centres near water bodies will experience convective forces and wind pattern could regulate heat transfer (Environmental Protection Agency, 2008).

2.3.5 Retrieval of land surface temperature

Wegmann *et al.* (2016) noted that Landsat data obtained from Earth explorer comes in 8-bit radiometric resolution usually known as digital numbers (DNs) (in order to reduce file size). OLI and TIRS comes in 16-bit data which means it has a pixel value ranging from 1 to 65,535. They also found out that sensor and band specific calibration parameters (multiplication terms often referred to as gain or mult and an additive term referred to as offset or add) need to be applied to DNs in order to recalculate the actual radiation measurement on the sensor. Remote sensing in the solar reflective range (300 to 2500 nm) is been impacted by the Earth's atmosphere.

Theoretically, in remote sensing the basic thing is that, remote sensor measures the thermal radiance of a feature from ground emittance which according to the theorem of blackbody radiance can be determined as a function of temperature at a specific wavelength (Wang *et al.*, 2015). In addition, Wang *et al.* (2015) revealed that, since the observed thermal emittance travel through space, it is being significantly affected by the atmosphere before it gets to the remote sensor. This means the retrieval of LST from the thermal band have to consider the effect of both atmospheric and ground in order to obtain accurate result and this has complicated the retrieval of LST as earlier mentioned.

The process of removing this atmospheric effect on the imagery is called atmospheric correction. There are several approaches for performing atmospheric correction. Dark object subtraction approaches rely on the estimation of atmospheric haze based on dark pixels thus, dark pixels are assumed to have zero reflectance. Hence, the haze values are estimates of path radiance, which can be subtracted in a dark object subtraction (DOS)

procedure (Wegmann *et al.*, 2016). Therefore, typically, haze is estimated in blue, green and red bands, occasionally also in the NIR band.

2.3.6 Impact of urban heat island

Reduction in outgoing long wave radiation caused by urban environment and the anthropogenic activities is noted to hinder distribution and loss of sensible heat and this has resulted in increases in ambient land surface temperature of about 2 to 3°C higher than the surroundings (Oke, 1982; Ifatimehin *et al.,* 2009). Similarly, UHI has also been implicated in the health sector. The normal human body temperature is about 37°C but this has been altered due to increase in temperature and UHI effect. Health effects of UHI has increase this optimal temperature value at which the human body functions to a significant value higher than the average thereby hindering the ability of the body to adapt, cool and fight some diseases (De Carolis, 2012).

Camilo (2010), reviewed the effect of urban heat island and found a direct relationship between urban heat intensity and cardiovascular and respiratory diseases. Chan *et al.* (2007) in their finding further revealed that increase in the internal body temperature due to UHI could exacerbate heat related sicknesses such as heat stroke, cramps, exhaustion, syncope, rashes, fainting and organ dysfunction. Patz *et al.* (2005) also warned that often times when extreme heat event is prolonged, that mortality can occur with increase in admissions in hospitals as a result of chronic conditions such as respiratory, diabetic, renal, nervous disorder and cardiovascular diseases (Chan *et al.,* 2007).

Another sector where the impact of UHI is significantly felt is in weather pattern. The primary manifestation of UHI on the weather is through its effect on the local temperature

of the environment with its secondary effect being felt on other local meteorological processes such as development of clouds, humidity, fogs, precipitation and altering of the pattern of wind (NASA, 2004). A study by Camilo (2010) has reported that relative low air pressure that could cause cooling are created by anomalous warming of cities (UHI) and condensate and precipitate. Urban induced precipitation, thunderstorm events, reduction in diurnal and seasonal freezing temperature, physiological and phonological disturbances on urban plant and forest, winds, are all affected by UHI. The study concluded that the degree to which UHI currently affects global temperatures is still unclear.

According to the Environmental Protection Agency (EPA) (2008), high pavement and rooftop surface runoff, with temperature of about 37°C can raise the original temperature of rainwater from 21°C to over 35°C. They revealed that such run off water when discharged into streams, rivers and lakes could negatively affect aquatic animals and plants by creating thermal shocks and an unconducive habitat for aquatic life. Similarly, Akbari (2005) has also noted that rain water could be heated via conduction from surface when runoff occurs.

Further important impact is on increase in energy consumption rate in an environment. De carolis (2012) noted that cities in hot climates are characterised with warmer surfaces all through the day and this has led to high energy consumption rate needed for air conditioning and refrigerators. For example, in order to be comfortable and safe in hot climatic environment, there will be increasing use of air conditionings and electric generators which will in turn increase the demand for energy. In addition to the above findings Environmental Protection Agency (2008) in their studies showed that in every $0.6^{o}C$ increase in temperature there is about 1.5-2.0% demand for electricity demand for

each house and 5-10% of community electricity demand for cooling the environment and pay off for the UHI effects and this increases the total consumption of energy needed to cool the environment, thus, increase energy production through power plant which in turn leads to higher release of greenhouse gases that could be trapped in the Earth-atmosphere (Camilo, 2010).

2.3.7 Methods of mitigating against urban heat island

In order to reverse the causes of increasing LST and associated UHI effect, some mitigation techniques have been put in place and are been practiced in many countries. These strategies are implemented to increase emissivity, evapotranspiration cooling, albedo and reduction in the construction of impervious surfaces in urban areas for example implementation of urban greening, continuous planting of selected trees and green roofing (De Carolis, 2012). The overall temperature of cities is majorly influenced by vegetation (Doick and Hutchings, 2013; Ishola *et al.,* 2016) and can be reduced through selecting and placing trees and green infrastructure in a more strategic way in cities which would consequently cause cooling of air to about $2^{o}C$ and $8^{o}C$.

Furthermore, Byomkesh *et al.* (2011) have persuasively argued that for the proper functioning of any ecosystem, the importance of green environment can never be over emphasized and hence, it is particularly essential and indispensable in achieving reduction in the overall temperature of cities centres and its surrounding. Also Alavipanah *et al.* (2015) while expressing similar opinion argued that urban vegetation regulates climate and also support social structure and wellbeing of the people. Hadi *et al.* (2014) have observed that for a green environment, control eco-environmental degradation and

sustainable development to be achieved, there will be need to regulate vegetation of an urban environment.

In adopting this view, De Carolis (2012) noted that in order to achieve significant reduction in the amount of accumulated heat and heat being radiated in the urban areas, the concept of green roofing (planting vegetation on roof tops in urban centres) and green wall are important; since vegetation in any landscape can provide greenspace and help to regulate the local climate. He consequently suggested that the use of traditional roofing and walls items such as shingles, tiling, gravel and asphalt which have lower albedo than vegetation and as such can increase surface temperature thereby contributing to urban heat island should be minimized.

This view was also adopted by Buyadi *et al*. (2013), through his finding by showing that there is significant decrease in vegetated area and that urban micro climate has been modified and temperature is increasing because of this loss in vegetation. A conclusion that was echoed by Peterson (2003) who noted that the effect of UHI on the global temperature was small or negligible. On the contrary, Mcktrick and Michaels (2007), reported a considerable influence of urban heat release on temperature estimates.

2.3.8 Application of remote sensing and geographic information system tools for land surface temperature, land use and land cover and urban heat island detection

"Remote sensing (RS) tools and data are the utmost instrument for the study of temporal and spatial dynamics of the thermal land cover of urban centres and the energy budgets of urban surface" (Weng, 2009 cited by Alavipanah *et al.,* 2015). RS provide detailed LULC information and a more complete and uniform sample of land surface temperature

observation when compared to in situ air temperature measurement (Alavipanah *et al.*, 2015). Satellite Remote Sensing (SRS) can be used to track land cover change and habitat distribution (Nagendra *et al.*, 2013 cited by Wegmann *et al.*, 2016).

The use of RS and GIS methods has been revealed by several research. In remote sensing, to obtain true, false and arbitrary colour composite red, green and blue (RGB) have been extensively applied to visualize images (Mahmoud, 2016). However, the two prominent composite are the false colour composite (FCC) and the natural colour composite (NCC) (Mahmoud, 2016). Balogun *et al.* (2011) used RS and GIS to analyse land use change and urban growth in Akure, south western part of Nigeria. Satellite imagery for 1986 and 2007 was analysed and result showed that, there exist rapid increase in urban build ups and decline in forest.

Furthermore, Ejaro and Abdullahi (2013) applied RS and GIS on their studies perform a post classification and to examine the spatiotemporal dynamics of LULC in Suleja area of Niger State, north central part of Nigeria. Their study revealed that there is constant expansion of built areas and decrease in vegetation cover in the area. Landsat imagery is capable of deriving LST (Weng, 2001; Alavipanah *et al.*, 2007; Buyadi *et al.*, 2013). Landsat OLI & TIR, ETM+ and TM (Landsat 8, 7 and 5) are extensively used to analyse land use changes, and to model the biological and physical features of the earth surfaces (Weng *et al.*, 2004; Sobrino *et al.*, 2008; Wang *et al.*, 2015; Avdan and Jovanovska, 2016; Li *et al.*, 2017).

Goslee (2011) noted that for large scale or long period studies SRS data can be used as an alternative or even a complement to ground based data but the problem attributed to this kind of data is the atmospheric, radiometric and topographic corrections that are

required before further analysis is carried out and also concluded that for most applications atmospheric correction is required because reflectance from the ground surfaces is of greater interest than that at the sensor when land surface emissivity and temperature is to be estimated.

Theoretically, in remote sensing the basic thing is that, remote sensor measures the thermal radiance of a feature from ground emittance which according to the theorem of blackbody radiance can be determined as a function of temperature at a specific wavelength (Wang *et al.*, 2015). In addition, Wang *et al.* (2015) revealed that, since the observed thermal emittance travel through space, it is being significantly affected by the atmosphere before it gets to the remote sensor. This means the retrieval of LST from the thermal band have to consider the effect of both atmospheric and ground in order to obtain accurate result and this has complicated the retrieval of LST as earlier mentioned. Landsat and other satellite data are readily available freely with more demand for atmospheric and radiometric corrections in which most research depends on a more complex GIS software.

Open source software like R can help bridge that gap to provide a more improved correction method to fill in the gaps between research and implementation (Goslee, 2011). Over the last decades, R has become one of the most frequently used tool for both classical and cutting-edge statistical analysis across many research (Wegmann *et al.,* 2016).

2.3.9 Novel approaches on land use and land cover classification

One major problem with classification result especially when scale-based textural methods are included in the classification is edge effect (Zhou and Lam, 2008). Zhou and Lam (2008), introduced a new approach which indicates that, all pixels in a moving

window make use of the textural information instead of only the centre and results showed that higher accuracy are acquired when the window size are set to be smaller than the land use polygons with a less complex class boundary. The moving window approach as the name implies stops for every pixel and calculate a summary statistic for the neighbourhood and then moves on to the next pixel (Wegmann *et al.*, 2016). This concept is used to analyse the heterogeneity of the various classes in image classification. Instead of having a smaller pixels appearing all over the map this approach makes the classification more homogenous by setting all smaller pixels to take the neighbouring classes and filtering out smaller pixels to avoid salt and pepper effect.

It is possible to acquire multi temporal and spatial images for a particular year from the free Landsat archive. Different optical images have been used by several studies to perform image classification (Gao *et al.,* 2006; Hilker *et al.,* 2009; Watts *et al.,* 2011; Thenkabail and Wu 2012; Wu, Thenkabail and Verdin, 2014). Combining data from multi-temporal scales from one sensor is another approach that can improve LULC classification accuracy and the advantage is that images from a single sensor will give a more consistent spatial radiometric calibration (Gómez *et al.,* 2016).

One of the limitation optical images is their inability to capture cloud free data during wet season or winter (Forkuor *et al.,* 2014). Therefore, many studies used different spectral images for their analysis. For example, Forkuor *et al.* (2015) in their studies compared the result obtained from a one-step classification method and a sequential classification method. They derived a SAR sensor (TerraSAR-X; TSX) and two optical sensors (Landsat 8 and Rapid Eye) for 2013. Accuracy obtained from the multi temporal image classification for a particular year was stated to be 6% and 9% when compared to a single step image classification in the West Africa. LULC analysis can be improved by a

combining both optical and microwave images (Solberg *et al.,* 1994; Blaes *et al*., 2005; McNairn *et al.,* 2009; Forkuor *et al.,* 2014; Hütt *et al.,* 2016). Forkuor, *et al*., (2017) also acquired multi-temporal data from Rapid Eye (March, April, and May 2013) and Landsat (June 2013) to carry out their analysis.

Microwave images like the satellite-borne Synthetic Aperture Radar (SAR) images are active sensor systems which makes them to be independent from cloud cover. Overall accuracy of above 85% can be reordered when SAR and optical images are stacked together to produce a single classification (Forkuor *et al.,* 2015). Past research have concluded that this observed increase is attributed to the application of sets of data acquired at different time steps (Solberg, *et al*., 1994; McNairn *et al.,* 2009; Forkuor *et al.,* 2014; Forkuor *et al.,* 2015; Hütt *et al.,* 2016).

Recent studies have shown that accuracy of land use classification can be improved when multi temporal images are used for classification (Guerschman *et al.,* 2003). It is assumed that any observed changes in a year are phenology changes when such images are used for classification and this is attributed to the fact that vegetation cover types show difference in their phenology characteristics.

Forkuor *et al.* (2014) also added that under cloud free conditions optical images from Landsat, MODIS can be used independently in any area of interest. Hutt *et al.* (2016), performed a repeated stepwise analysis by adding several bands until the best accuracy is attained. Another contribution to land cover classification accuracy was achieved by Sinha *et al.* (2011), in their research on "Seasonal land use/land cover mapping: Accuracy comparison of various band combinations". They used six multi-temporal TM digital images (from January 2007, August, and September 2007; March 2008 and November

2009) to perform land-cover classification on both derived and original images by combining several bands by stacking all the 13 bands to generate a final image (Sinha *et al.,* 2011). Information that is not obtainable on a particular image can be obtained from another by fusing the two or several images together (Dong *et al.,* 2009 cited by Forkuor, 2014).

Single date approach for LULC classification have been proved to be inferior to temporal approach (Gómez *et al*., 2016). Although a more sophisticated tool is needed to analyse a multi-temporal spectral data because they contain rich information (Kennedy *et al.,* 2014 cited by Gómez *et al.,* 2016). Random Forest (RF) classification is a learning algorithm that guess a class from sets of sample data by creating multiple decision trees and cumulate their outcomes (Forkuor *et al.,* 2014).

2.4 Summary

In most developing countries like in Nigeria vegetation cover have been lost in thousands of hectares annually. Forest are being deforested, land covers are being converted and modified at dramatic rate just to meet the request and advancement of the economy. The literatures reviewed showed that urbanization, anthropogenic activities, are major contributors to LULC change. Land cover type in Kano suburbs is noticed from field observations and satellite imagery collected to be changing fast as a result of conversion of forest/dense fields with shrubs and grasses to agricultural lands in order to meet the demand of the commercial market and the population. Buildings and roads are being constructed by the government not considering the effect it will have in the environment and putting down an alternative plan to combat this effects especially on the increasing land surface temperature. This is noted to have significant impact on LST and cause UHI

effect to be noted. It was also pointed out that application of RS and GIS techniques are accurate geospatial techniques for analysing different LULC classification, examine their transitions and influence on land surface temperature but atmospheric correction is noted to be over looked by many research because of its complexity.

Research have refrained from using several satellite imageries because of the problems of atmospheric correction and the inability to analyse these data on time and with less cost. Open source software like R can help bridge that gap to provide a more improved correction method (Goslee, 2011) and can work on several data. The gap of LULC and it continuous influence on LST have been bridged and studied to some extend but in what dimension and trend is this land surface temperature developing on different LULC within a year or two? This study employed the use of spatiotemporal satellite imagery (Landsat 8 to be precise) to assess the different LULC types, perform radiometric and atmospheric corrections on the imageries, examine the impact on land surface temperature by using a different methodology that is more robust, accurate and reliable techniques (R statistics and QGIS) to ascertain the aim and objectives of the study.

CHAPTER THREE

3.0 MATRERIALS AND METHODS

The methodology of this study involves different material, methods and approaches used for data collection and analysis. The methodology to achieve the set objectives involved the following; materials and methods, satellite image correction, land use and land cover and different land use index extraction, land surface temperature extraction, class based analysis for land surface temperature time series and analysing the impact of Land Use and Land Cover (LULC) on Land Surface Temperature (LST).

3.1 Dataset and Tools Used

Majorly secondary data was acquired in order to show the temperature trend and changes over time and the current impact of the different LULC type on LST in the study area. Existing maps, land use and land cover map of the study area was used as well. Socio-economic data (population data at district level) and training samples were also of importance to the study. Primary data like satellite data and training samples acquired on the field were used to detect LULC and LST extraction.

One great tool among many tools used in carrying out studies on LST and LULC is the Quantum Geographic Information System (QGIS). The tool has different version like 2.1, 2.2, 2.3, 2.4, 2.18.0 and many more. Version 2.18.0 was preferred in this study because it contains all the necessary cartographic tools and plugins that is needed to carry out the map design and data analysis in this study.

R is a multipurpose environment for statistical computing, graphics and programming language and also an open source like QGIS. R has extensions usually called packages that need to be installed simply on the command line by writing a short script or on the CRAN repository. For this study, several packages like RStoolbox, rgdal, maptool, stringr, ggplot2, raster, randomForest, rpart, caret (R development core team, 2011; Keitt *et al.,* 2011; Pebesma *et al.,* 2017; Leutner and Horning, 2017) were used to successfully carryout the data analysis. This packages were designed by remote sensing and GIS experts who are good in script writing and programming and the packages contains all the functions that are needed for analysing a robust set of satellite data in the study.

Another great tool used was Global Positioning System (GPS). GPS is a hand-held satellite-based navigation system with a set of twenty-four satellites used to collect coordinates for different features. For the purpose of this research, preferably Garmin GPSmap 62Sc model was used to collect training samples on the field and it was set to carry Universal Tranverse Mercator (UTM zone 32) projection which is the accurate coordinate system for the study area. In addition, the error margin at which the data was collected was between 3-4m so as to have maximum numbers of satellite available at that point to collect the exact location of the feature.

3.2 Data Acquisition and Source

Spatial and non-spatial (ancillary data) data that are significant for this study were collected and used. Table 3.1 shows a complete list of the satellite data, other ancillary data date acquired and the source acquired from.

3.2.1 Socio-economic data

On the socio-economic data of the study area population data on LGA level was obtained from http://vts.eocng.org/population for 2017 which was subtracted from the population data of 2006 population census provided by National Bureau of Statistics in 2012 in order to see the trend of growth and its possible impact on the current LULC of the study area (Table 1.1 and 4.1).

3.2.2 Satellite imagery and training data

Multi-temporal spatial Landsat 8 OLI/TIRS satellite imageries for 2015 and 2016 of path 188 and Row 052 (Table 3.1) were collected from the United States Geological Survey (USGS) to calculate land cover index, LULC classification and derive LST. Landsat imagery was used because of its cost effectiveness and availability to the research work. In order to perform image classification and accuracy assessment training data were collected from the field. In the same view field photographs was taken to visualize different LULC classes and to ascertain the reliability of the ground-truth data.

Table 3. 1 Dataset used in this study

Items	Acquisition Date	Source
Ancillary Data		
Administrative boundary	2017/05/12	EHealth System Africa (EHA)
Population data for study area	2017/05/12	EHealth System Africa (EHA)
Population for 2016	2016 census	National Bureau Statistics
Sample points	2017/05/04	Field work
Spatial Data		
Landsat 8 (OLI/TIRS)	2015/01/01 (D001)	USGS Earth Explorer website (http://earthexplorer.usgs.gov/)
	2015/01/17 (D017)	
	2015/02/02 (D033)	
	2015/04/23 (D113)	
	2015/05/25 (D145)	
	2015/06/10 (D161)	
	2015/10/06 (D289)	
	2015/11/22 (D305)	
	2015/12/09 (D353)	
	2016/01/20 (D020)	
	2016/02/05 (D036)	
	2016/04/09 (D100)	
	2016/04/25 (D116)	
	2016/05/27 (D148)	
	2016/07/14 (D196)	
	2016/09/16 (D260)	
	2016/11/15 (D324)	
	2016/12/21 (D356)	

Source: Authors compilations, 2017.

3.3 Data Pre-processing and Conversion

Landsat 8 consists of 2 sensors, the Operational Land Imager (OLI) and the Thermal Infrared Sensor (TIRS). Band 6 and 7 of this sensor acquired shortwave infrared data while band 10 and 11 are of the thermal band. Data processing and conversion was done using 'R' on the entire imagery (not selected bands) and these involves extracting files and metadata, radiometric and atmospheric correction.

3.3.1 Extraction of files and metadata

The study used three primary colour (red, green and blue RGB) to visualize a colour composite of the RS images which contains at least three bands (5, 4 and 3). However, since R software could handle several combination of bands all the visible bands were used for LULC classification. RStoolbox package in R statistics software was used to read in the metadata for all the Landsat imagery collected. This step also involves extraction of the files that is the associated bands and files that were needed for further processing and it was carried out by writing a script in the R statistics software by first calling the RStoolbox package and running the analysis before further processes were carried out.

3.3.2 Radiometric and atmospheric correction

This study used Simple Dark Object Subtraction (SDOS) method of the DOS approach found in the RStoolbox package in R statistics tools to perform atmospheric correction on the blue, green, red and near infrared band as seen in equation 11, based on the principle that there are always few pixels that reflect almost no radiation and hence should appear dark It is assumed that any radiation originating from dark pixels is due to

atmospheric haze and not the reflectance of the surface itself. Dark object subtraction approaches rely on the estimation of atmospheric haze based on dark pixels thus, dark pixels are assumed to have zero reflectance. Hence, the haze values are estimates of path radiance, which can be subtracted in a dark object subtraction (DOS) procedure.

3.4 Data Analysis

3.4.1 Determination of Land Cover Index

In order to achieve the second objective of this research, this study used different land cover indices namely: Normalized Difference Vegetation Index (NDVI); Normalized Difference Built-up Index (NDBI) and Modified Normalised Difference Water Index ((MNDWI) Land Cover Index was determined using Several band in Landsat 8 obtained from Adeyeri *et al*. (2017), as indicated in Table 3.3 below to retrieve land cover indices of the study area by applying the equations adopted by McFeeters (1996); Wegmann *et al.* (2016); Landsat 8 handbook (2016) and Li *et al.* (2017).

1) Normalised Difference Vegetation Index: This was done using the Red (band 4) and NIR (band 5) and by applying the equation below in a script using the R statistics tool.

$$\mathrm{NDVI} = \frac{\mathrm{P_{NIR}} - \mathrm{P_{RED}}}{\mathrm{P_{NIR}} + \mathrm{P_{RED}}} \quad (1)$$

2) The Normalised Difference Built-up Index: It was calculated using the shortwave infrared (band 6) and near infrared (band 5).

$$NDBI = \frac{P_{SWIR} - P_{NIR}}{P_{SWIR} + P_{NIR}} \quad (2)$$

3) The Modified Normalised Difference Water Index: This was done by using the green (band 3) and shortwave infrared (band 6).

$$MNDWI = \frac{P_{GREEN} - P_{SWIR}}{P_{GREEN} + P_{SWIR}} \quad (3)$$

Where,

P is the respectively bands,

Green is band 3,

Red is band 4,

NIR is band 5 (near Infrared),

SWIR is band 6 (short wave infrared) and

TIR is band 10 thermal infrared).

Table 3. 2 Landsat 8 spectral bands used for calculating land cover indices and LST

Spectral Band	Wavelength (µm)	Resolution (m)
Band 1 (Coastal band)	0.43-0.45	30
Band 2 (Blue band)	0.45-0.51	30
Band 3 (Green band)	0.53–0.59	30
Band 4 (Red band)	0.64–0.67	30
Band 5 (Near Infrared, NIR band)	0.85–0.88	30
Band 6 (Short Wave Infrared, SWIR 1)	1.57–1.65	30
Band 7 (Short Wave Infrared, SWIR 2)	2.11-2.29	30
Band 8 (Panchromatic band)	0.5-0.68	15
Band 9 (Cirrus band)	1.36-1.38	30
Band 10 (Thermal Infrared Sensors, TIRS 1)	10.6-11.19	100
Band 11 (Thermal Infrared Sensor, TIRS 2)	11.5-12.19	100

Source: Adeyeri *et al*. (2017)

3.4.2 Image classification

The study used 0.01% cloud satellite images and training samples collected from a rigorous fieldwork by validating the field data with a very high resolution satellite image source like Google Earth before performing the image classification. An automated classification method (Supervised and unsupervised) was used to carry out image classification. This study uses supervised classification method, which is a computer algorithm to classify pixels that requires collection of training samples from the field for the algorithm to run, to generate LULC maps of the study area.

The method was carried out using the superclass function in R statistics tools and by indicating random forest as the algorithm. The study collected data all through the two years of interest to perform its image classification rather than using one-time step. The rationale behind the use of all the images for a year was to use the phenology information (or time series information) in the image. In February agricultural fields might have the same digital number (DN) in Near Infrared than settlement, but could have a different value in August/September. Evergreen trees might have similar values than agricultural lands in the rainy season, but different in the dry season. Therefore, the information of the change in the existing spectral bands were used. This was done in order to attain a more accurate image classification (Figure 4.1 and 4.2). This is attributed to the fact that a powerful classification algorithm and computing techniques used.

The classification classes used are built up (residential areas, industrial, and commercial), vegetation (such as forest, grassland and shrubs and agricultural lands), water bodies (ponds, rivers, streams and lakes) and bare land (crop outcrop, hills, soils). This set of class were preferred in this study because many studies have used this data to carry out their classification analysis and have revealed an accurate result (Weng *et al.*, 2007; Ejaro and Abdullahi 2013; Faqe, 2017). There were also used in order to achieve the objectives of this study and because these features are widely distributed in an environment. The classes are described as follows:

a) **Residential areas:** These are characterized by several-unit structures of high density urban centres and less dense areas (Plate I) covered with buildings that are lots more than an acre and almost reserved for residential use.


Plate I Field photograph of residential areas

b) **Industrial areas:** This include a wide arrangement of land from heavy to light manufacturing plants (Plate II) with mostly large building types, structures and roof materials different from that of residential or commercial.


Plate II Field photograph of Industrial areas

c) **Commercial areas:** These are areas primarily for the buying and selling of goods and services such as in shops, commercial strips, urban central business districts

and markets. They are characterised of smaller shops and mostly of zinc and metal roof types and can be populated with people.

d) **Forest:** This vegetation type includes every forest cover types such as forest deciduous cover, evergreen, dense and sparse forested areas of about 70% cover (Plate III).

Plate III Field photograph of forest

e) **Shrubs and Grasslands:** Consist of grasses and shrubs and mostly known to be abandoned lands with natural vegetation cover that are dried up in dry season (Plate IV) found around hills.

Plate IV Field photo of grasslands and shrubs

f) **Agricultural lands:** They consist of croplands and farmlands and pasture of about two hectares of land. This land could be fully dedicated for irrigation agriculture which means all through the year the land will be cultivated and it could be purely rain fed (Plate V).

Plate V Field photograph of rain fed agricultural land

g) **Water body:** This class was divided into rivers and ponds, streams or lakes which are stationary or flowing, seasonal or dammed as shown in Plate VI below.

Plate VI Field photograph of water bodies

h) **Bare lands:** These are surfaces that are left bared with neither vegetation nor buildings such as crop outcrops, bare soils and hills (Plate VII).

Plate VII Field photographs of bare lands

In land use and land cover image classification, edge effect is one major problem. Moving window approach is a new approach used to correct this edge effect (Zhou and Lam, 2008 and Wegmann *et al.*, 2016) carried out by analysing the heterogeneity of the various classes in image classification. Therefore, instead of having smaller pixels appearing all over the map, more homogenous classification map is created by setting all smaller pixels to take the neighbouring classes. This study applied the moving effect concept because the study is more interested in homogeneous areas and so neglect the smaller pixels in the classification. In doing this, a weight matrix was defined. The weight matrix used was of 3 x 3 pixel (90 x 90m) moving window and this was used to weight the contribution of neighbouring cells using the raster function (focal () in R) as shown below:

1 1 1
1 1 1
1 1 1

3.4.3 Image classification accuracy assessment

LULC map classification accuracy assessment is also known as contingency table or confusion matrix. This is done in order to ascertain the extent to which reality reflect in

the map. Therefore, User Accuracy (UA) was used to give information on error of commission, which is estimated when pixels belonging to a particular class is correctly assigned to it while, Producer Accuracy (PA) was used to compute the errors associated with omission, which is estimated when pixels belonging to a different class is classified into another class error of omission is committed (Congalton, 2001).

Accuracy assessment for this study was calculated from the equations:

$$\mathrm{OA} = \frac{\sum(\text{diagonal correctly classified classes})}{\sum(\text{row total})} \tag{4}$$

$$\mathrm{PA} = \frac{\text{correctly labelled class in the column}}{\text{column total of the item}} \tag{5}$$

$$\mathrm{UA} = \frac{\text{number of correctly predicted class}}{\text{sum of row total}} \tag{6}$$

$$\mathrm{Pr(c)} = \sum(\mathrm{OA} * \mathrm{PA}) \tag{7}$$

$$Kc = \frac{(OA - \mathrm{Pr}\,(c))}{(1 - \mathrm{Pr}\,(c))} \tag{8}$$

Where;

OA is overall accuracy

PA is producer's accuracy

UA is user's accuracy

Pr(c) is probability by chance

Kc is Kappa coefficient

The study used Kappa coefficient to calculate the observed agreement between the ground reference and classification map and the agreement between the map that might be by chance. The accuracy level includes Kc > 0.75 (which means there is a strong or excellent agreement); Kc between 0.4 and 0.75 (fair to good agreement) and Kc = 0.4 and Kc < 0.4 (which shows a poor agreement).

3.4.4 Sampling techniques

Simple random sampling and a purposive technique were used in this study and this was carried out by taking a subset of the specific locations in the study area, and this was mainly applied to the metropolis of the study area. In order to achieve the objectives of the study, the sample size used in this study was derived based on the number of LGAs, the number of wards in each LGAs and the features contained in this wards. The wards were selected at random and a purposive technique was used to identify each ward based on the features contained in the ward. This resulted to 1367 sample training used to perform both classification and accuracy assessment.

3.4.5 Retrieval of land surface temperature

Land surface temperature was retrieved from thermal band 10 of the satellite imageries and time series analysis was determined following the equations stated in Landsat 8 Handbook, (2016) and other recent studies (Avdan and Jovanovska, 2016; Faqe, 2017; Adeyeri *et al.,* 2017). This was carried out as follows:

a) **Conversion of DN to Top Of Atmosphere (TOA) Radiance**: The rescaling factors provided in the metadata file of OLI and TIRS was used to convert the band data to TOA spectral using the equation below:

$$L_{r\lambda} = M_r Q_{cal} + A_r \quad (9)$$

Where,

Lr_λ is TOA spectral radiance (in watts/m^2*srad* μm)

M_r is obtained from the metadata and known as band-specific multiplicative rescaling factor (radiance-mult band y where y is the band number)

A_r is obtained from the metadata, also called band specific-additive rescaling factor (radiance-add band y where y is the band number)

Q_{cal} is standard product pixel values (DN) which are quantized and calibrated.

b) **Conversion of DN values to TOA reflectance:** The reflectance rescaling coefficients found in the metadata file (MTL file) can be used to convert the OLI band data to TOA planetary reflectance. The following equation was used to convert DN values to TOA reflectance for OLI data as follows:

$$\rho_\lambda = M_{r\rho} Q_{cal} + A_{r\rho} \quad (10)$$

Where,

ρ_λ is planetary reflectance (TOA), without corrections for solar angle

Mrρ is derived from the metafile and known as band-specific multiplicative rescaling factor (reflectance-mult band y where y is the band number

A$r\rho$ is also derived from the metafile and known as band specific additive rescaling (reflectance-add band y where y is the band number)

Q_{cal} is standard product pixel values (DN) which are quantized and calibrated.

c) **Dark object subtraction (DOS):** DOS is also known as haze removal is used to remove apparently small reflectance caused by air diffusion, atmospheric scattering or haze. This was corrected using the equation below.

$$DOS = R_1 min - R_1(DOI\%) \quad (11)$$

Where,

$R_1 min$ means the radiance corresponding to the minimum DN from the sum of all the pixels of the image and *R1(DOI%)* is the radiance dark object with a value of 0.01.

d) **Land surface emissivity:** Recently, studies have used the NDVI threshold method (NTM) for estimating emissivity of diverse land surfaces that range between 10-12 µm (Sobrino *et al.,* 2004; Sobrino *et al.,* 2008; Wang *et al.,* 2015; Avdan and Jovanovska, 2016; Adeyeri *et al*., 2017). Particularly, Wang *et al.* (2015) stated that since the spectral range of thermal band 10 falls in this range NTM approach can be effective in extracting the land surface emissivity of Landsat 8 image and the emissivity can be modelled as follows:

$$\varepsilon_\lambda = \varepsilon_{ve\lambda} P_{ve} + \varepsilon_{so\lambda}(1 - P_{ve}) + C_{s\lambda} \quad (12)$$

Where,

ε_λ is land surface emissivity,

$\varepsilon_{ve\lambda}$ and $\varepsilon_{so\lambda}$ are the vegetation and soil emissivity respectively,

P_{ve} is vegetation proportion

$C_{r\lambda}$ is roughness of surfaces (C = 0 for a flat surface) calculated from:

$$C_{r\lambda} = (1 - \varepsilon_{so\lambda})\varepsilon_{ve\lambda}F'(1 - P_{ve})$$

F' is geometric factor between 0 and 1.

e) Estimation of proportion of vegetation (Pv): The proportion of vegetation at pixel scale was derived from NDVI as follows (Sobrino *et al.,* 2004 cited in Wang *et al.,* 2015).

$$P_v = \left[\frac{NDVI - NDVI_{so}}{NDVI_{ve} - NDVI_{so}}\right]^2 \quad (13)$$

Where,

$NDVI_{ve}$ and $NDVI_{so}$ are the NDVI for a completely vegetated pixel and soil respectively. Note that, on a global scale $NDVI_{ve}$and $NDVI_{so}$values are proposed to be 0.5 and 0.2 respectively (Sobrino *et al.,* 2008). In contrast, atmospheric conditions determines $NDVI_{ve}$ and $NDVI_{so}$ values on a regional scale and can be obtained from the NDVI histogram plotted over a particular region (Jiménez-Muñoz *et al.,* 2009; Avdan and Jovanovska, 2016; Adeyeri *et al.,* 2017). This study obtained 0.2 and 0.45 values from the NDVI map and used it to calculate the proportion of vegetation.

f) **At-satellite brightness temperature:** The TIR band converted to spectral radiance can be further converted to at-satellite brightness temperature using the thermal constants details shown in the metafile:

$$T_{bt} = \frac{K_{b2}}{\ln(\frac{K_{b1}}{L_{r\lambda}} + 1)} \quad (14)$$

Where

T_{bt} is brightness temperature At-satellite level (K)

Lr_{λ} is spectral radiance (TOA) (Watts/ (m^2 * srad * μm))

K_{b1} is known as band-specific thermal conversion constant obtained from the metafile (K_1_constant_band y where y is the thermal band number (666.09 to 774.89) for band 10)

K_{b2} is also known as band-specific thermal conversion constant obtained from the metafile known (K_2_constant_band y where y is the thermal band number (1282.71 to 1321.08) for band 10).

g) **Estimating Land surface temperature in Kelvin:**

$$T_k = \frac{T_{bt}}{\{1 + \left[\left(\frac{\lambda_{b10} T_{bt}}{\rho}\right) \ln \varepsilon_{\lambda}\right]\}} \quad (15)$$

Where,

T_k is surface temperature

T_{bt} is At-satellite brightness temperature

λ_{b10} is wavelength for band 10

ε_{λ} is land surface emissivity

$\rho = h\frac{c}{\sigma} = 1.438 \times 10^{-2} mK$ or $14388 \mu m$ which was used in this study. (σ is the Stefan Boltzmann constant $(1.438 \times 10^{-23} j/k,)$ h is Planck's constant $(6.626 \times 10^{-32} js)$ and c is speed of light $(2.998 \times 10^{8} m/s)$ (Weng *et al.,* 2004).

h) Kelvin to Celsius: Conversion of LST kelvin to Celsius as follows,

$$T_s = T_k - 273 \tag{16}$$

3.5 Statistical Analysis of Land Surface Temperature, Land Use and Land Cover and Land Cover Indices

The instabilities in LST have prompted several application of spatial statistical approaches to enhanced the understanding of LST and indicate the factors that can cause its variabilities. Thus, this study applied three statistical tools to evaluate land cover indices, LULC and LST and also determine, if there is cause-effect relationship between the variables. This was carried out using the steps listed below.

1. **Descriptive and Exploratory Analytic tools:** Tables, maps and boxplots where used to explore, display and describe the data for simplicity and better understanding of the analysis. Boxplot was used to determine mean LST and explore the relationship between LST and LULC, land cover indices between different time steps.

2. **Correlation Analysis**: Correlation test checks the association between variables. This statistical tool determines a correlation coefficient (r) known as a measure of the degree to which a variable *a* is linearly related to another variable *b*. Pearson's' correlation analysis method was used in this study. This was done using the formula below:

$$\mathbf{r} = \frac{\sum_{\mathbf{K=1}}^{\mathbf{Nc}} (\mathbf{X_{aK}} - \boldsymbol{\mu}_\mathbf{a})(\mathbf{X_{bK}} - \boldsymbol{\mu}_\mathbf{a})}{\mathbf{Nc} - \mathbf{1}}$$

(17)

Where Nc represent the total number of cells, K is number of specific cells, X is the different values of cells, μ denotes the mean of a layer and a and b are the different layers stack.

The correlation coefficient "r" values range from -1 to +1. It explains a negative correlation if r is < 0, positive correlation when r > 0 and shows no correlation when r = 0.

3. **Simple linear regression model (SLRM):** Correlation analysis is limited in determining the causation of one variable to another. SLRM was used to determine not only the linear relationship between variables but also the cause-effect relationship between the variables. This study applied a SLRM in order to determine the coefficient determination (R^2) so as to know the effect of vegetation on LST dynamics. This was carried out using the formula below:

$$y = a + b_x + e$$

(18)

Where a+bx are the linear explanatory variable and e is the error.

This was calculated using the *lm* function in R software. NDVI, NDBI, MNDWI were set as independent variables/predators, while LST was set as dependent variables.

CHAPTER FOUR

4.0 RESULTS AND DISCUSSION

This chapter present and discuss the results of the population data acquired for 2006 and 2017, LULC classification and validation, analysis of land cover indices, land surface temperature extraction from the OLI/TIRS imagery for 2015 and 2016 and finally the relationship between land cover indices and LST in order to understand the influence of different LULC types on land surface temperature.

4.1 Analysis of Population Data and its Impact on LULC

Data collected from eHealth system Africa has shown that population is dynamic and not static. There is increase of about 3,330,681 from 2006 population census collected from National Bureau of Statistics archive as compared to the population data collected from eHealth system Africa in 2017 as shown in Table 4.1. This will imply that anthropogenic activities will increase along with the increasing population. In order to meet the wants of man and demand for food and shelter, land cover will continue to change and thus affect the micro climate of the study area. Government has to improve on social amenities and infrastructure in order to develop the study area and to meet the growing population, and thus cause more asphalt in the surrounding which retain heat and can contribute to increase in land surface temperature and urban heat island effect

Table 4. 1 Statistical description of population increase

Local Government Areas	2006 Population	2017 population
Dala	418,759	445,554
Dawakin kudu	225,497	378,387
Dawakin tofa	246,197	421,130
Fagge	200,095	265,042
Gwale	357,827	667,297
Kano municipal	371,243	679,426
Nassarawa	596,411	725,388
Ungogo	365,737	881,268
Tarauni	221,844	312,019
Kumbotso	294,391	967,366
Tofa	98,603	123,625
Mingibir	219,611	357,502
Gezawa	282,328	447,033
Warawa	131,858	196,534
Bebeji	191,916	257,025
Garun mallam	118,622	153,426
Bunkure	174,467	217,833
Tudun wada	228,658	284,110
Rano	148,276	185,562
Madobi	137,685	191,359
Kibiya	138,618	147,131
Kura	143,094	182,927
Garko	161,966	220,603
Rimin gado	103,371	200,208
Total	**5,577,074**	**8,907,755**

Source: National Bureau of Statistics (NBS), (2012) and EHealth Africa (EHA), (2017).

4.2 Assessment of Land Use and Land Cover in Kano Metropolis and its Suburbs

4.2.1 Land use and land cover image classification

A composite of red, green and blue (RGB) was used to produce land use and land cover thematic map of the study area. The thematic map for the study area generated for 2015 (Figure 4.1) showed that agricultural land is the dominant land use type covering about 84.17%, followed by built up (residential) areas which covered 9.91%, river occupied 2.01%, bare surface occupied 1.76%, forest occupied 1.10%, shrub/grass occupied 0.74%, lakes/ponds/stream occupied 0.28% and built up industrial areas and built up commercial areas occupied 0.02% and 0.01% respectively (Table 4.2). This study conforms to the finding of Ayila *et al.* (2014) in their studies "Statistical Analysis of Urban Growth in Kano Metropolis", that reveal that the built environment in Kano State could increase to 21.70%, while this study estimated 9.91% for Kano metropolis and its suburbs could be true.

In 2016, the thematic map generated show only slight changes which could be neglected. Agricultural land dominated about 83.74%, built up (residential) area occupied 10.23%, bare surface 2.01%, River 1.93%, forest 1.07%, shrubs/grasses 0.71, lake/ponds/stream occupied 0.28% and industrial and commercial area occupied 0.02% and 0.01% respectively (Table 4.2). Table 4.2 shows the total proportion coverage for each class and the surface areas in meters square and hectares. Figure 4.2 further indicate that, the study area is mainly dominated by agricultural land which is distributed all over the study area. The core of the area is mostly dominated by built-up areas comprising of residential, industrial and commercial buildings. Forest lies after Tiga river which is located in the southern part (Figure 4.1 and 4.2).

Table 4. 2 Area and proportion coverage of each class

Land use types	Surface area coverage (2015)		Proportion	Surface area coverage (2016)		Proportion
	meters (m^2)	Hectares (ha)	(%)	Meters (m^2)	Hectares (ha)	(%)
Residential	9880	889.7	9.91	10310	929.25	10.23
Industrial	16	1.44	0.02	16	1.44	0.02
Commercial	13	1.17	0.01	15	1.35	0.01
Forest	1094	98.46	1.1	1087	97.83	1.07
Lake/pond/stream	280	25.2	0.28	287	25.83	0.28
River	2004	180.36	2.01	1944	174.96	1.93
Agricultural land	84213	7557.17	84.17	84551	7609.59	83.74
Shrubs/grasses	742	66.68	0.74	718	64.62	0.71
Bare surface	1758	158.22	1.76	2025	182.25	2.01
Total	100000	8978.5	100	100968	9087.12	100

Source: Author's compilation, 2017.

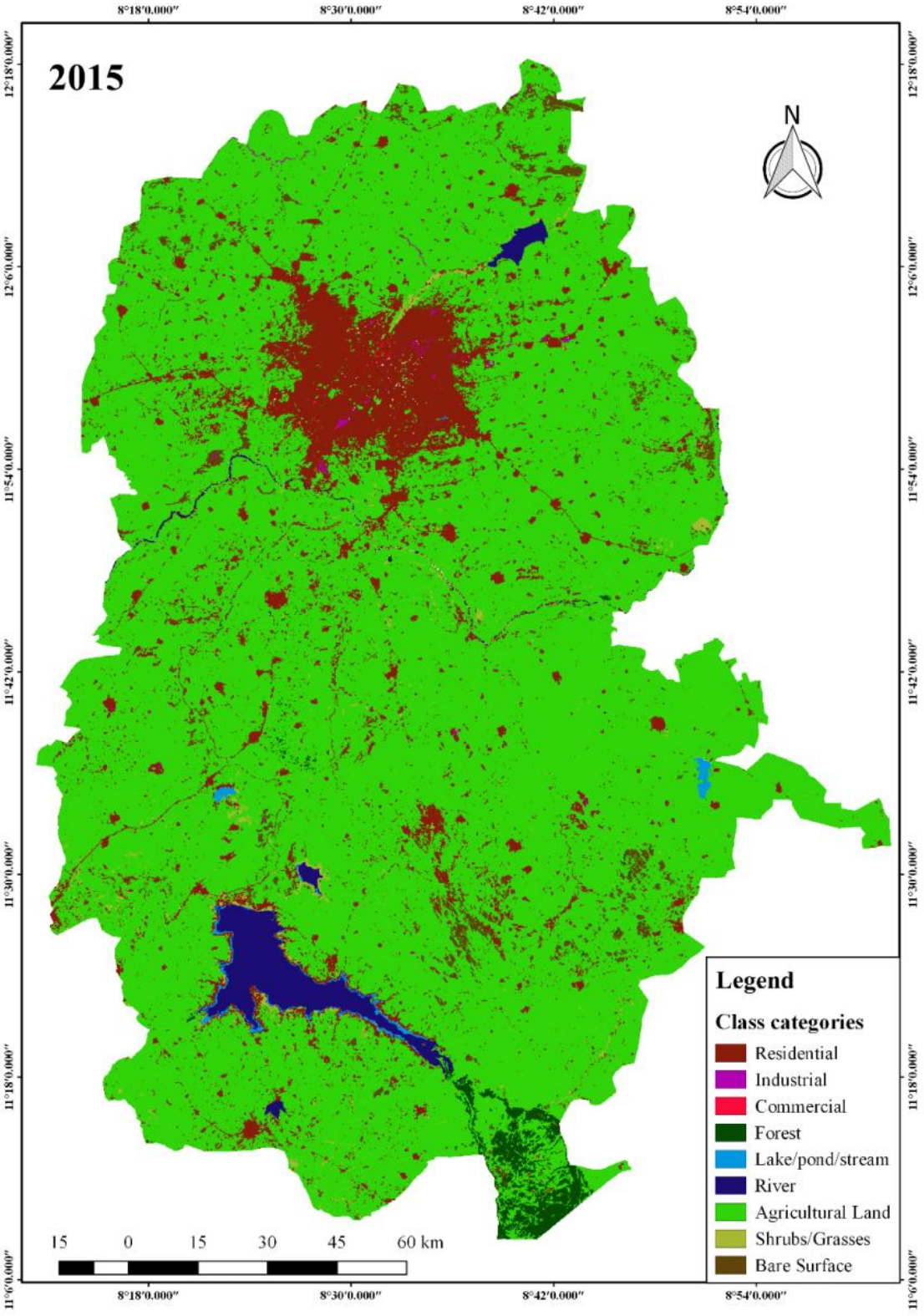

Figure 4. 1 Land Use and Land Cover Map of Kano Metropolis and its Suburb in 2015

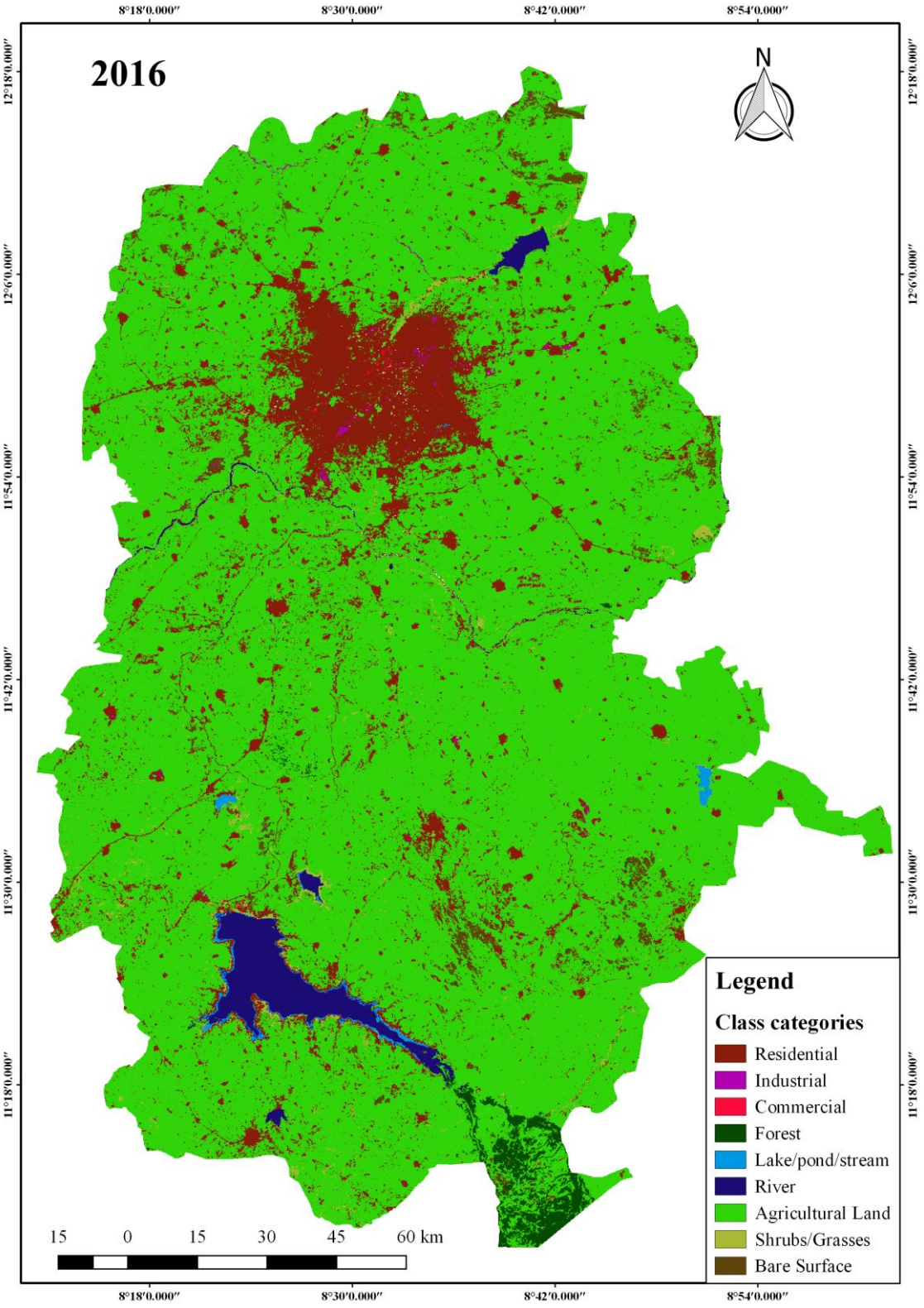

Figure 4. 2 Land Use and Land Cover Map of Kano Metropolis and its Suburb in 2016

The produced LULC maps as shown in Figure 4.1 and 4.2 were used to generate area coverage of each class and to further determine the relationship between each class and LST within the time periods.

4.2.2 Accuracy assessment

Thirty percent of the training data collected from the field was used to validate the accuracy of the classified image and the result obtained is highlighted in Table 4.3 and 4.4. In accordance with the computed error matrix shown in the contingency table, the overall accuracy the 2015 image yielded 0.8462 (Table 4.3). The producer accuracy for built up industrial and commercial areas were low because few sample points were collected for these and this is due to the fact that on the actual ground commercial and industrial areas are few in number in the study area and also because the areas were confused for built up residential. In fact, these areas were observed to be heterogeneous areas with a similar spectral reflectance with built up residential areas and bare surfaces. The areas were highly mixed up with residential and other land use types.

Table 4. 3 Contingency matrix for 2015 image classification

2015		Ground Reference information										
Remote Sensing		BUR.	BUI.	BUC.	FOR.	LPS.	RIV.	AGR.	SG.	BS.	RT	UA
Classification	BUR.	163	4	3	0	0	0	5	4	6	185	0.881
	BUI.	0	5	0	0	0	0	0	0	0	5	1.000
	BUC.	0	0	3	0	0	0	0	0	0	3	1.000
	FOR.	0	0	0	7	0	0	0	0	0	7	1.000
	LPS.	0	0	0	0	10	1	0	0	0	11	0.909
	RIV.	0	0	0	0	0	8	2	0	0	10	0.800
	AGR.	10	0	0	1	1	0	61	10	2	85	0.718
	SG.	0	0	0	0	0	0	0	10	0	10	1.000
	BS.	0	0	0	0	0	0	1	0	8	9	0.889
	CT	173	9	6	8	11	9	69	24	16	**325**	
	PA	0.942	0.556	0.500	0.875	0.909	0.889	0.884	0.417	0.500		
OA = 0.8462												
Pr (c) = 9.849												
Kc = 1.017												

BUR=Built up residential; BUI=Built up industrial; BUC=Built up commercial; FOR=Forest; RIV=River; LPS=Lakes/ponds/stream; AGR=Agricultural land; SG=Shrubs/Grasses; BS=Bare surface; RT=Row total; PA= Producers' accuracy; CT= Column Total; UA= User accuracy; OA=Overall accuracy, Pr (c)= Probability of chance; Kc= Kappa coefficient.

Source: Author's compilation, 2017.

Table 4. 4 Contingency matrix for 2016 image classification

2016		Ground Reference information										
Remote Sensing Classification		BUR.	BUI.	BUC.	FOR.	LPS	RIV.	AL.	SG.	BS.	RT	PA
	BUR.	163	2	6	0	0	0	9	6	3	189	0.862
	BUI.	0	6	0	0	0	0	0	0	1	7	0.857
	BUC.	0	0	5	0	0	0	0	0	1	6	0.833
	FOR.	0	0	0	6	0	0	0	0	0	6	1.000
	LPS.	0	0	0	0	9	0	0	0	0	9	1.000
	RIV.	0	0	0	0	1	11	0	0	0	12	0.917
	AGR.	6	0	0	1	2	1	61	3	2	76	0.803
	SG.	0	0	0	0	0	0	0	7	1	8	0.875
	BS.	1	0	0	0	0	0	1	1	9	12	0.750
	CT	170	8	11	7	12	12	71	17	17	325	
	UA	0.959	0.750	0.456	0.857	0.750	0.917	0.859	0.412	0.529		
OA = 0.852												
Pr (c) = 5.743												
Kc = 1.031												

BUR=Built up residential; BUI=Built up industrial; BUC=Built up commercial; FOR=Forest; RIV=River; LPS=Lakes/ponds/stream; AGR=Agricultural land; SG=Shrubs/Grasses; BS=Bare surface; RT=Row total; PA= Producers' accuracy; CT= Column Total; UA= User accuracy; OA=Overall accuracy, Pr (c)= Probability of chance; Kc= Kappa coefficient

Source: Author's compilation, 2017.

The producer accuracy for shrubs/grasses and bare surface were recorded to be low due to the confusion between the two land cover types. The percentage coverage for most shrubs/grass areas were low and mostly dried up in dry season. And during the wet season bare surface are covered with natural vegetation for example on mountains and hills. This result is in agreement with past research which have concluded that the observed increase is attributed to the application of sets of data acquired at different time steps (Solberg *et al*., 1994; McNairn *et al.,* 2009; Forkuor *et al.,* 2014; Forkuor *et al.,* 2015; Hütt *et al.,* 2016). Specifically, in accordance to Forkuor *et al.* (2015), in their study titled "Evaluating the sequential masking classification approach for improving crop discrimination in the Sudanian Savanna of West Africa" overall accuracy of 85% and above is good for LULC image classification.

The contingency table (Table 4.4) indicates 0.852 of overall accuracy for 2016 image. Based on this, the kappa coefficient for this study showed a 1.017 and 1.031 value for 2015 and 2016 respectively. In agreement to Batisani and Yarnal, (2008), there is a strong agreement between the classification with the ground reference data. On this ground, the accuracy derived from the thematic map is within the satisfactory range when compared to the ground truth points, with 84.62% and 85.20% accuracy recorded.

4.3 Generation of Land Cover Indices

The result of Table 3.3 shows that a total of three land cover indices were extracted using various bands of the OLI/TIRS image for 2015 and 2016. The NDVI, NDBI and MNDWI estimated were used to understand the relationship between LST and different land cover classes.

4.3.1 Extraction of the normalised difference vegetation index (NDVI)

The result of Figure 4.3a and 4.4a depicts the NDVI values for dry periods in the study area which range from 0.270 to 0.690 and 0.361 to 0.791 for 2015 and 2016 respectively. For wet periods NDVI values range from -0.310 to 0.849 and 0.035 to 0.954 for 2015 and 2016 respectively (Figure 4.3b and 4.4b). This results agrees with other findings by (Sims and Gamon, 2002; Mfondoum *et al*.; Adeyeri *et al.,* 2017) that, the negative and near negative values, observed were during the wet season and high positive values observed indicate that there is increase in both man-made and natural vegetation such as shrubs/grasses and agricultural lands.

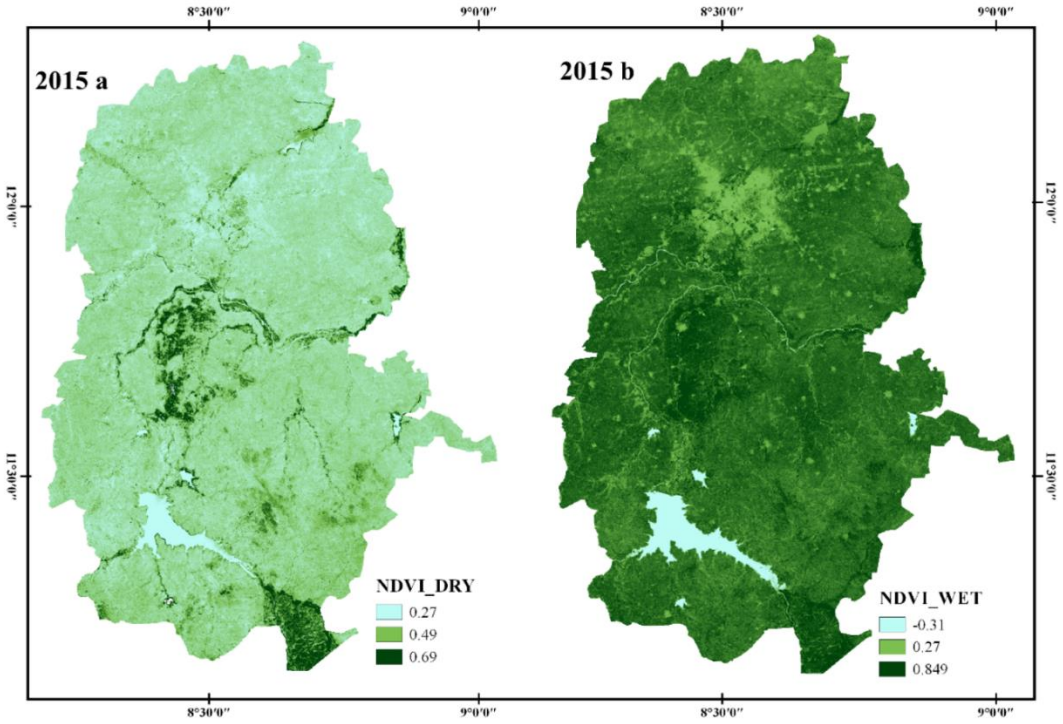

Figure 4. 3 Normalised difference vegetation index map for 2015 (a and b)

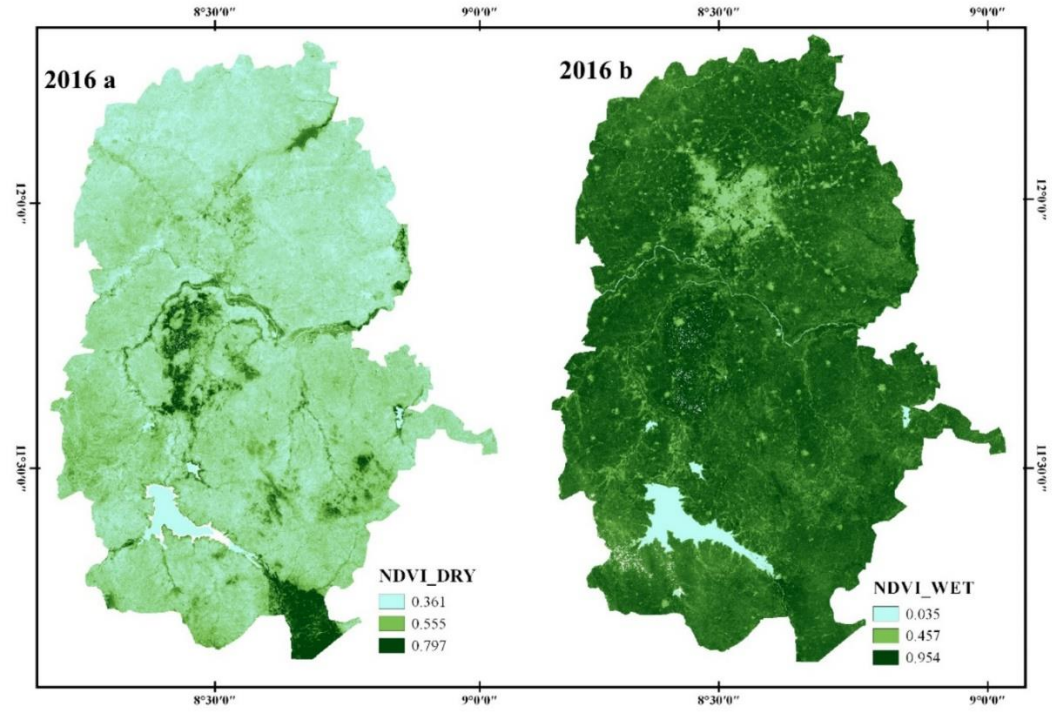

Figure 4. 4 Normalised difference vegetation index map for 2016 (a and b)

The time series analysis shown in Figure 4.5 and 4.6 shows how NDVI changes in different seasons and periods. There is a consistent variation in the NDVI of the various maps in 2015 and 2016 and it is noticed that during dry season NDVI value is low except in the southern part where the forest is located and the middle western area where there is an irrigation fed agricultural land which is observed from fieldwork to be cultivated all through the year.

In wet periods, NDVI values were recorded to be high because of increase in vegetal cover. A noteworthy example is in the early days of both year (D017, D020) which is most likely to be the beginning of dry period when the study area is less vegetated and thus low NDVI values are recorded and late days of both year (D289, D260) which is the end of wet period when the study area is fully vegetated and thus have a higher value of NDVI. From Figure 4.5, the trend of increase in NDVI value is increasing from D001 to D161 which is noted to be from January to early days in June which in the study area is known to be dry periods with little or no vegetal cover in the environment.

NDVI records high value from D289 to D305 which are wet periods when the environment is highly vegetated with both natural and agricultural vegetation. Low NDVI value was recorded at D353 and this could be attributed to the fact that at this period agricultural vegetation and cultivation have being removed, thus leaving most of the environment bared and this means there will be little or no vegetation cover. This explains that NDVI values are not constant, it varies with time, period and the season it was examined. This result could help in making adequate decisions.

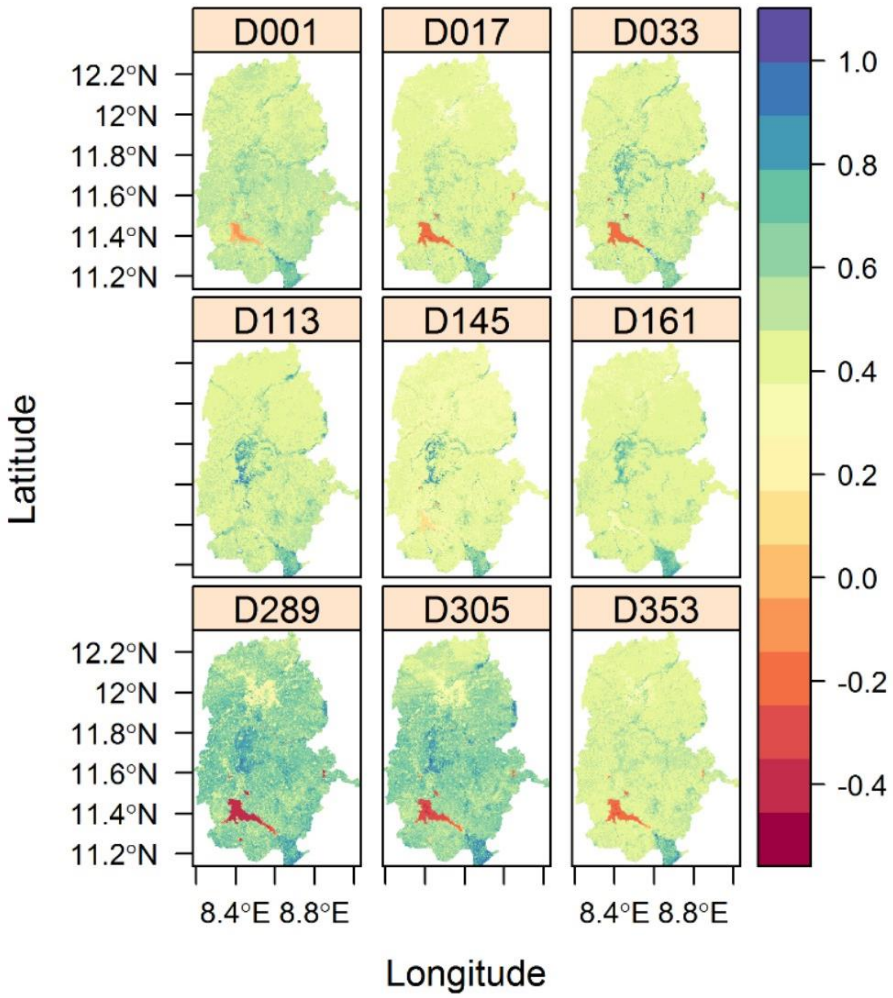

Figure 4. 5 Time series analysis of NDVI for 2015 images

The variation in NDV values recorded in Figure 4.5 is similar to the values recorded in Figure 4.6. NDVI shows low values from the first five months (January to May) and start increasing from the end of July up to September when the environment becomes vegetated. There is a decrease recorded in the value at the end of the year which is towards November to December as shown in the figure below.

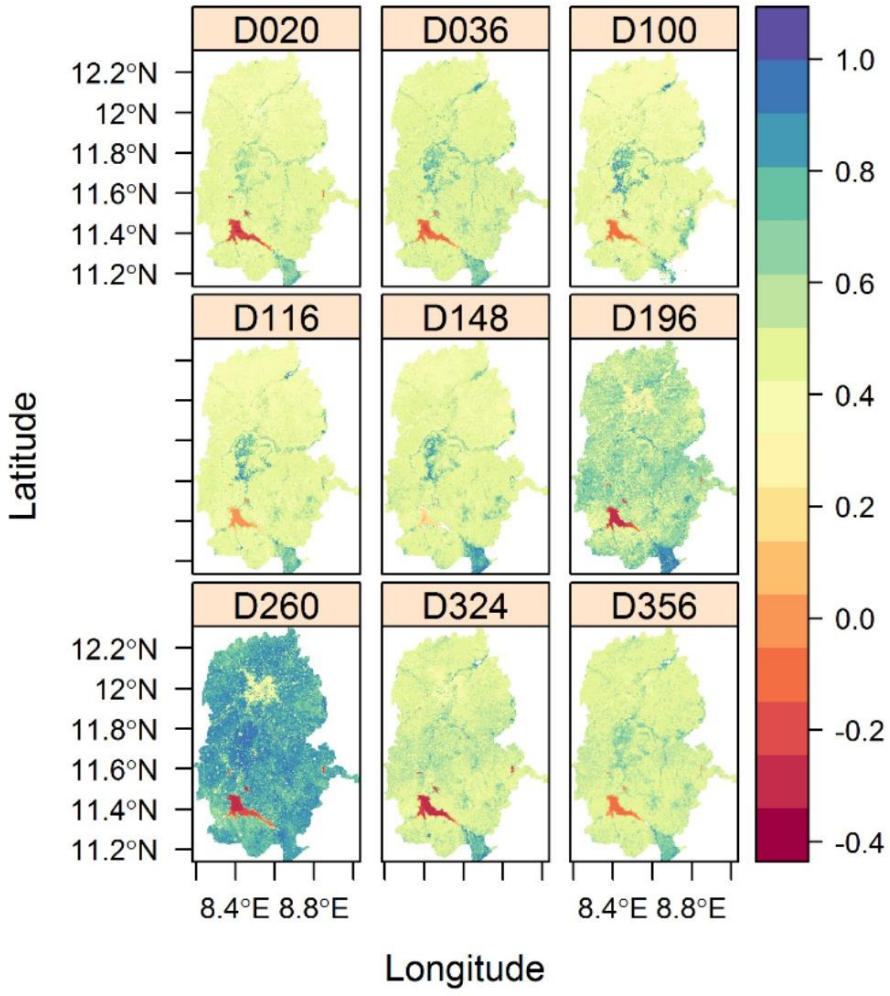

Figure 4. 6 Time series analysis of NDVI for 2016 images

4.3.2 Extraction of the normalised difference built-up index (NDBI)

The estimated NDBI values as shown in Figure 4.7a and 4.8a for dry periods range from -0.177 to 0.150 and -0.279 to 0.134 for 2015 and 2016 respectively and during wet periods NDBI value range between -0.319 to 0.0596 and -0.475 to -0.036 in 2015 and 2016 respectively (Figure 4.7b and 4.8b).

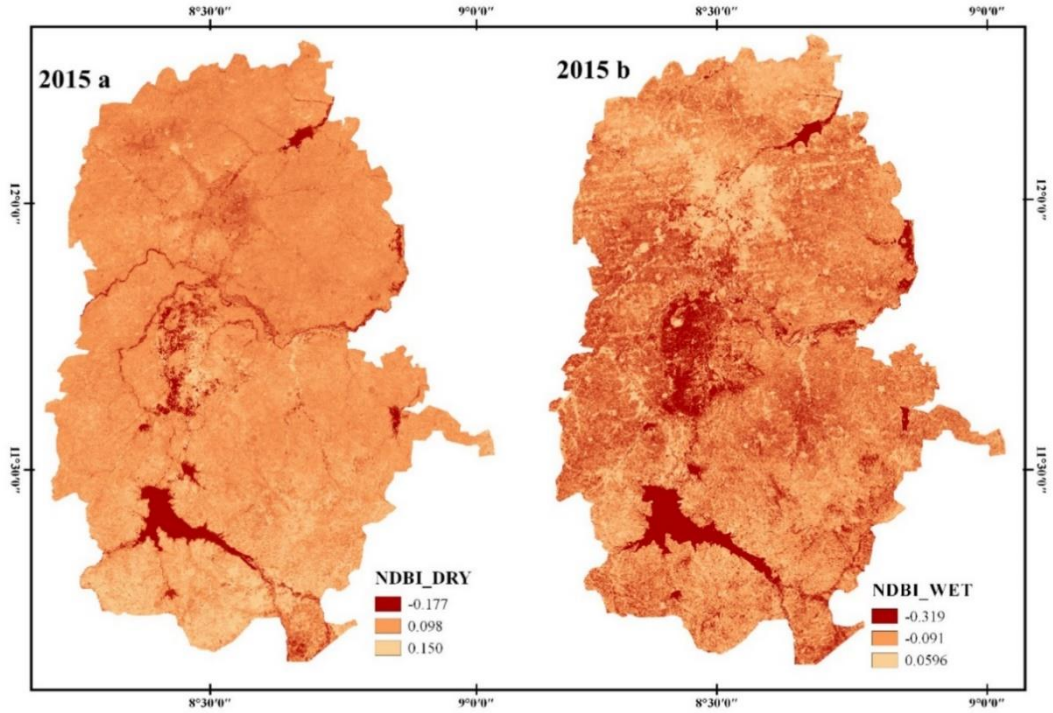

Figure 4.7 Normalised difference built up index map for 2015 (a and b)

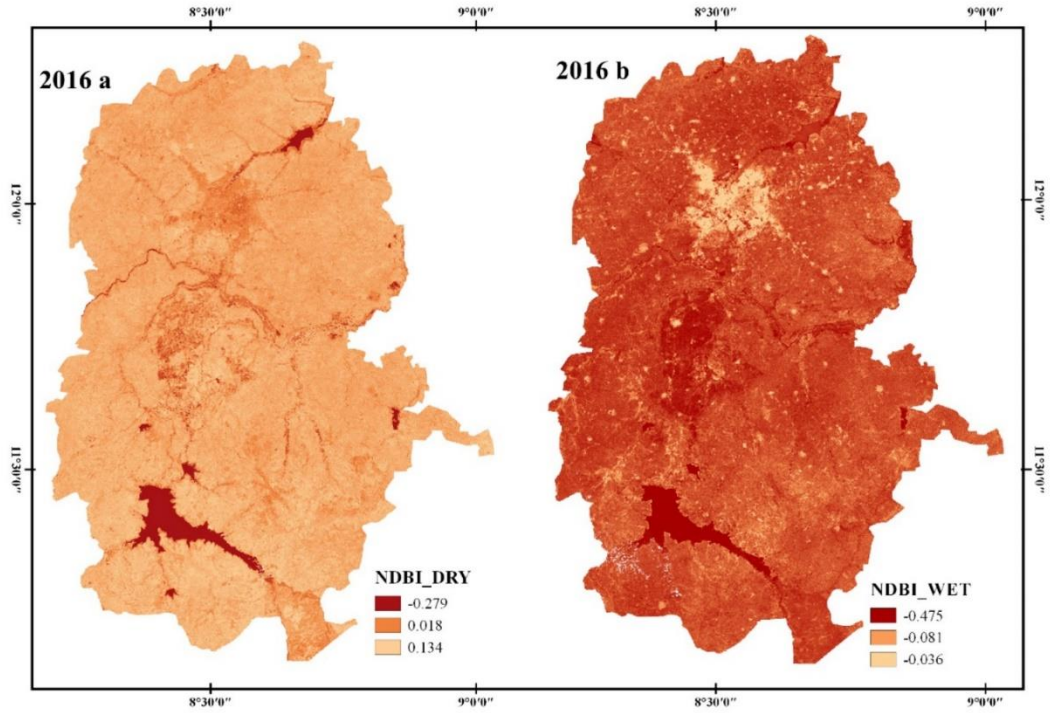

Figure 4. 8 Normalised difference built up index map for 2016 (a and b)

The NDBI estimated for both years indicate a very high negative values for wet periods and a very low value for dry periods. This means the pixel record areas with almost no vegetation. Figure 4.9 and 4.10 below indicate that for both years, during the dry season NDBI has an index value of between 0.1 to 0.2, which covers almost all the environment except for water which indicate otherwise and this is dues to the fact that bare surface and built up have similar reflectance. This is somewhat different in wet seasons where the whole environment is vegetated and thus the NDBI is clearly differentiated as seen in day 289 (D289) and 260 (D260) in 2015 and 2016 respectively.

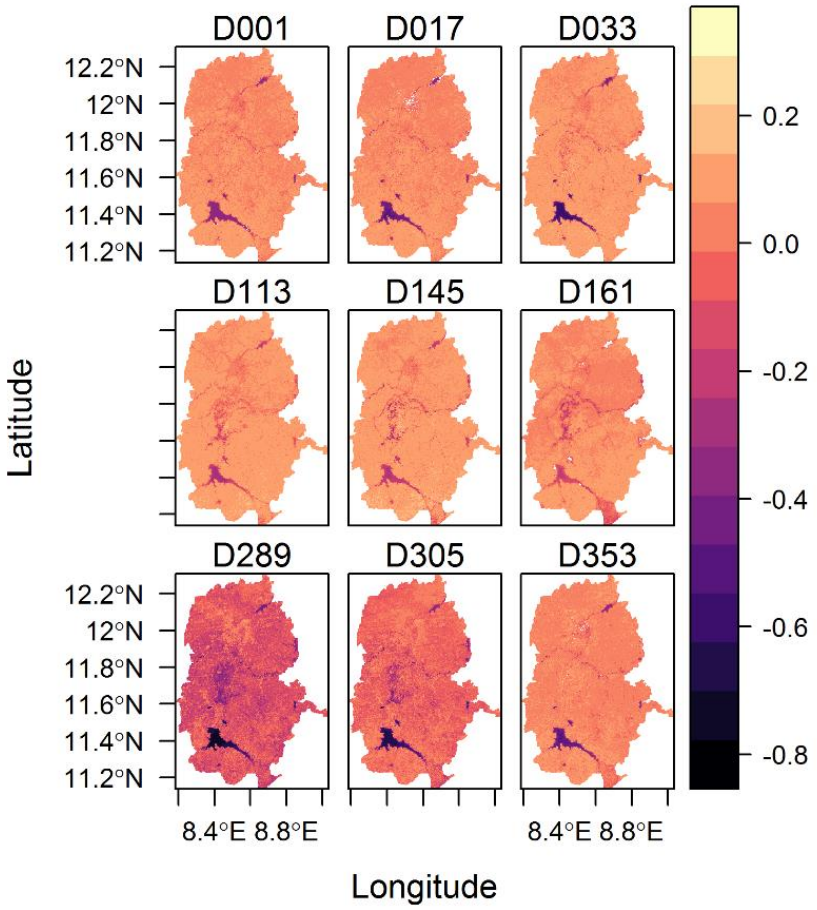

Figure 4. 9 Time series analysis for 2015 NDBI images

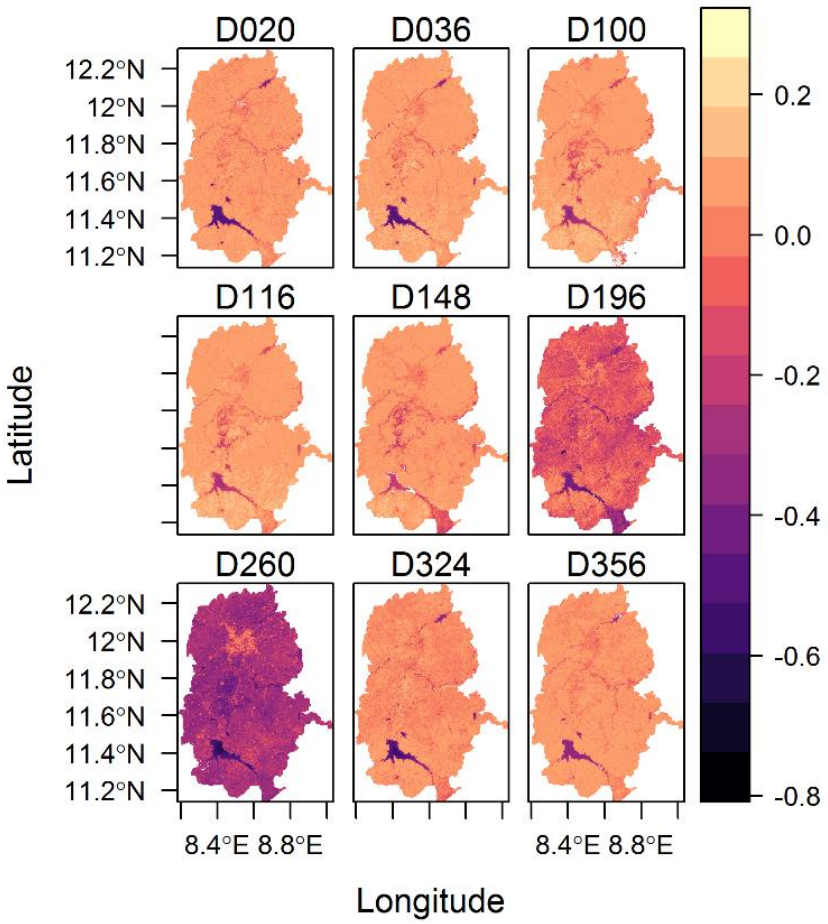

Figure 4. 10 Time series analysis for 2016 NDBI images

4.3.3 Extraction of the modified normalised difference water index

MNDWI value estimated for dry period range from -0.780 to 0.193 and -0.769 to -0.0041 for 2015 and 2016 respectively (Figure 4.11a and 4.12a). In wet periods, MNDWI value ranges from -0.756-0.671 and -0.877 to 0.369 in 2015 and 2016 respectively (Figure 4.11b and 4.12b). This means that very low negative values indicate pixels of water bodies.

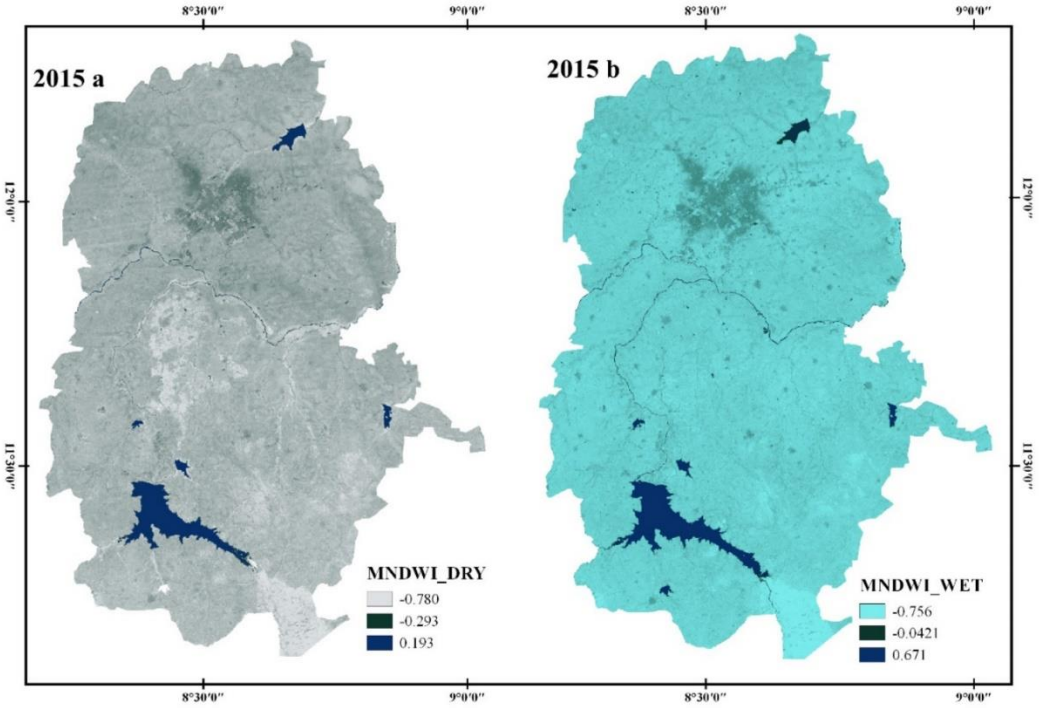

Figure 4. 11 2015 Modified normalised difference water index map (a and b)

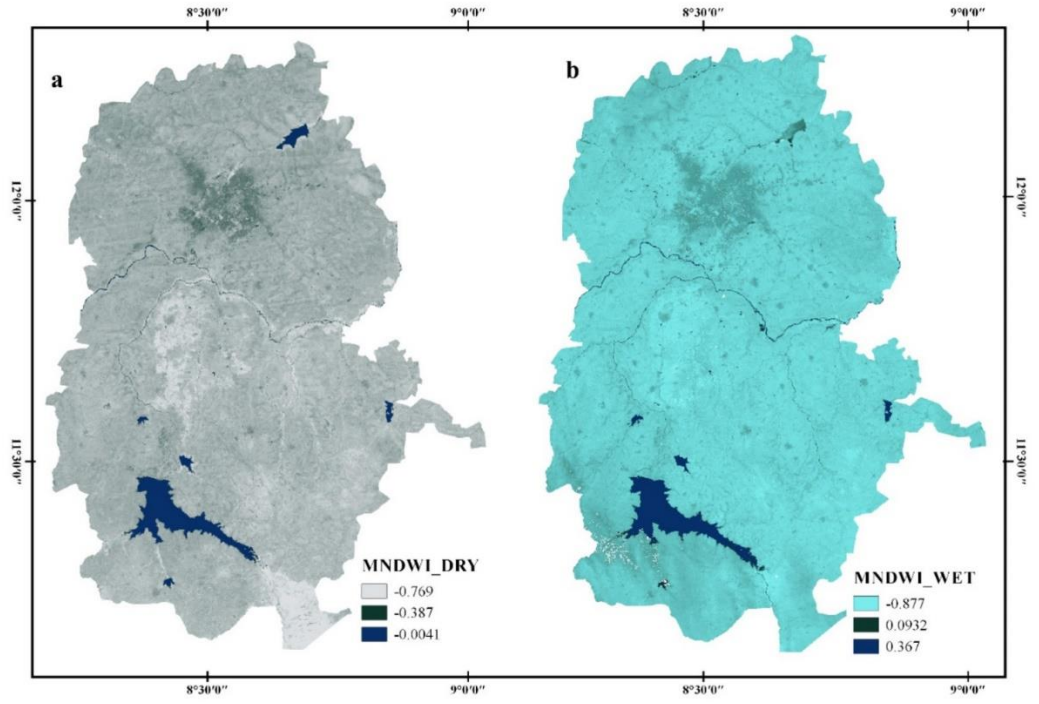

Figure 4. 12 2016 Modified normalised difference water index map (a and b).

The time series analysis for MNDWI shows only slight changes in the different periods analysed. The difference is seen slightly on lakes, ponds and stream where the water bodies have reduced in quantity and also have mixed up with the soil content thus MNDWI index values of -0.5 as shown in Figure 4.13 and 4.14.

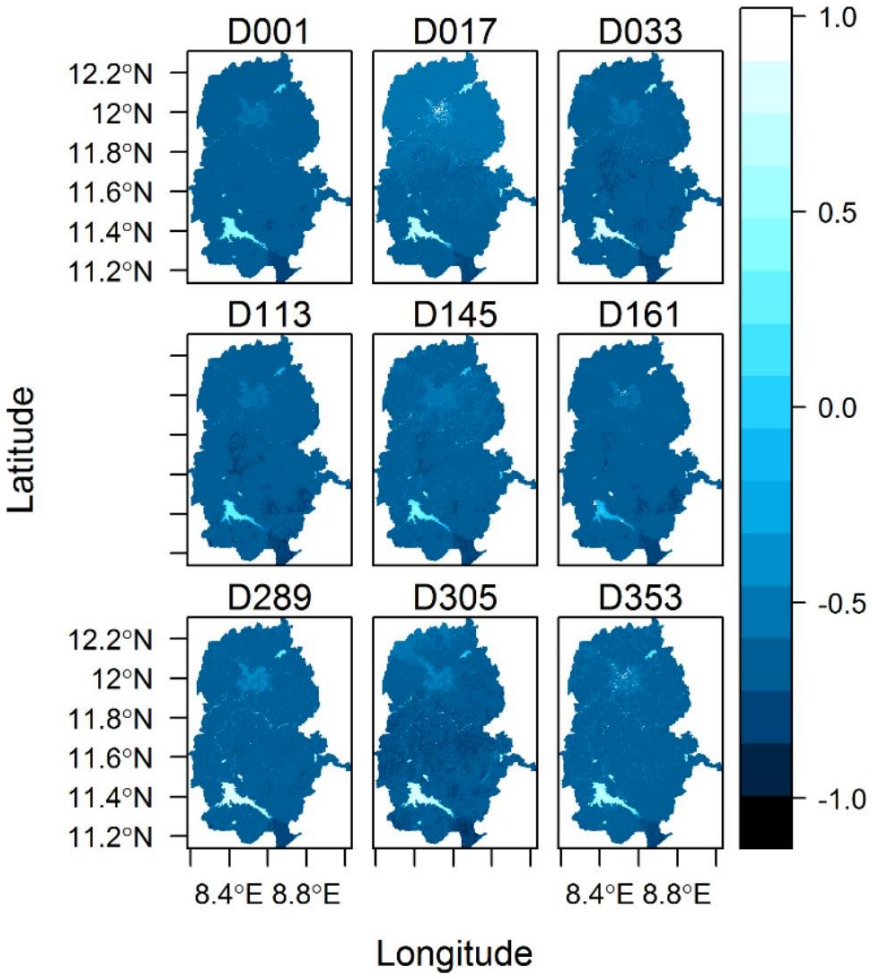

Figure 4. 13 Time series analysis of MNDWI map for 2015

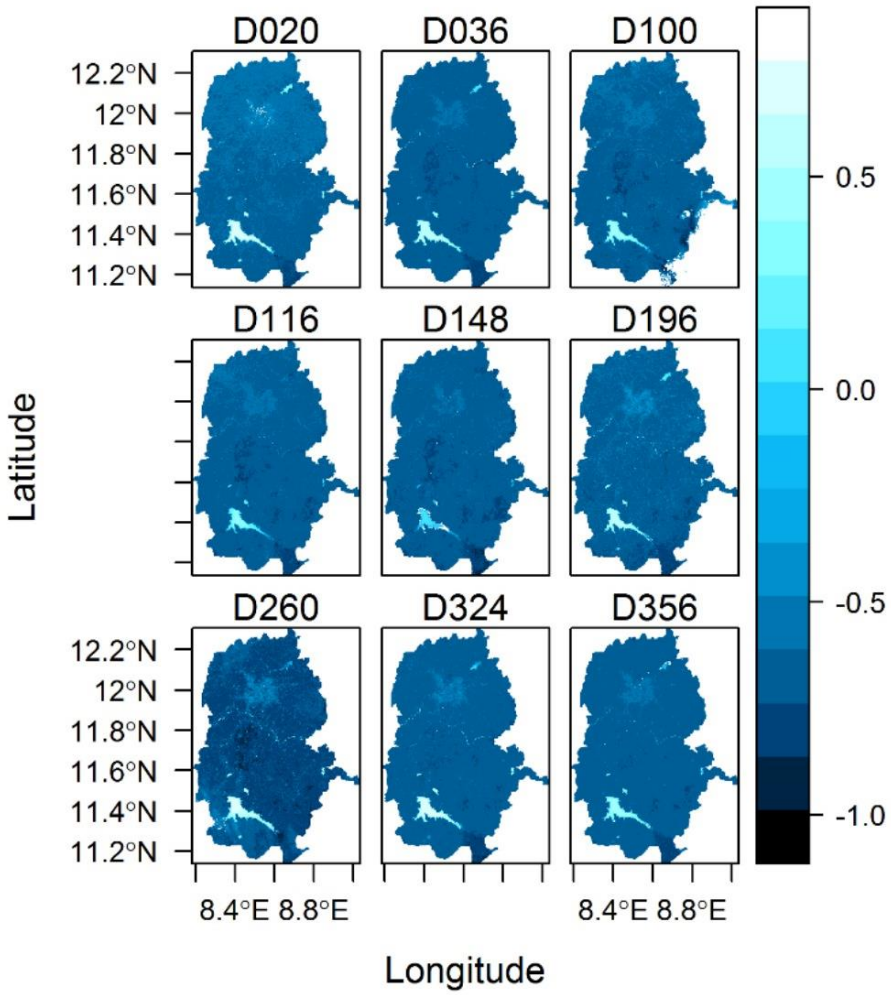

Figure 4. 14 Time series analysis of MNDWI map for 2016

4.4 Analysis of Retrieved Land Surface Temperature

Previous study carried out in Abuja revealed that, there is a wide variation between result obtained from the minimum and mean air temperature with land surface temperature (Mahmoud, 2016), hence this study concentrated on estimating the continuous LST of the study area using several Landsat imageries. Figure 4.15 and 4.16 show the retrieved LST maps and these maps reveals varying intensity of LST over the study area on the various seasons.

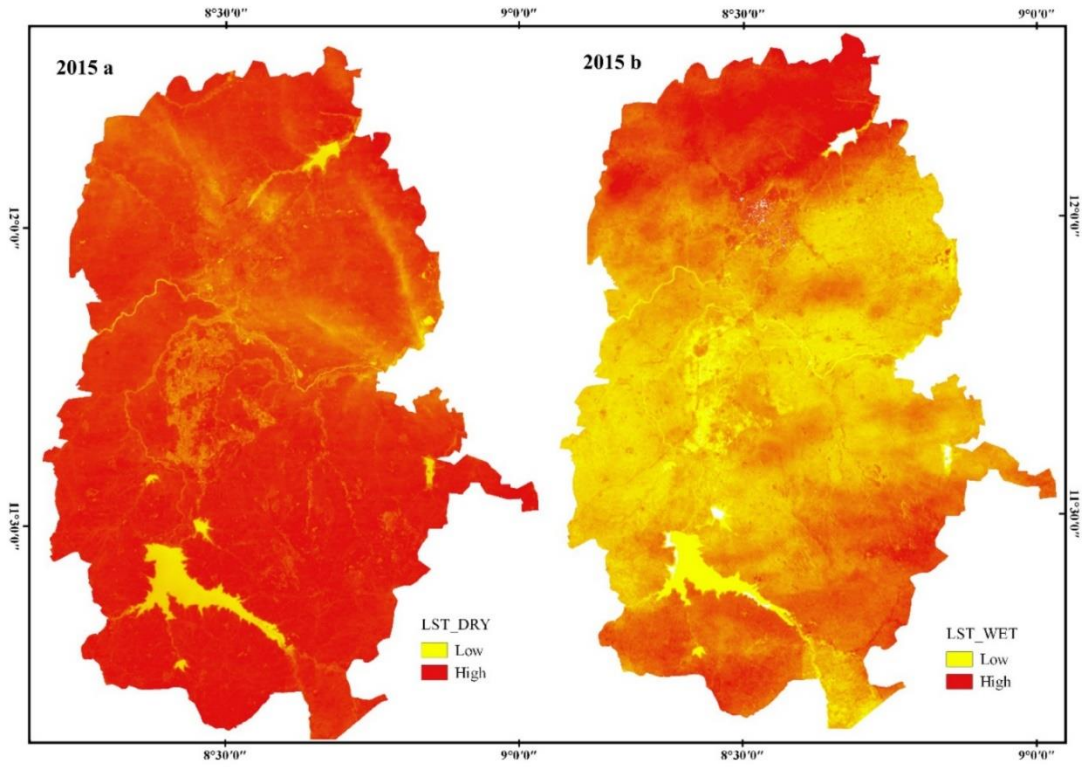

Figure 4. 15 Retrieved LST maps (a and b) for dry and wet season in 2015

In 2015, LST in dry periods as shown in Figure 4.15a reveals a high land surface temperature which is clearly seen in the core of the study area that consist of built ups such as residential, commercial and industrial areas. The surroundings, which are mainly bare surfaces also recorded a high surface temperature except for areas that are observed to be irrigated farmlands and water bodies which showed low land surface temperature record. During wet seasons Figure 4.15b reveals a low surface temperature around the suburbs of the study area and high surface temperature at the northern areas of the study area and this could be as a result of presence of bare surfaces such as hills. The core of the study area in this period also record moderate to low surface temperature and this could be attributed to the fact that natural vegetation cover within the core plays a vital role in regulating the temperature of the core.

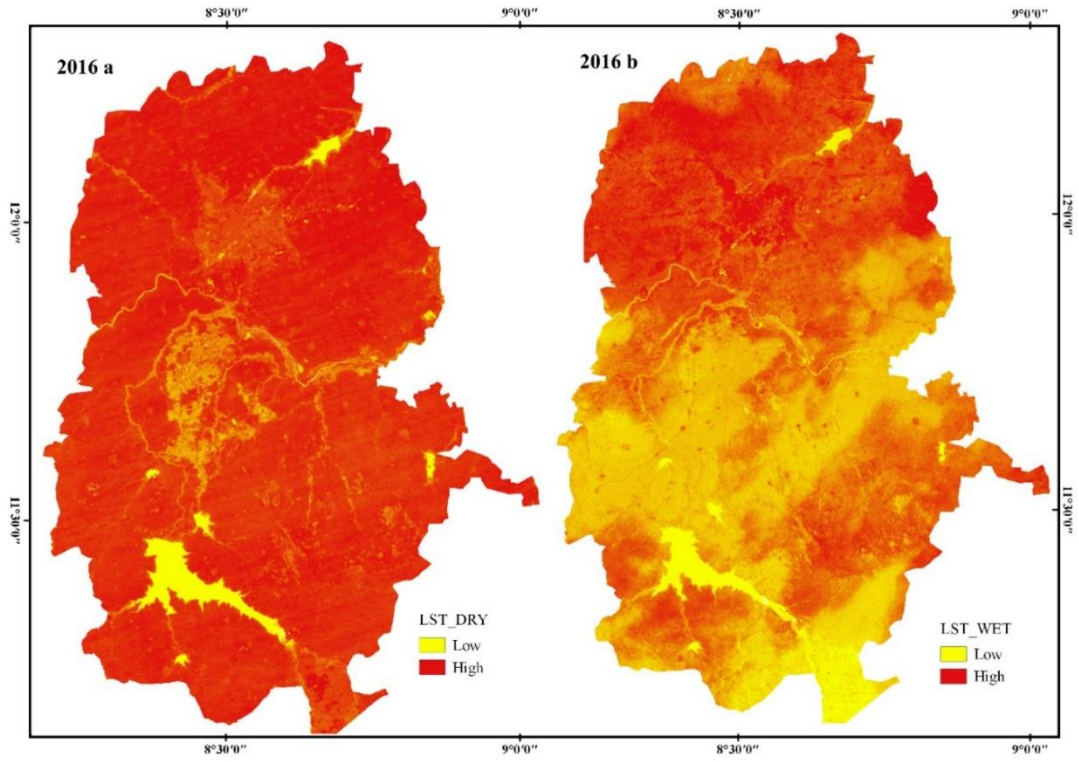

Figure 4. 16 Retrieved LST maps (a and b) for dry and wet season in 2016

Figure 16a shows a similar record for LST during dry season. The core of the study area indicates a very high surface temperature as compared to other area like the suburbs which record a low surface temperature. It is also seen from the figure that water bodies such as lakes, ponds, rivers and streams reveals a low surface temperature. Likewise, the suburbs that are irrigated almost all through the year, they show low LST in the study. Surprisingly, forest areas recorded a high temperature during dry season. In wet periods for 2016, Figure 4.16b revealed a low temperature mostly around the suburbs and this could be as a result of increase in both natural and agricultural vegetation cover in this period. Forest in this period showed low surface temperature due to increase in vegetation, foliage and tree cover. The derived LST can be used to further analyse it relationship with LULC classes and various land cover indices. Areas with high LST indicate areas with either little or no vegetal cover and these areas are mostly residential, industrial,

commercial and bare surface areas. The core of the study area is known to be characterised with built up materials like tarred roads, buildings and high population hence, more pressure is on land resources (Figure 4.15 and 4.16). This may be the reason why such areas have higher land surface temperature when compared to other areas like in the southern part known to be characterised with less buildings, untarred roads, less population and more vegetal cover.

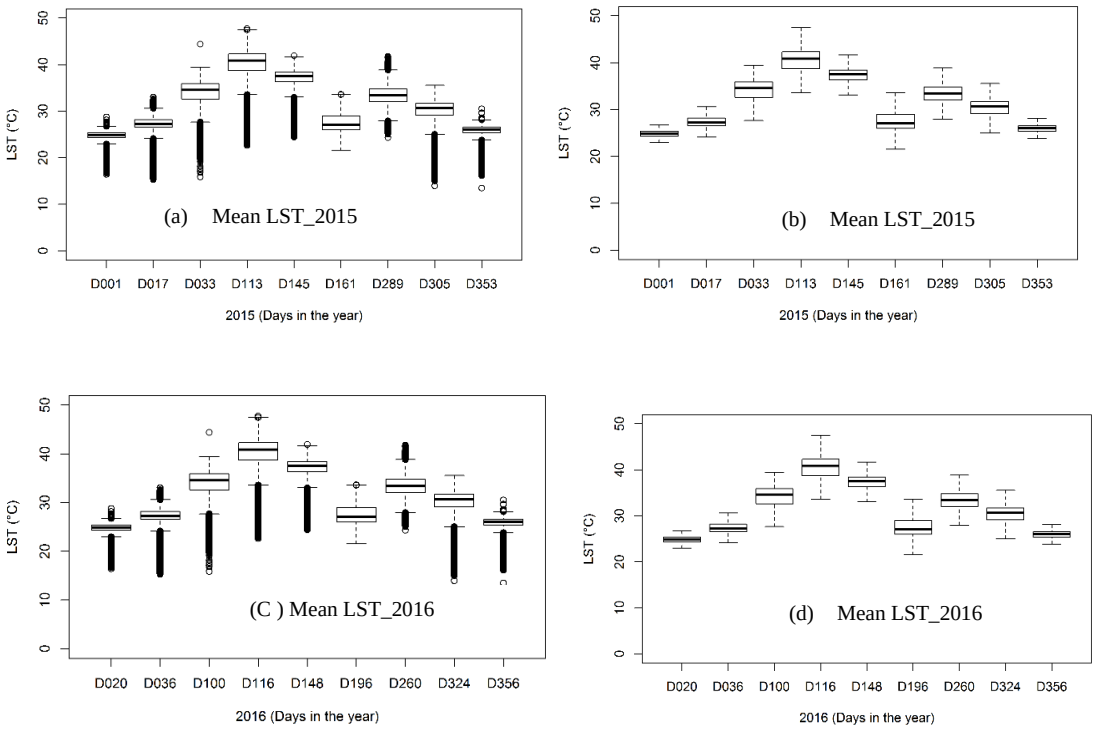

Figure 4. 17 Check for normality and removal of outliers of land surface temperature.

Figure 4.17 describe the mean land surface temperature of the study area for the two years under study. The boxplots further indicate an exploratory analysis of the mean land surface temperature in the study area and the removal of outliers. LST could be as high as 38^{o}C to 40^{o}C in hot seasons and as low as 22^{o}C to 25^{o}C in wet seasons.

Visual display of the time series analysis of LST in 2015 and 2016 (Figure 4.18 and 4.19) reveals how LST intensity varies from one period to the other. During harmattan period which in the study area is known to be from December to February and from this analysis falls between D353 to D033, LST was retrieved to be low in this period.

Figure 4.18 indicates that in this period LST record is between 20-25^{o}C. LST begins to increase from the D113 to D145 with surface temperature of about 35-45^{o}C when the environment is hot, brightness of the sun is intense, surfaces absorb more heat and when there is no vegetation cover. The study area in this period could be uncomfortable and unbearable because of high LST especially at the core due to the presence of buildings, asphalts and other materials that absorb and retain more heat. Surface temperature is shown in figure 4.18 to decrease again from D161 to D305 during the raining season when the environment is covered with vegetation which helps to regulate LST.

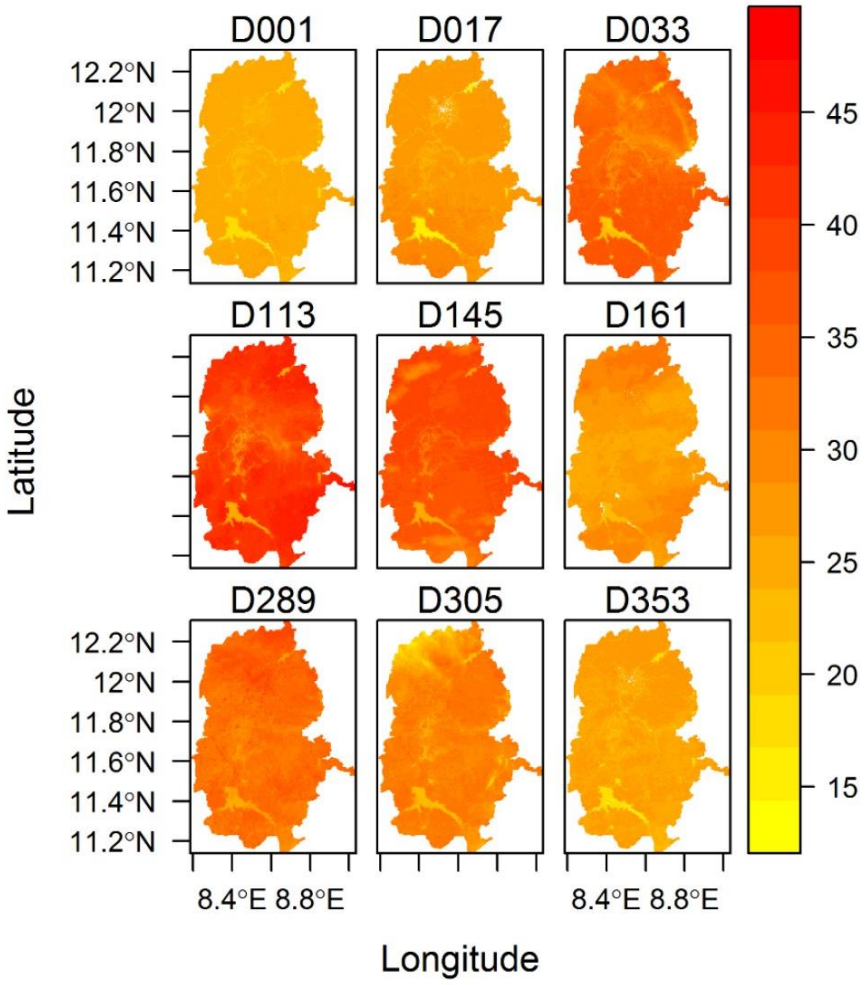

Figure 4.18 Time series analysis of land surface temperature for 2015

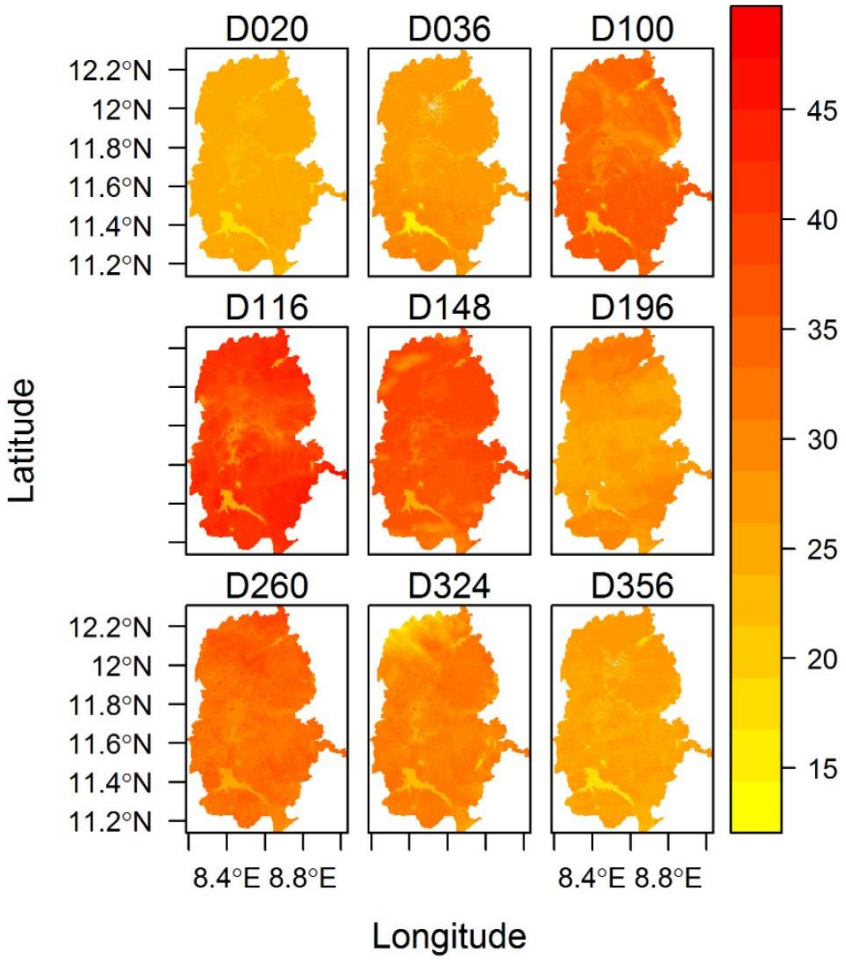

Figure 4. 19 Time series analysis of land surface temperature for 2016 images

In 2016, Figure 4.19 shows a similar trend of variation in LST. Low LST is retrieved from December to February which is also harmattan period in the study area. There is an increase in LST recorded during dry seasons from D100 to D148, which is from April to June when there is no rain and a moderate surface temperature of between 25 to 30^{o}C in wet season.

This can be better explained when two close dates of same periods in the two years under study are analysed. D017 and D020 for dry periods (Figure 4.18), LST image for 017 and 020 and D289 and D260 for end of wet periods (Figure 4.19), image for day 289 and 260,

the LST maps reveals that there is high LST recorded in dry periods and low LST in wet season in both years. This implies that LST consistently varies in different seasons of both years and varies slightly between the two years. Hence, the effect of season and time of the year are very important factors to be considered in determining the LST of the area.

4.5 Land Surface Temperature and Land Use and Land Cover

A simple descriptive analysis was used to describe LST and the different LULC types used in this study. From the descriptive and visual presentation carried out in Figure 4.20 (a-i) and Figure 4.21 (a-i) it is evident from this study that LST is dynamic on different LULC classes and a constant trend analysis of surface temperature and LULC classes in different time step is observed. The variation of LST on various LULC category is obvious.

From Figure 4.20a-d, the dynamic nature of LST retrieved is described for residential, industrial, commercial and forest land cover. The boxplot for residential, industrial and commercial land use shows a similar trend for built up environment. Figure 4.20a-d further reveals that, even within the same land use type LST is not the same all through the year, it varies in different time, periods and seasons. The peak at which LST is recorded to be high in the plots is D113 which period with very high temperature and no vegetation cover and it is lowest at D353 during harmattan. Forest land cover reveals almost the same trend of change in LST and it indicates a low LST generally when compared to the built up areas.

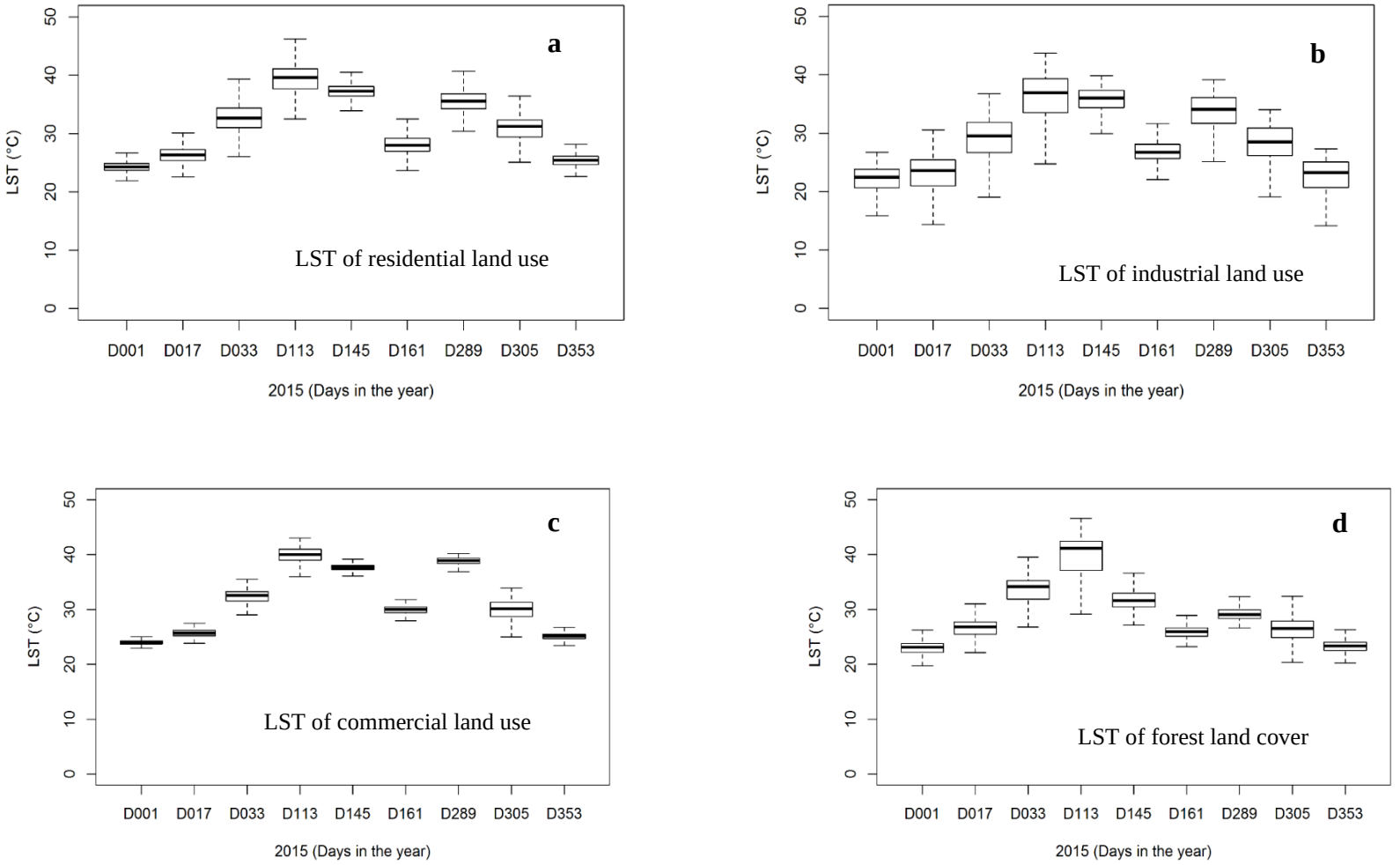

Figure 4.20a-d Descriptive analysis of land surface temperature of different land use and land cover types for 2015 images

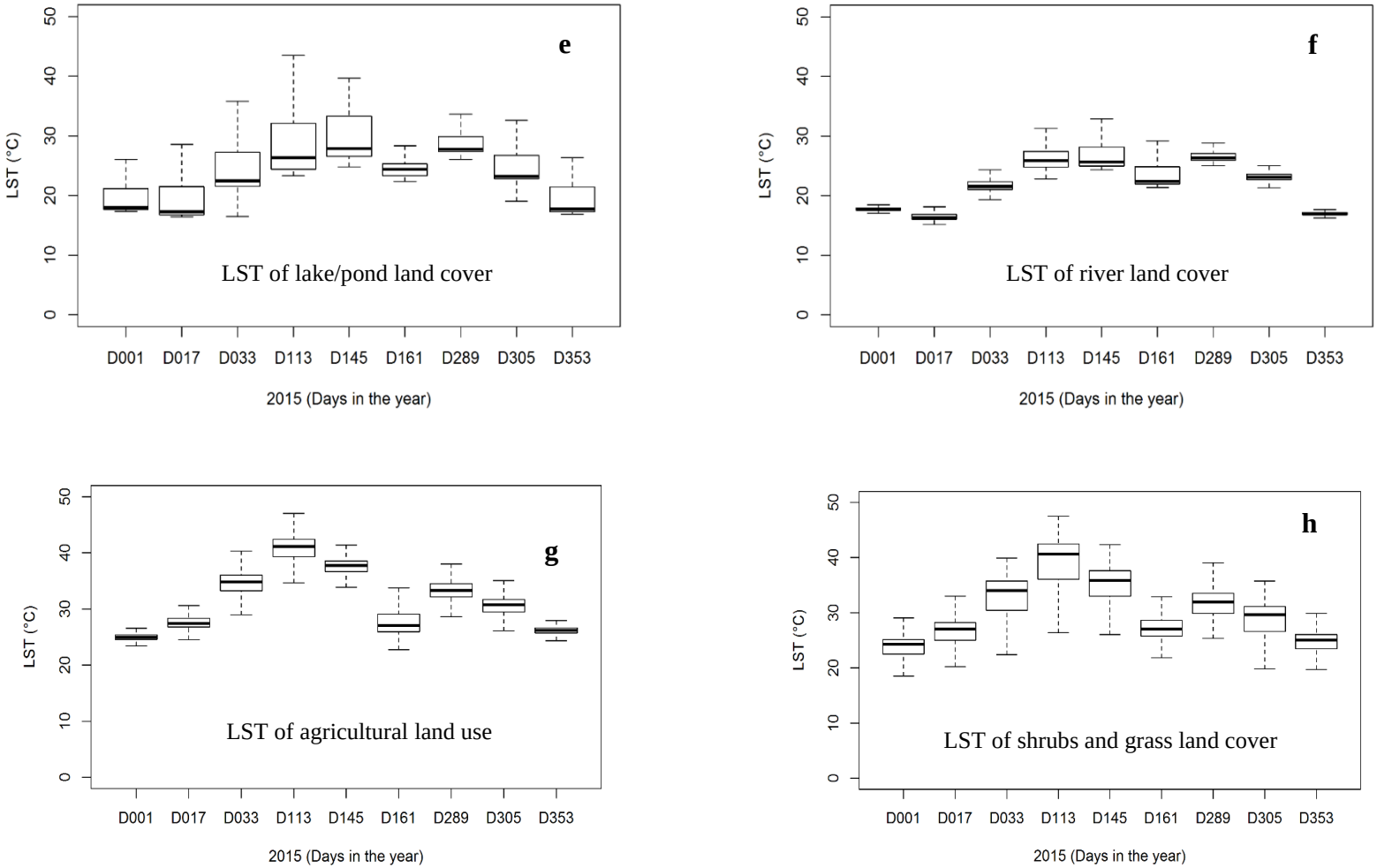

Figure 4.20e-h Descriptive analysis of land surface temperature of different land use and land cover types for 2015 images.

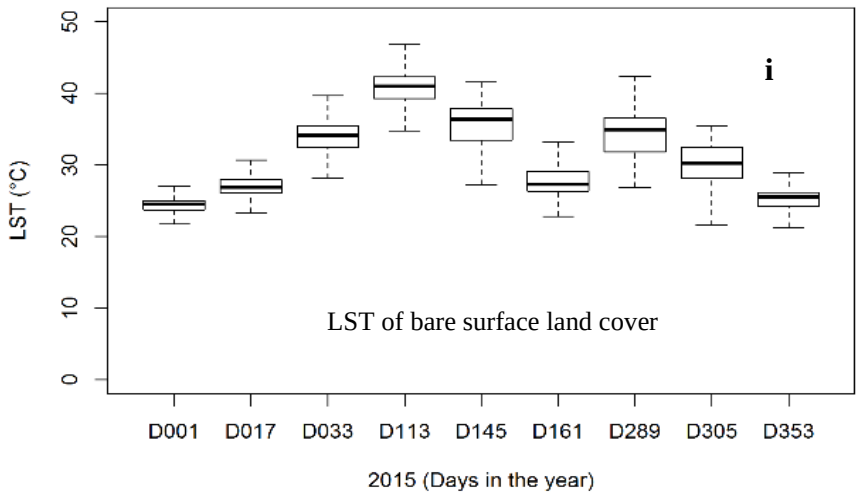

Figure 4. 20(i) Descriptive analysis of land surface temperature of different land use and land cover types for 2015 images.

Figure 4.20e-h and figure 4.20(i) also describe LST of different LULC types in 2015. In Figure 4.20e-h, water bodies such as lakes, ponds, streams and river shows low LST could be recorded all through the year when compared to build up areas, agricultural lands and bare surfaces. The highest LST recorded was 25^{o}C in D145 for all water bodies and the lowest in D353 and in this period LST over water bodies could be as low as 14-15^{o}C. Agricultural and shrubs/grasses shows a different trend of LST when compared to water bodies and forest. During wet season LST records for this LULC are low when there is enough vegetation cover and high when there is little or no vegetation cover. Bare surface shows a very high temperature in D113 when the environment is bared with no vegetation.

Each class show variation in LST in different time and season of the year. For example, in 2015, for each LULC class, from day one (D001) temperature begins to increase until day 161 (D161)

when it decreases. D161 is around June the beginning of rain in the study area, thus surface temperature could be low for each class and LST begins to decreases for each class up till December (D353).

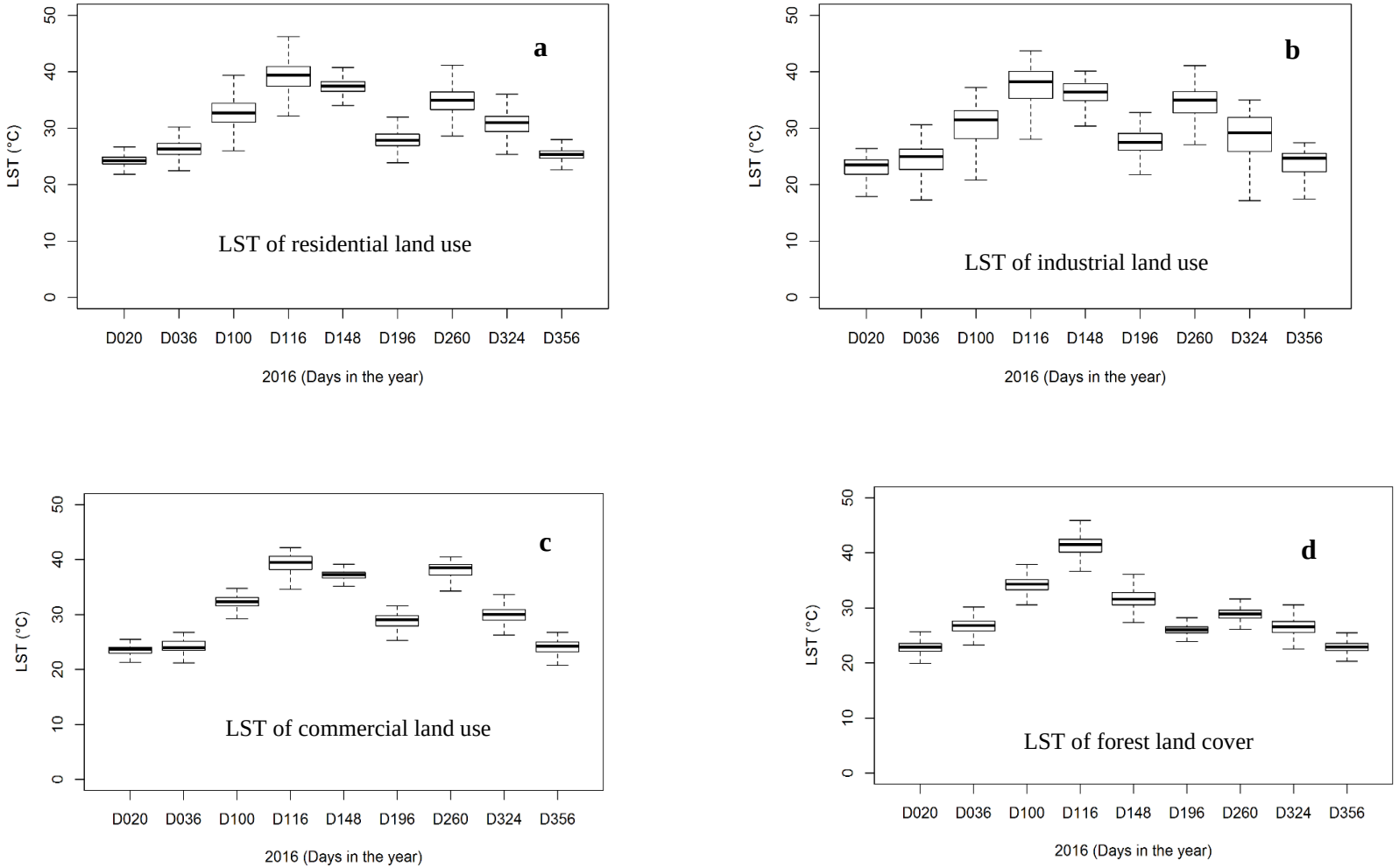

Figure 4.21a-d Descriptive analysis of land surface temperature of different land use and land cover types for 2016 images.

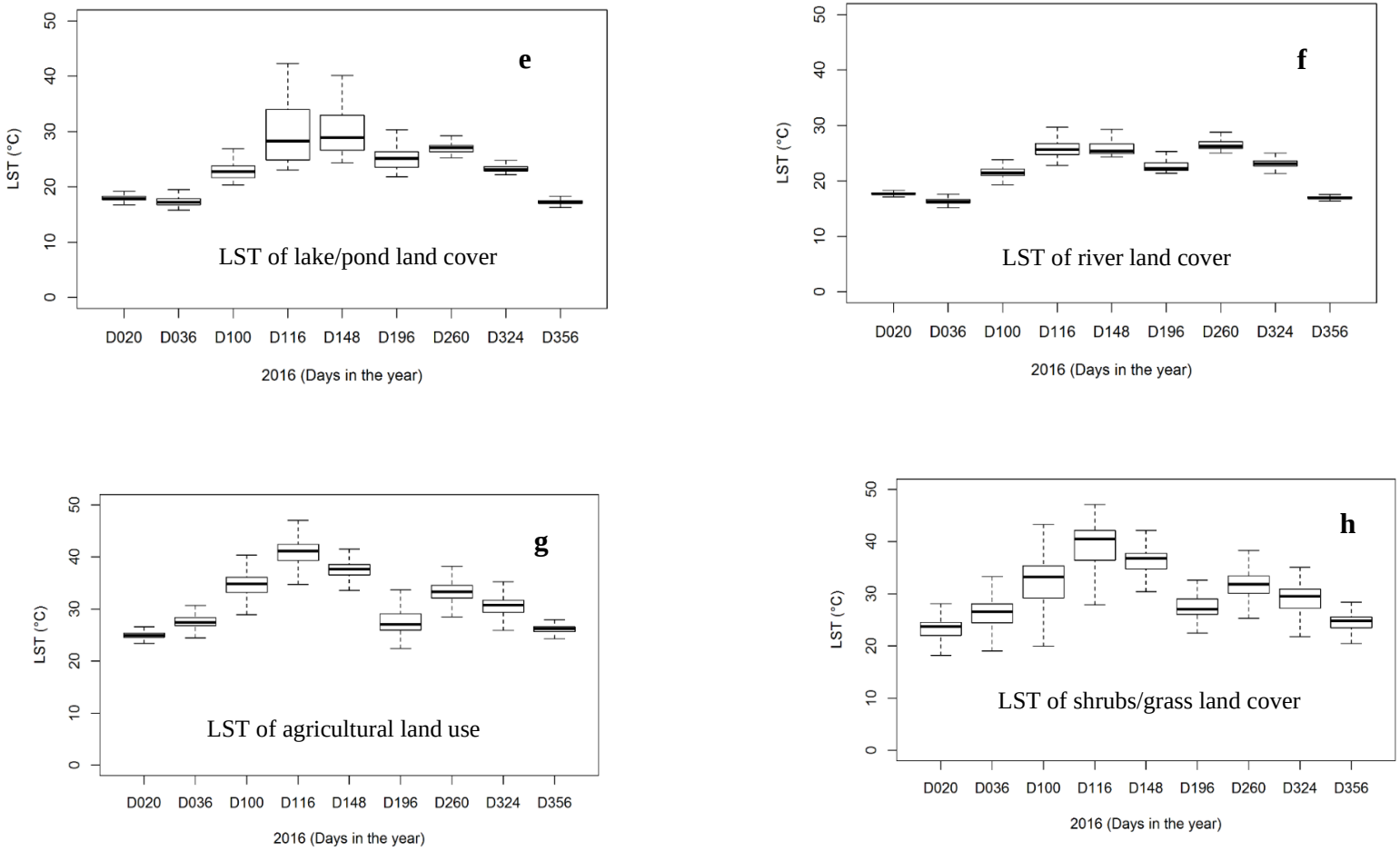

Figure 4.21e-h Descriptive analysis of land surface temperature of different land use and land cover types for 2016 images.

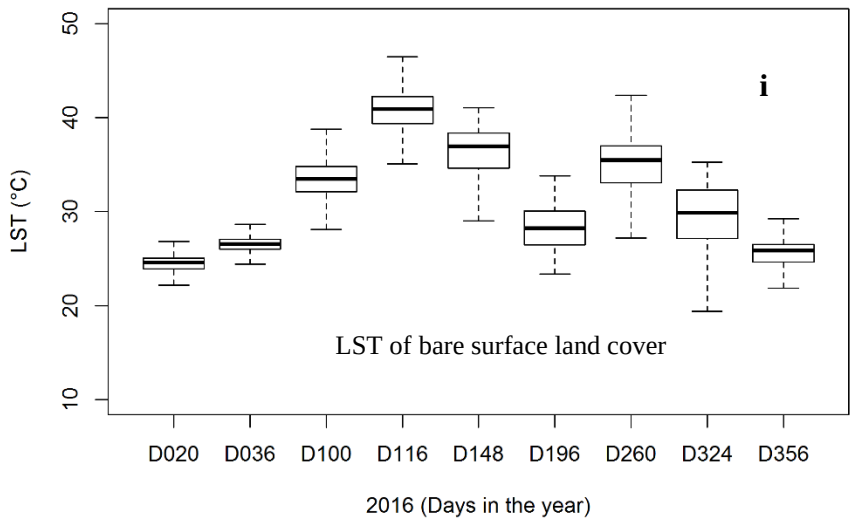

Figure 4. 21(i) Descriptive analysis of land surface temperature of different land use and land cover types for 2016 images.

In 2016, Figure 4.21a-d, figure 4.21e-h and figure 4.21(i) describes the trend analysis of LST on different LULC classes in different time periods under study. In both LULC classes LST also varies from one period to another. LST was revealed to increase from the early days in the year for instance from day 20 to 116 (D020 to D116) which is around January to April when it has not started raining and the surfaces are bare hence more heat is trapped. LST decreases from day 196 to 260 (D196-D260) when rain is intense and almost all the surfaces are covered with vegetation thus more heat is reflected from the surfaces. LST is noticed to be higher on each LULC class on day 116 (D116) and this is because in this period (April) the study area has a very dry climate and could be unconducive.

For better description of the relationship between LST, LULC classes, time series analysis of LST was plotted against various LULC classes in different time as shown in figure 4.22 and figure 2.23.

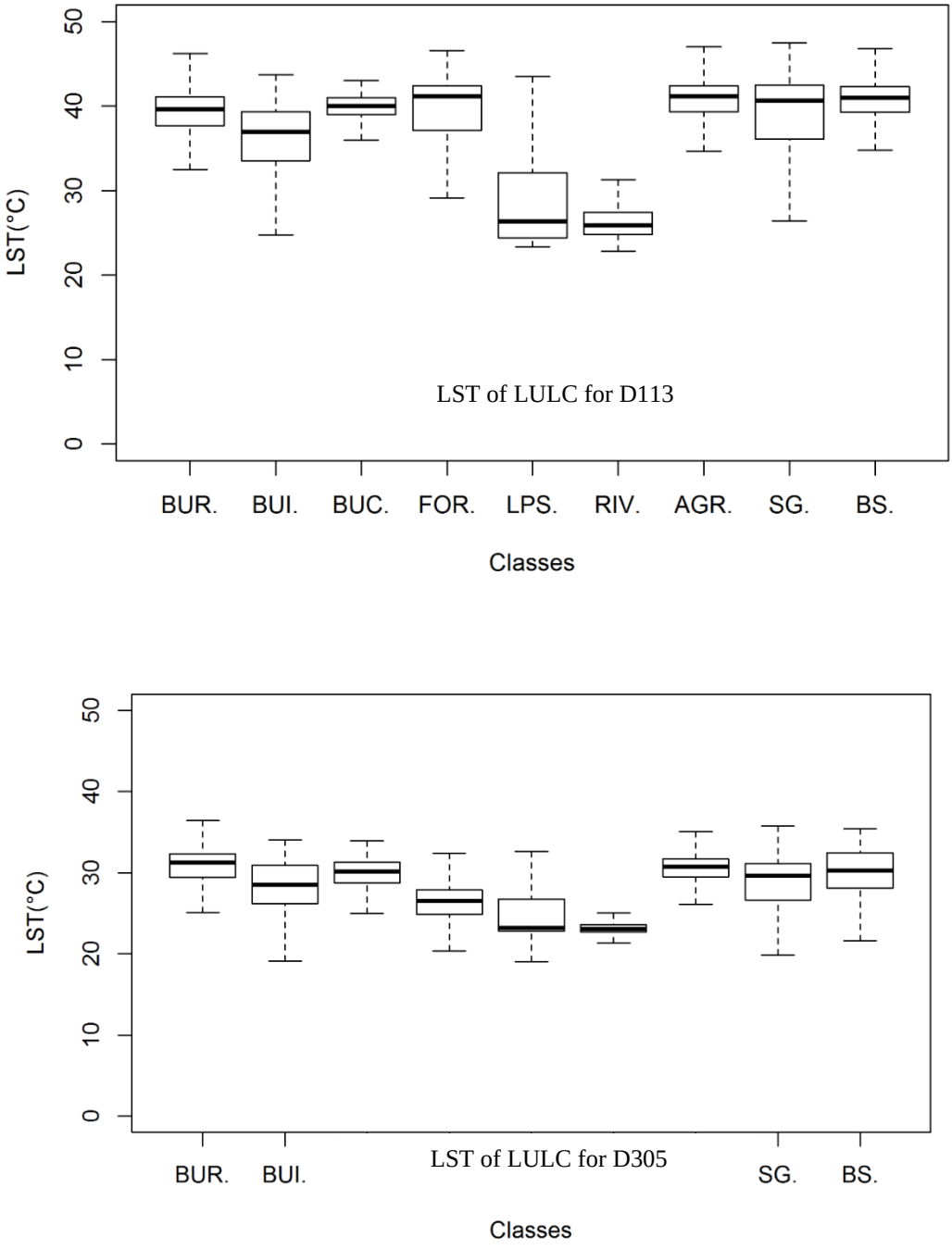

Figure 4. 22 Relationship between LST and LULC for a dry and wet day in 2015

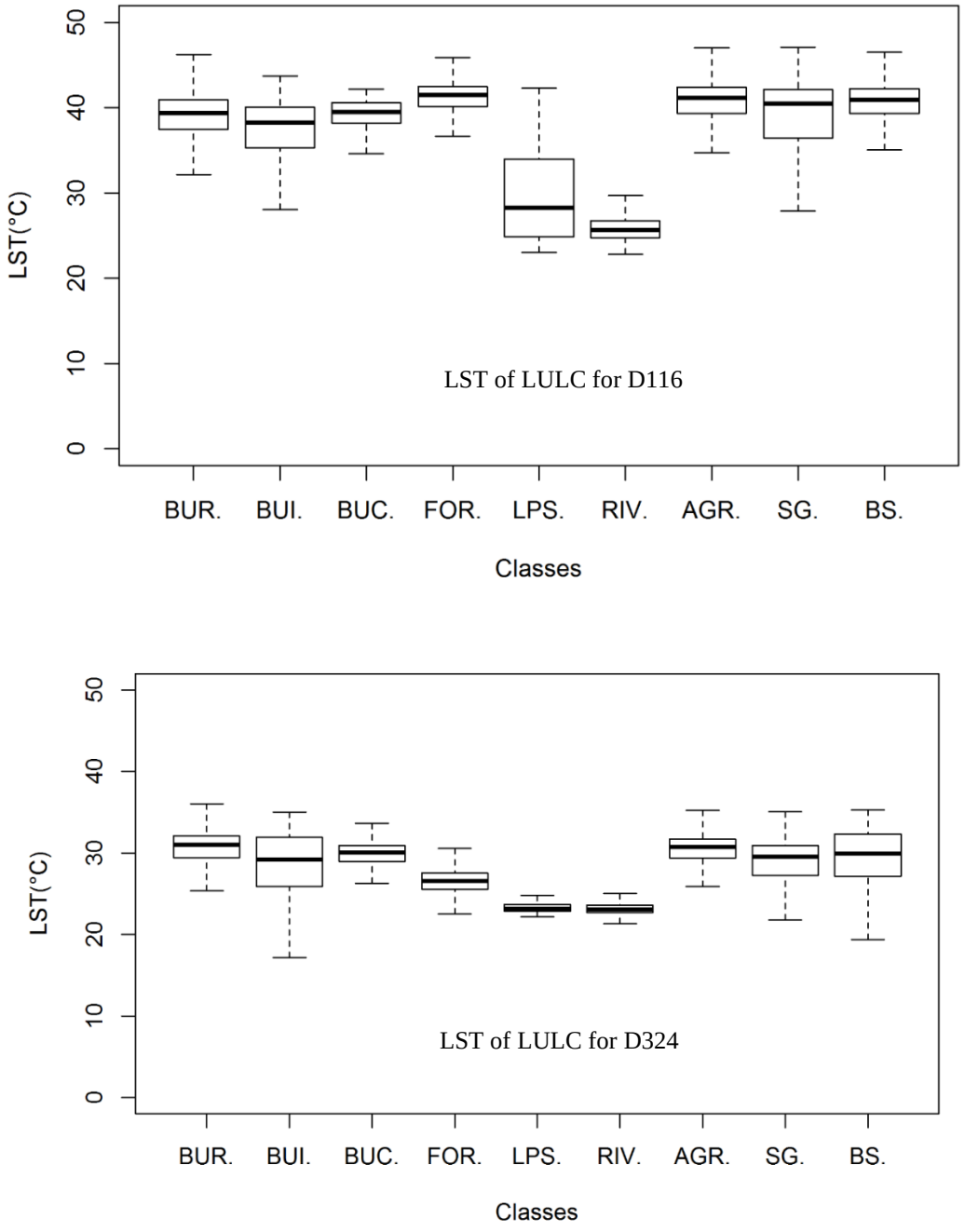

Figure 4. 23 Relationship between LST and LULC for a dry and wet day in 2016

The result in figure 4.22 and 4.23 reveals that in all the time steps, LST varies from water bodies to bare surfaces and built up areas (residential, industrial and commercial areas) which have the highest temperature in every time step because bare surfaces are characterised with a thin cover thus all the solar energy incident on it are absorbed and this warms up the surface faster than other classes. In hot periods like D113 LST could

be as high as 40^{o}C in all LULC except on water bodies, which show low LST. In wet periods or harmattan like in D305 LST for water bodies also show a low value but higher value on other LULC types. The western part of the study area is covered with vegetation all through the year because the area is engaged in irrigation farming hence the reason for low LST. This can also be seen in the forested area and on water bodies as indicated in the southern part of the map.

In accordance to previous studies, time series analysis of LST for various time steps reveals the spatial distribution of surface temperature and this indicates that the higher the vegetation cover in an area the lower the LST and the higher the built-ups and transformation of vegetated cover to bare surfaces or buildings the higher the LST in that area (Ishola *et al.*, 2016; Mahmoud *et al.*, 2016; Adeyeri *et al.*, 2017).

This finding is similar to other findings by Emmanuel (2005) and Blake *et al.* (2011) cited by Adeyeri *et al.* (2017), which reflects that built up areas stores large quantity of incident radiation that makes it warmer, while natural vegetation like shrubs and grasses, forest and agricultural lands maintain a lower LST majorly because, vegetation cover reflect more radiation incident on it. Water bodies have the lowest LST because of its high specific heat capacity when compared to other built up areas.

Thus, vegetal cover is an important and necessary land cover that should not be excluded from the earth surface rather it should be reserved and included in any urban planning system. Its importance cannot be under-emphasized in regulating LST and UHI effect in any environment. This is because it aids in cooling the environment and reduce the concentration of carbon in the atmosphere, serves as means of evapotranspiration and also

provide shades in urban areas thus lowers both surface and air temperature (Adeyeri, 2016).

4.6 Relationship Between Land Surface Temperature and Land Cover Indices

To determine and comprehend the relationship between LST and vegetation, built ups and water bodies, NDVI, NDBI and MNDWI were used to perform the analysis. This is because NDVI in remote sensing serves as an alternative to determine the vegetation greenness (Weng *et al*., 2004), NDBI was used for built ups because it is more sensitivity to build environment and MNDWI for water bodies. The relational analysis was carried out by superimposing LST on LULC and the various land cover indices used in this study. Values for LST were extracted and a linear association analysis using Pearson's correlation analysis was conducted as shown in Table 4.5.

Table 4. 5 Correlation analysis between land surface temperature and different land cover indices

Day	Mean LST(ºC)	NDVI (r)	NDBI (r)	MNDWI (r)
		2015		
D001	23.9	-0.304	0.701	-0.621
D017	26.1	-0.212	0.748	-0.753
D033	32.4	-0.128	0.742	-0.686
D113	38.6	-0.297	0.721	-0.606
D145	36.7	-0.436	0.667	-0.521
D161	28.2	-0.365	0.581	-0.313
D289	34.7	-0.344	0.804	-0.385
D305	29.6	-0.127	0.491	-0.378
D353	24.9	-0.211	0.713	-0.679
		2016		
D020	27.1	-0.275	0.806	-0.766
D036	28.4	-0.389	0.834	-0.786
D100	33.1	-0.309	0.728	-0.637
D116	40.1	-0.388	0.749	-0.675
D148	27.8	-0.271	0.666	-0.434
D196	27.6	-0.391	0.746	-0.389
D260	26.7	-0.137	0.711	-0.208
D324	33.1	-0.280	0.839	-0.749
D356	28.9	-0.242	0.818	-0.766

Source: Author's compilation, 2017.

Table 4.5 displays the result of the descriptive statistics and correlation analysis of the land cover indices parameters and the LST. The table reveals that mean LST ranges from 23.9ºC to 38.6ºC and 27.1ºC to 40.1ºC in 2015 and 2016 respectively. It further explains how LST varies from one day to another, in different months and season in a particular year. This study removed the values for water bodies on the derived NDVI in order to avoid its influence on the correlation analysis. Table 4.5 shows that NDVI have a negative correlation with LST. The association between the two variables ranges were between -0.127 to -0.436 and -0.137 to -0.391 for 2015 and 2016 respectively. This means that there is variation on the relationship between NDVI and LST depending on the time and season the data was collected and used for the analysis. NDVI indicate a high negative

correlation values when vegetation cover increases. NDBI indicate a positive correlation between LST and built up environment. The correlation coefficient values range from 0.491 to 0.804 and 0.666 to 0.834 for 2015 and 2016 respectively. Table 4.5 also reveals that there is a slight variation between the coefficient values.

In accordance to the findings of Pal and Ziaul, (2016); Mahmoud *et al*. (2016), that point out that pixels of water bodies always show low values and indicate a very strong negative correlation between water and LST, this study determined value ranging from -0.291 to -0.753 and -0.208 to -0.786 for 2015 and 2016 respectively MNDWI. This study reflects that there is a very poor correlation between LST and water. In the concept of urban greening, vegetation weakens UHI and the result revealed above on LST and NDVI showing a negative correlation indicates that vegetation cover is a weakening measure for UHI effect in the study area. In this context it means green parks, gardens and landscapes should be improved on and constructed in the core of the city so as to reduce the impact of high LST on the environment.

To determine the cause-effect relationship between built-up environments, vegetation and LST, this study used a simple linear regression model to analyse the coefficient of determination R^2. Figure 4.24 and figure 4.25 shows the line of linearity, r and R^2 for different time steps at p-value less than 0.5 at 95% confidence interval which means there is it is statistically significant for land surface temperature analysis. This result reveals that as vegetation cover decreases LST is said to increase and it increases while LST decreases. The finding of this study is related to the view of Doick and Hutchings (2013) and Adeyeri (2017) in their findings that explains that vegetal cover provides shade effect and support evapotranspiration in the environment which in turn cause cooling in the environment.

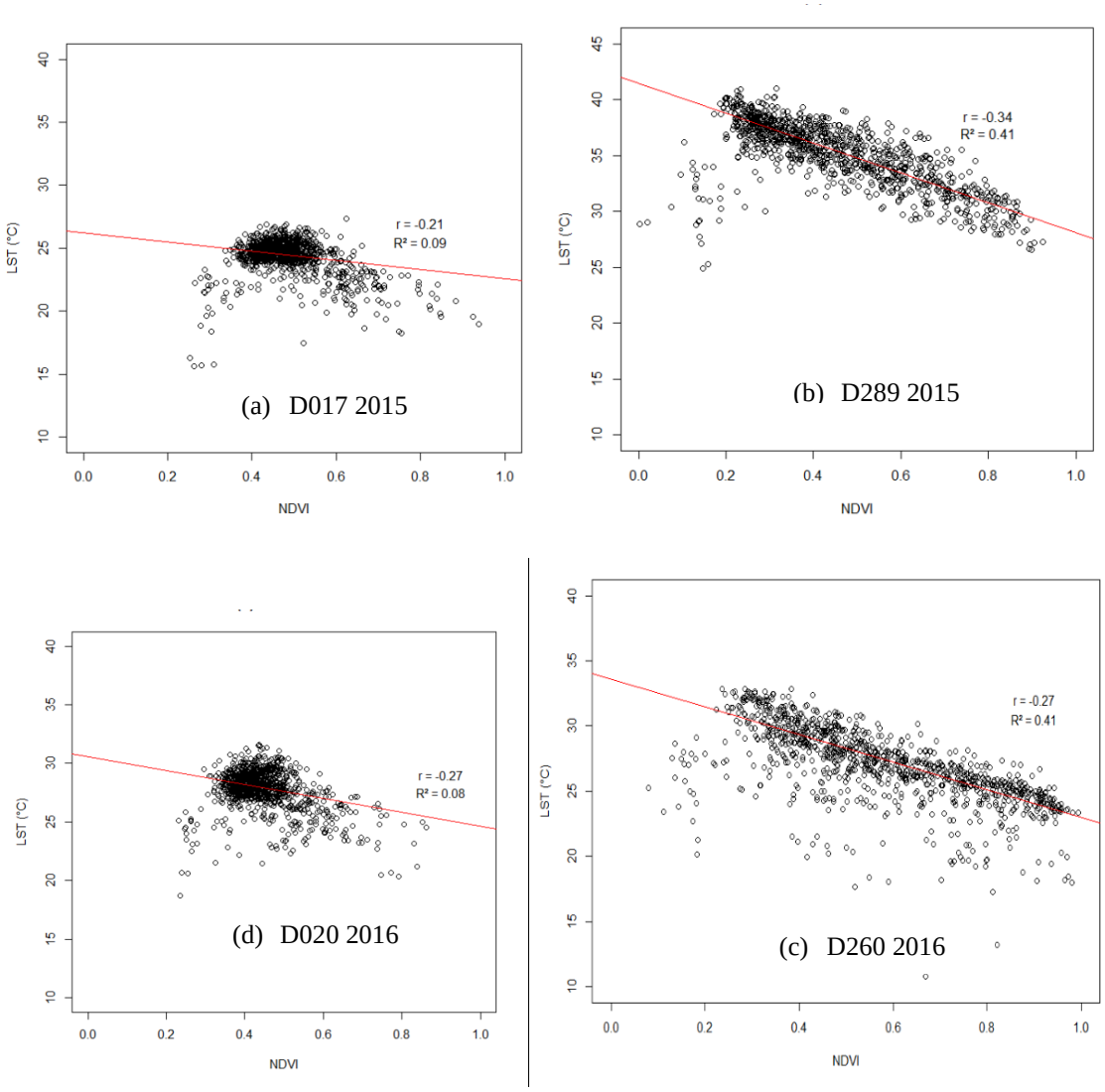

Figure 4. 24 Relationship between LST and vegetation indicators in 2015 and 2016

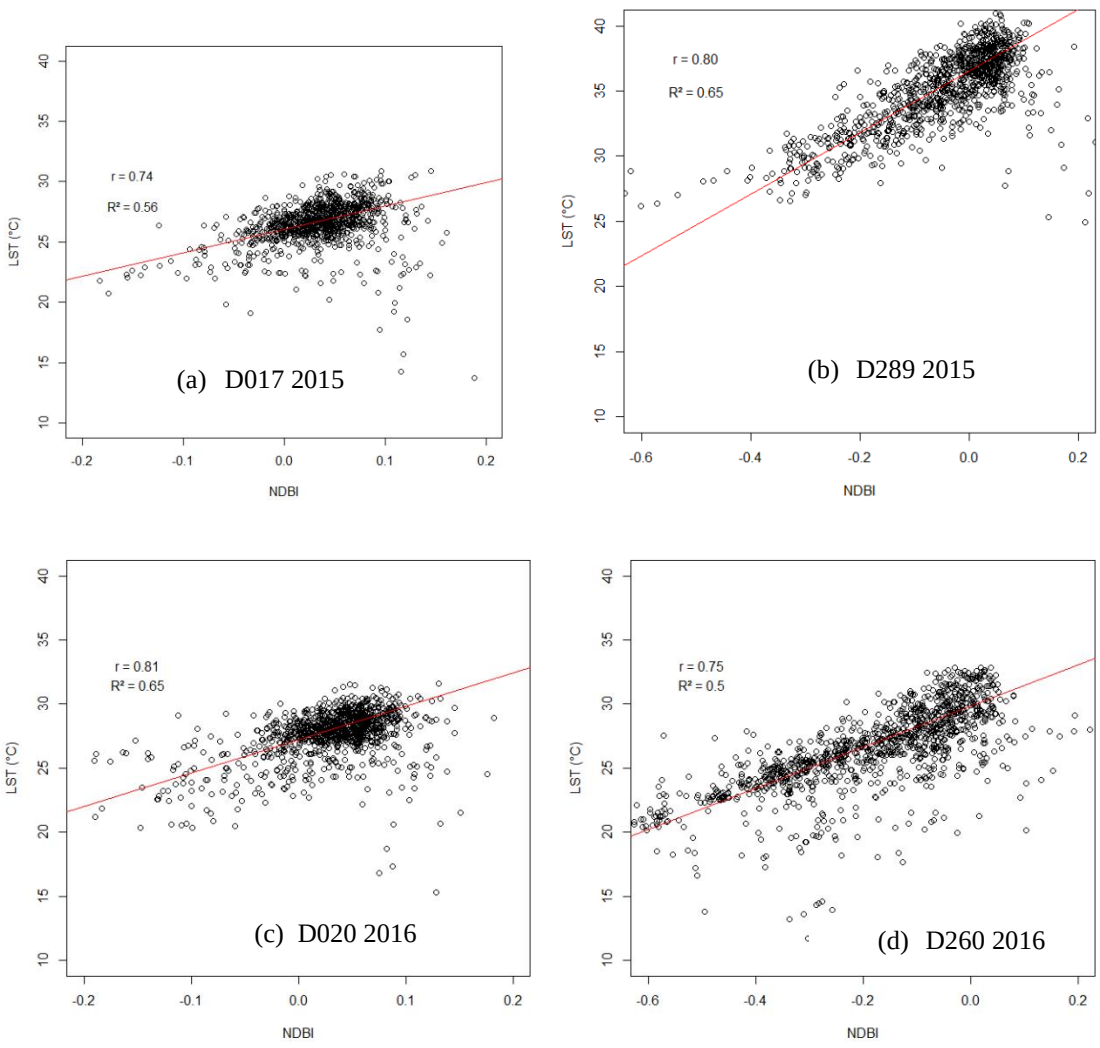

Figure 4. 25 Relationship between LST and NDBI in 2015 and 2016

Figure 4.24 reveals a very low coefficient of determination R-squared for NDVI and LST of 0.09 and 0.08 in dry days for 2015 and 2016 respectively as seen in D017 and D020 and a moderately low coefficient of determination of 0.41 when vegetation cover is more. When NDBI and LST was explored a different situation was revealed (Figure 4.25). The coefficient of determination for LST and NDBI is 0.5 and 0.6 in both dry and wet seasons of both years and this is said to be higher than that of NDVI and LST. This means LST increases with increase in NDBI and decreases with increase in NDVI (Figure 4.24 and figure 4.25). The cause-effect relationship between NDBI and LST is that increase in LST

can be 50-65% caused by NDBI and it can be increased by NDVI by only 8-9% which means NDVI can cause LST to decrease by approximately 91%.

4.7 Descriptive and Spatial Visualization of UHI

UHI effect in the study area is shown mostly in the urban core and its neighbouring towns. The core of the study area tends to indicate more of built-up areas covering residential, commercial and industrial use with little vegetal cover and open surface and thus influence more heat than in the periphery where agricultural activities are intense with less buildings. It can be deduced from this study that as one moves from the core to the periphery LST tends to decrease because of the influence of vegetation at the periphery but increases when one moves from the periphery to the core of the study area.

In order to examine features of hot spots and cold spots and to highlight the influence of homogeneous LULC on LST in the study area, LULC and LST retrieved were zoomed as shown in Figure 4.26 and 4.27.

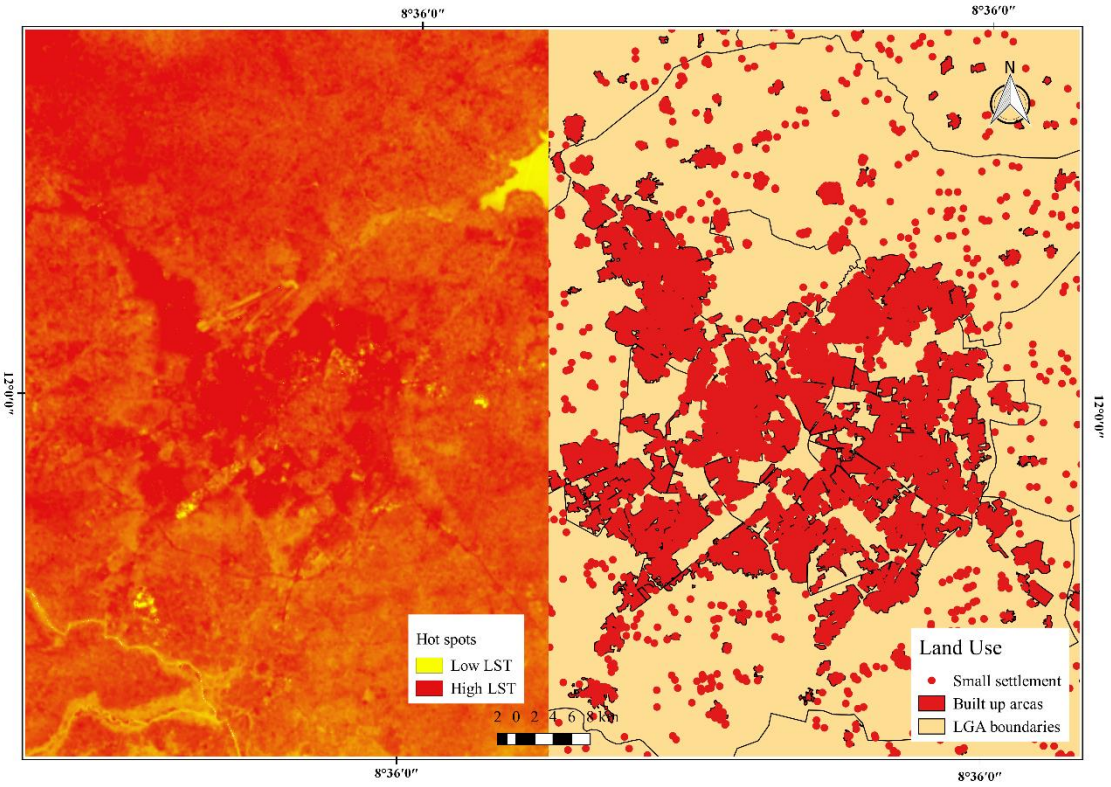

Figure 4. 26 Spatial visualization of hotspots in the study area

Figure 4.26 reflects that a more homogenous built up environment have clusters of high LST hot spots ranging from 33^{o}C to 40^{o}C which are visible across the core of Kano State. This result is in line with the findings of Mahmoud (2016), who observed that the formation of UHI is dependent on a more homogenous built up environment with no vegetation cover.

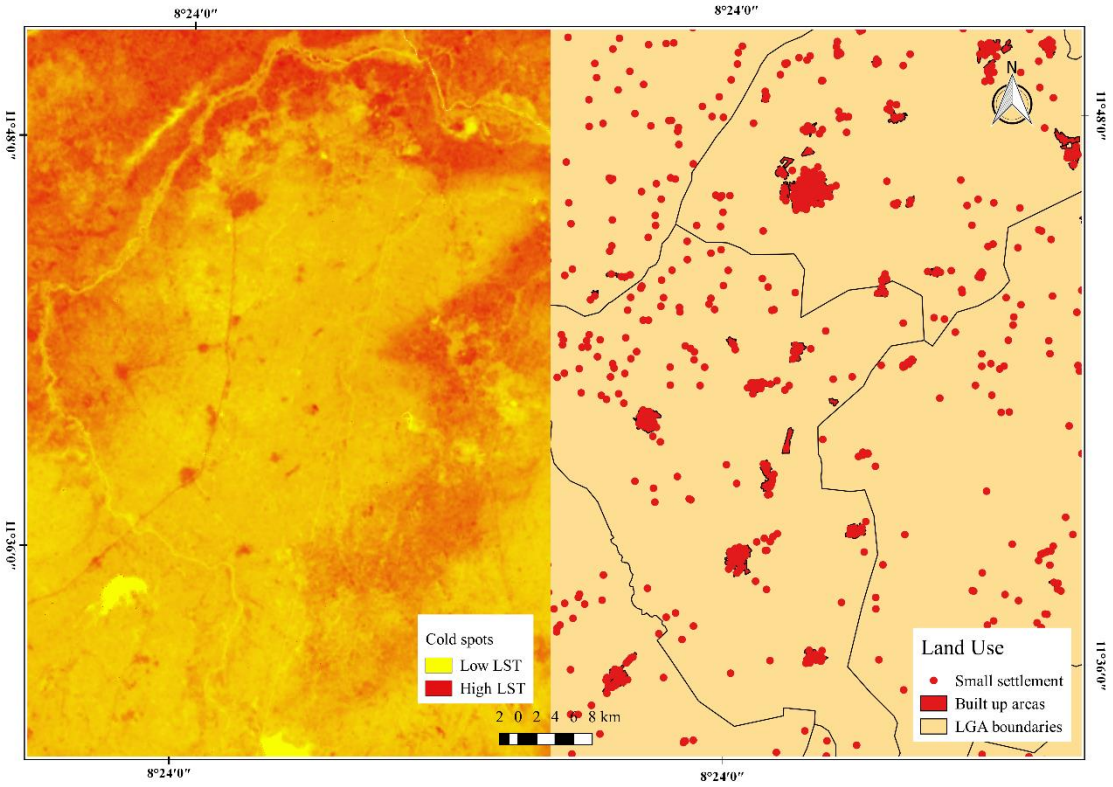

Figure 4. 27 Spatial visualization of cold spots in the study area

The result of figure 4.27 further shows that a more homogenous vegetated environment has a clusters of land surface temperature ranging from 18^{o}C to 22^{o}C and are visible across the periphery of Kano State.

This study therefore indicates that vegetation plays essential role in modifying LST and the findings of this study is in agreement with Ishola *et al.* (2016) and Adeyeri *et al.* (2017), who points out that vegetation should be preserved and built up environment should be planned by improving on landscaping activities so as to reduce the influence of clusters of hotspots in the core of the study area. This will result to LULC modification and could transform clusters of hotspots to cold spots and thus address issues related to UHI effect (Doick and Hutchings, 2013; Adeyeri, 2017).

CHAPTER FIVE

5.0 CONCLUSION AND RECOMMENDATIONS

In this chapter, conclusions were drawn and possible recommendations were highlighted from the findings of the study.

5.1 Conclusion

The study employed and demonstrated the use of multi-temporal spatial Landsat OLI&TIRS images for 2015 and 2016 to produce LULC map and land cover indices like NDVI, NDBI and MNDWI that were relevant to the aim and objectives of the study. In order to understand the influence of urbanization on landscape and the micro climate of the environment this study collected population data for 2006 and 2017 in order to analyse population growth. The study showed that over three million people have increased from 2006 to 2017 and this could have possible spatial impact on the different land cover categories. However, for further study, more in-situ data that could explain better the influence of urbanization on LULC class and LST should be considered.

Considering the periods and seasons the Landsat 8 images were collected and noting that an optical satellite image like Landsat contains cloud, care was taking in selecting a less cloud image in the respective months of interest. However atmospheric and radiometric correction of all the satellite images was performed using more sophisticated tools known as R software. This was also possible as a result of the availability of powerful computing system that was used for analysing the data collected. The images were processed and a digital map for 2015 and 2016 was produced using the three true colour composite bands of all the nine satellite images processed. A more accurate and powerful machine learning

algorithm and supervised classification classifier known as random forest (RF) was used. In order to analyse the development trend of LST on the different LULC categories that were of interest to this study, RF algorithm was used to classify all the multi-temporal images stacked for each year to produce a single LULC map taking into account the phenology information of the different time steps used. The LULC map for both years showed that agricultural lands are the dominant land, followed by built up residential, river, bare surface, forest, shrub/grass, lakes/ponds/stream, built up industrial areas and the least cover is built up commercial. This is true basically because government created an irrigation scheme program which is basically involved in rice and maize production in the western part of the study area and thus covers a large area. Higher accuracy was achieved considering the techniques, algorithm and method used in this study. Kappa coefficient estimated in this study showed an excellent agreement between the classification map and the ground truth data. Hence, when carrying out such study in other regions or similar study, the approaches used in this study is strongly advised and encourage in order to attain a better result.

In a particular time and season LST is not constant and it also differs on different LULC categories. Built up environment such as residential, industrial and commercial areas showed higher LST, bare surface such as open soils, rocks, hills indicate also high LST while vegetated areas like agricultural lands, forest and shrubs/grasses showed a low temperature. Lower LST over water bodies was retrieved and this explains why the micro climate around water bodies and vegetated surfaces are different from built up areas. To further understand the relationship between LST and LULC, correlation and regression techniques were used to ascertain the association between LST and three relevant land

cover indices (NDVI, NDBI and MNDWI) and determine the cause-effect relationship between these variables.

It can be deduced from results found that there are variations in the relationship between LST and different LULC categories and NDVI, NDBI, MNDWI and this is being reflected in different climatic seasons and periods. A negative correlation exists between LST, MNDWI and NDVI and this further explains that NDVI weakens LST and MNDWI could regulate to a great degree the LST of the environment. While LST and NDBI showed a strong positive correlation which means NDBI can strengthen LST and make the environment unconducive for life and other activities especially during harsh and hot periods when the vegetated areas are bared and open, thus more heat will be trapped and surface temperature will be high. The cause-effect relationship examined using regression statistics showed that increase in NDBI can cause high LST and increase in NDVI can cause decrease in LST. Hotspots spotted at the core of the study area showed higher surface temperature because of high amount of the use of asphalt for construction of roads, but this was somewhat different from the periphery of the study area which form cold spots because of the abundant of agricultural activities. From this study it can be inferred that, if the trend and changes in LST is left unchecked and not regulated in the study area, it will have impact on its citizens by causing heat related illnesses and diseases. For further related studies in Kano state and urban cities with similar climatic zones, same methodology could be applied and also the use of other multi-spectral and temporal satellite images like RADAR, Rapid-Eye, LIDAR could be used to analyse LST and LULC. Findings from this study also reveal that for simulation and prediction of LST and LULC, several multi-temporal satellite imageries should be considered in order to get a more accurate result and validation.

5.2 Recommendations

This study has drawn some recommendations that could be useful to regulate LST and helpful to urban planners and development. The recommendations are as follows below:

1. Government policy should include city planning by focusing on urban greening and landscaping in street and along roads. Street trees provide shading effect such as ever greening and high level of canopy which will help in regulating ambient land and air temperature that could affect human comfort. This can be achieved by setting policies that guide:
    - planting of flowers and trees along any building by house owners;
    - compulsory landscaping activities in streets and on building pavements and roof tops.

2. Government should improve on irrigation schemes in all part of the state in order to regulate land surface temperature. This can be achieved by channelling dams and rivers to areas where there are dependent on rain. This will increase vegetal cover and will help to regulate land surface temperature.

3. Government and individuals should engage in tree planting program. This program can be achieved by:
    - Replacement of dead trees with new trees in urban centres and along permeable pavements.
    - Improvement of afforestation activities and putting down penalties for deforestation activities so as to stop individuals from cutting down trees.

4. Permeable pavements such as interlocks should be used for constructing access roads to reduce the retention of heat. Interlocks provide space for some patches of vegetation to grow and reduce the retention of heat unlike tarred roads which retain more heat.

REFERENCES

Adebayo, A. A., & Zemba, A. A. (2003). Analysis of micro climatic variations in Jimeta-Yola, Nigeria. *Global Journal of Social Sciences*, *2*(1), 79–88. Retrieved from https://www.ajol.info/index.php/gjss/article/view/22769

Adeyeri, O. E., Akinsanola, A. A., & Ishola, K. A. (2017). Investigating surface urban heat island characteristics over Abuja, Nigeria: Relationship between land surface temperature and multiple vegetation indices. *Remote Sensing Applications: Society and Environment*, *7*(June), 57–68. https://doi.org/10.1016/j.rsase.2017.06.005

Agarwal, C., Green, G. M., Grove, J. M., Evans, T. P., & Schweik, C. M. (2002). *A Review and Assessment of Land-Use Change Models : Dynamics of Space , Time , and Human Choice Chetan Agarwal*. U.S. Retrieved from https://www.nrs.fs.fed.us/pubs/gtr/gtr_ne297.pdf

Ahmed, B., Kamruzzaman, M., Zhu, X., Rahman, M., & Choi, K. (2013). Simulating Land Cover Changes and Their Impacts on Land Surface Temperature in Dhaka, Bangladesh. *Multidisciplinary Digital Publishing Institute*, *5*(11), 5969–5998. https://doi.org/10.3390/rs5115969

Akbari, H. (2005). Energy Saving Potentials and Air Quality. In *First International Conference on Passive and Low Energy Cooling for the Built Environment*. Berkeley, CA (US): Ernest Orlando Lawrence Berkeley National Laboratory, Berkeley, CA (US). Retrieved from https://www.osti.gov/scitech/biblio/860475

Alavipanah, S., Wegmann, M., Qureshi, S., Weng, Q., & Koellner, T. (2015). The role of vegetation in mitigating urban land surface temperatures: A case study of Munich, Germany during the warm season. *Sustainability*, *7*(4), 4689–4706. https://doi.org/10.3390/su7044689

Alexander, P. J., & Mills, G. (2014). Local climate classification and Dublin's urban heat island. *Atmosphere*, *5*(4), 755–774. https://doi.org/10.3390/atmos5040755

Alkali, J. L. S. (2005). Planning Sustainable Urban Growth in Nigeria : Challenges and Strategies. In *Planning Sustainable Urban Growth and Sustainable Architecture* . 1-9, New York, US. Retrieved from http://www.un.org/en/ecosoc/meetings/2005/docs/Alkali.pdf

Anjana, V., Shastri, B., & Joshi, Y. (2014). Spatio-Temporal Analysis of UHI Using Geo-Spatial Techniques : A Case Study of Ahmedabad City. *The International Archives of the Photogrammetry, Remote Sensing and Spatial Information Sciences*, XL(8), 9-12. https://doi.org/10.5194/isprsarchives-XL-8-997-2014

Avdan, U., & Jovanovska, G. (2016). Algorithm for automated mapping of land surface temperature using Lansat 8 satellite data. *Journal of Sensors*, *2016*, 1–8. https://doi.org/10.1155/2016/1480307

Ayedun, C. A, Durodola, O. D., & Akinjare, O.A. (2011). Towards ensuring sustainable urban growth and development in Nigeria: Challenges and Strategies. *Society*

for Business and Management Dynamics, *1*(2), 99–104. Retrieved from www.bmdynamics.com

Ayila, A. E., Oluseyi, F. O., & Anas, B. Y. (2014). Statistical Analysis of Urban Growth in Kano Metropolis , Nigeria. *International Journal of Environmental Monitoring and Analysis: Scirnce Publishing Group*, *2*(1), 50–56. https://doi.org/10.11648/j.ijema.20140201.16

Balogun, I. A., Adeyewa, D. Z., Balogun, A. A., & Morakinyo, T. E. (2011). Analysis of urban expansion and land use changes in Akure, Nigeria, using remote sensing and geographic information system (GIS) techniques. *Journal of Geography and Regional Planning*, *4*(9), 533–541. Retrieved from http://www.academicjournals.org/JGRP

Batisani, N., & Yarnal, B. (2008). Urban expansion in Centre County , Pennsylvania : Spatial dynamics and landscape transformations. *Applied Geography*, *29*(2), 235–249. https://doi.org/10.1016/j.apgeog.2008.08.007

Bharath, S., Rajan, K. S., & Ramachandra, T. (2013). Geostatistics : An Overview Land Surface Temperature Responses to Land Use Land Cover Dynamics. *A SciTechnol Journal*, *1*(4), 1–10. https://doi.org/http://dx.doi.org/10.4172/2327-4581.1000112

Bhatta, B. (2010). Analysis of Urban Growth and Sprawl from Remote Sensing Data. *Advances in Geographic Information Science*, *1*, 1–172. https://doi.org/Doi 10.1007/978-3-642-05299-6

Braimoh, A. K., & Onishi, T. (2006). Spatial determinants of urban land use change in Lagos , Nigeria. *Land Use Policy*, *Elsevier*, *24*, 502–515. https://doi.org/10.1016/j.landusepol.2006.09.001

Blaes, X., Vanhalle, L., and Defourny, P., 2005. Efficiency of crop identification based on optical and SAR image time series. *Remote Sensing of Environment*, 96 (3–4), 352–365. Retrieved from http://www.sciencedirect.com/science/article/pii/S0034425705001045

Bruzzone, L., & Prieto, D. F. (2002). *An Adaptive Semi-parametric and Context-based approach to Unsupervised Change Detection in Multi-temporal Remote Sensing Images. IEEE Transactions on Image Processing*. 11(4), 1-37. Retrieved from ieeexplore.ieee.org/document/999678

Buyadi, S. N. A., Mohammed, W. N. M., & Misni, A. (2013). Impact of Land Use Changes on the Surface Temperature Distribution of Area Surrounding the National Botanic Garden, Shah Alam. *Procedia - Social and Behavioral Sciences*, 18(01), 516–525. http://doi:10.1088/1755-1315/18/1/012104

Byomkesh, T., Nakagoshi, N., & Dewan, A. M. (2011). Urbanization and green space dynamics in Greater Dhaka, Bangladesh. *Landscape and Ecological Engineering*, *8*(1), 45–58. https://doi.org/10.1007/s11355-010-0147-7

Camilo, P. A. (2010). Urban Heat Islands Effect. Retrieved March 31, 2017, from http://www.urbanheatislands.com/

Chan, C. F., Lebedeva, J., Otero, J., & Richardson, G. (2007). URBAN HEAT ISLANDS : A CLIMATE of the City of Montreal. The Climate Change Action

Partnership McGill University School of Urban Planning. Montreal. Retrieved from https://www.mcgill.ca/urbanplanning/files/urbanplanning/CCAPUHIFinalReport-2007.pdf

Chen, X. L., Zhao, H. M., Li, P. X., & Yin, Z. Y. (2006). Remote sensing image-based analysis of the relationship between urban heat island and land use/cover changes. *Remote Sensing of Environment*, *104*(2), 133–146. https://doi.org/10.1016/j.rse.2005.11.016

Congalton, R. G. (2001). Accuracy assessment and validation of remotely sensed and other spatial information. *International Journal of Wildland Fire*, *10*(4), 321–328. Retrieved from http://www.publish.csiro.au/WF/search?q=Accuracy+assessment+and+validation+of+remotely+sensed+and+other+spatial+information&sjournal=on

Danba, E. P., David, D. L., Wahedi, A. J., Buba, U. N., Usman, D., Bingari, M. S., & Tukur, U. K. (2015). Physicochemical analysis and fish pond conservation in Kano State , Nigeria. *Archives of Applied Science Research*, *7*(6), 28–34. Retrieved from atwww.scholarsresearchlibrary.com Scholars

De Carolis, L. (2012). *The Urban Heat Island Effect in Windsor, ON: An Assessment of Vulnerability and Mitigation Strategies*. Windsor. Retrieved from http://www.citywindsor.ca/residents/environment/environmental-master-plan/documents/urban heat island report (2012).pdf

Doick, K., & Hutchings, T. (2013). *Air temperature regulation by urban trees and green infrastructure Forestry commission.* Retrieved from http://www.forestry.gov.uk/pdf/FRN012.pdf/$FILE/FRN012.pdf

Ehealth System Africa, (2017). Population estimate. Retrieved from *http://vts.eocng.org/population/LGA?s=&l=&gender=MF&from=0&to=100*

Ejaro, S. P., & Abdullahi, U. (2013). Spatiotemporal Analyses of Land Use and Land Cover Changes in Suleja Local Government Area, Niger State, Nigeria. *Journal of Environment and Earth Science*, *3*(9), 72–84. Retrieved from http://www.iiste.org/Journals/index.php/JEES/article/view/7330

EPA (Environmental Protection Agency, 2008). *Reducing Urban Heat Islands: Compendium of Strategies Urban Heat Island Basics*. Washington, DC. Retrieved from http://www.epa.gov/heatisland/about/index.htm

Essa, W., Verbeiren, B., Van der Kwast, J., Van de Voorde, T., & Batelaan, O. (2012). Evaluation of the DisTrad thermal sharpening methodology for urban areas. *International Journal of Applied Earth Observation and Geoinformation*, *19*(1), 163–172. https://doi.org/10.1016/j.jag.2012.05.010

Forkuor, G., Conrad, C., Thiel, M., Ullmann, T., & Zoungrana, E. (2014). Integration of Optical and Synthetic Aperture Radar Imagery for Improving Crop Mapping in Northwestern Benin, West Africa. *Remote Sensing*, 21(6), 1–30. https://doi.org/10.3390/atmos7060078

Forkuor, G., Conrad, C., Thiel, M., Landmann, T., & Barry, B. (2015). Evaluating the sequential masking classification approach for improving crop discrimination in

the Sudanian Savanna of West Africa. *Computers and Electronics in Agriculture,* 118, 380–389. https://doi.org/10.1016/j.compag.2015.09.020

Forkuor, G., Hounkpatin, O. K. L., Welp, G., & Thiel, M. (2017). High Resolution Mapping of Soil Properties Using Remote Sensing Variables in South-Western Burkina Faso: A Comparison of Machine Learning and Multiple Linear Regression Models. *PLOS ONE, Public Library of Science,* 12(1), 1–13. Retrieved from http://doi.org.ololo.sci-hub.io/10.1371/journal.pone.0170478

Faqe, I. G., (2017). Urban Land Use Land Cover Changes and Their Effect on Land Surface Temperature: Case Study Using Dohuk City in the Kurdistan Region of Iraq. *Climate*, *5*(1), 13. https://doi.org/10.3390/cli5010013

Fonji, S. F., & Taff, G. N. (2014). Using satellite data to monitor land-use land-cover change in North-eastern Latvia. *Springer Plus*, *3*(61), 1–15. Retrieved from http://www.springerplus.com/content/3/1/61%0Aa

Gao, F., Masek, J., Schwaller, M., & Hall, F. (2006). On the blending of the landsat and MODIS surface reflectance: Predicting daily landsat surface reflectance. *IEEE Transactions on Geoscience and Remote Sensing,* 44(8), 2207–2218. https://doi.org/10.1109/TGRS.2006.872081

Gómez, C., White, J. C., & Wulder, M. A. (2016). Optical remotely sensed time series data for land cover classification: A review. *ISPRS Journal of Photogrammetry and Remote Sensing*, 116, 55–72. https://doi.org/10.1016/j.isprsjprs.2016.03.008

Goslee, S. C. (2011). Analyzing Remote Sensing Data in R : The landsat Package. *Journal of Statistical Software July*, *43*(4), 1–25. Retrieved from http://www.jstatsoft.org/

Guerschman, J. P., Paruelo, J. M., Di Bella, C., Giallorenzi, M. C., & Pacin, F. (2003). Land cover classification in the Argentine Pampas using multi- temporal Landsat TM data. *International Journal of Remote Sensing*, 24(17), 3381–3402. https://doi.org/10.1080/0143116021000021288

Hadi, S. J., Shafri, H. F., & Mahir, M. D. (2014). Modelling LULC for the period 2010-2030 using GIS and Remote sensing: a case study of Tikrit, Iraq. In *IOP Conference Series: Earth and Environmental Science* 20(1), (p. 012053). https://doi.org/10.1088/1755-1315/20/1/012053

Hilker, T., Wulder, M. A., Coops, N. C., Linke, J., McDermid, G., Masek, J. G., … White, J. C. (2009). A new data fusion model for high spatial- and temporal-resolution mapping of forest disturbance based on Landsat and MODIS. *Remote Sensing of Environment*, 113(8), 1613–1627. https://doi.org/10.1016/j.rse.2009.03.007

Hütt, C., Koppe, W., Miao, Y., & Bareth, G. (2016). Best accuracy land use/land cover (LULC) classification to derive crop types using multitemporal, multisensor, and multi-polarization SAR satellite images. *Remote Sensing*, 8(8). https://doi.org/10.3390/rs8080684

ICSC (International Climate Science Coalition, 2011). Urban Heat Island Effects. In D. T. Ball (Ed.), *Surface Measurements Underlying Recent "WARMER YEARS"* (p.6). British Columbia, Canada. Retrieved from

htttp://www.climatescienceinternational.org/index.php?option=com_content&view=article&id=378:timball-28-01-10&catid=1:latest&Itemid=17

Ifatimehin, O. O., Ishaya, S., & Fanan, U. (2010). An Analysis of Temperature Variations Using Remote Sensing Approach In Lokoja Area, Nigeria. *Patnsuk Journal*, *6*(2), 35–44. Retrieved from www.patnsukjournal.net/currentissue

Ifatimehin, O. O., Ujoh, F., & Magaji, J. Y. (2009). An evaluation of the effect of land use / cover change on the surface temperature of Lokoja town, Nigeria. *African Journal of Environmental Science and Technology*, *3*(3), 86–90. https://doi.org/10.5897/AJEST09.014

IPCC (Inter-governmental Panel of Climate Change, 2001). Climate Change 2001: Scientific basis. In J.T. Houghton, D.J. Griggs, M. Noguer, P. J. Van der Linden, X. Dai, K. Maskell & C. A Johson (Eds.), *Contribution of Working Group I to the Third Assessment Report of IPCC* (pp. 881). Cambridge University Press, 2001.

IPCC (Inter-governmental Panel of Climate Change, 2007b). Climate change 2007: Impacts, Adaptations and Vulnerability. In M. L. Parry, O.F. Canziani, J. P. Palutikof, P. J. Van der Linden & C. E. Hanson (Eds), *Contribution of Working Group II to the Fourth Assessment Report of the IPCC* (xc z=pp. 976). Cambridge, UK: Cambridge University Press

Ishii, A., Iwamoto, S., Katayama, T., Hayashi, T., Shiotsuki, Y., Kitayama, H., Nishida, M. (1991). A Comparison of Field Surveys on the Thermal Environment in Urban Areas Surrounding a Large Pond: when Filled and when Drained. *Energy and Buildings*, *15*(16), 965–971. Retrieved from http://moscow.sci-hub.io/5f238fc51594853af2678dbe212251ae/ishii1991.pdf

Ishola, K. A., Okogbue, E. C., & Adeyeri, O. E. (2016). Dynamics of surface urban biophysical compositions and its impact on land surface thermal field. *Modeling Earth Systems and Environment*, *0*(4), 1–20. https://doi.org/10.1007/s40808-016-0265-9

Jalan, S., & Sharma, K. (2014). Spatio-temporal Assessment of Land Use / Land Cover Dynamics and Urban Heat Island of Jaipur City Using Satellite Data. *The International Archives of the Photogrammetry, Remote Sensing and Spatial Information Sciences*, *XL-8*(December), 9–12. https://doi.org/10.5194/isprsarchives-XL-8-767-2014

Jamei, E., Rajagopalan, P., Seyedmahmoudian, M., & Jamei, Y. (2016). Review on the impact of urban geometry and pedestrian level greening on outdoor thermal comfort. Renewable and Sustainable Energy Reviews, 54(November), 1002–1017. https://doi.org/10.1016/j.rser.2015.10.104

Jiang, Y., Fu, P., Weng, Q., Baghdadi, N., & Thenkabail, P. S. (2015). Assessing the Impacts of Urbanization-Associated Land Use/Cover Change on Land Surface Temperature and Surface Moisture: A Case Study in the Midwestern United States. *Remote Sensing*, *7*, 4880–4898. https://doi.org/10.3390/rs70404880

Jiboye, A. D. (2011). Urbanization challenges and housing delivery in Nigeria: The need for an effective Policy framework for Sustainable Development. *International*

Review of Social Sciences and Humanities, *2*(1), 176–185. https://doi.org/www.irssh.com

Jiménez-Muñoz, J. C., Sobrino, J. A., Plaza, A., Guanter, L., Moreno, J., & Martínez, P. (2009). Comparison between fractional vegetation cover retrievals from vegetation indices and spectral mixture analysis: Case study of PROBA/CHRIS data over an agricultural area. *Sensors*, *9*(2), 768–793. https://doi.org/10.3390/s90200768

Kalnay, E., & Cai, M. (2003). Impact of urbanization and land-use change on climate. *Nature*, *423*, 528–531. https://doi.org/10.1038/nature01649.1.

Kaspersen, P., Fensholt, R., & Drews, M. (2015). Using Landsat Vegetation Indices to Estimate Impervious Surface Fractions for European Cities. *Remote Sensing*, *7*(6), 8224–8249. https://doi.org/10.3390/rs70608224

Kaya, S., Basar, U. G., Karaca, M., & Seker, D. Z. (2012). Assessment of Urban Heat Islands Using Remotely Sensed Data. *Ekoloji*, *113*(84), 107–113. https://doi.org/10.5053/ekoloji.2012.8412

Keitt T., Bivand R., Pebesma E., Rowlingson B. (2011). rgdal: Bindings for the Geospatial Data Abstraction Library. R package version 0.7-1, *http://CRAN.R-project.org/ package=rgdal.*

Lambin, E. F., Geist, H. J., & Lepers, E. (2003). Dynamics of land-use and land-cover change in tropical regions. *Annual Review of Environment and Resources*, *28*(1), 205–241. https://doi.org/10.1146/annurev.energy.28.050302.105459

Landsat 8 Handbook, (2016). Department of the Interior U.S. Geological Survey 2016. Retrieved from *https://landsat.usgs.gov/using-usgs-landsat-8-product*

Leutner B. & Horning N. (2017). RStoolbox: Tools for Remote Sensing Data Analysis. R package version 0.1.8. *https://cran.r-project.org/web/packages/RStoolbox/index.html*

Li, H., Wang, C., Zhong, C., Su, A., Xiong, C., Wang, J., & Liu, J. (2017). Mapping Urban Bare Land Automatically from Landsat Imagery with a Simple Index. *Remote Sensing*, *9*(3), 249. https://doi.org/10.3390/rs9030249

Li, Y., & Zhao, X. (2012). An empirical study of the impact of human activity on long-term temperature change in China: A perspective from energy consumption. *Journal of Geophysical Research Atmospheres*, *117*(17), 1–12. https://doi.org/10.1029/2012JD018132

Liu, L., & Zhang, Y. (2011). Urban heat island analysis using the Landsat TM data and ASTER Data: A case study in Hong Kong. *Remote Sensing*, *3*(7), 1535–1552. https://doi.org/10.3390/rs3071535

Ma, L., Li, M., Ma, X., Cheng, L., Du, P., & Liu, Y. (2017). A review of supervised object-based land-cover image classification. ISPRS Journal of Photogrammetry and Remote Sensing, 130, 277–293. https://doi.org/10.1016/j.isprsjprs.2017.06.001

Maduako, I., Ebinne, E., Zhang, Y., & Bassey, P. (2016). Prediction of Land Surface Temperature (LST) Changes within Ikom City in Nigeria Using Artificial Neural

Network (ANN). *Journal of Remote Sensing and GIS*, *5*(01). https://doi.org/10.14355/ijrsa.2016.06.010

Mahmoud, M. I. (2016). *Integrating Geoinformation and Socioeconomic Data of Abuja for Assessing Urban Land-use Vulnerability to Potential Climate-change Impacts.* (Unpublished doctoral thesis). Kwame Nkrumah University of Science and Technology , Ghana.

Mahmoud, I. M., Duker, A., Conrad, C., Thiel, M., and Ahmad, S. H., (2016). Analysis of Settlement Expansion and Urban Growth Modelling Using Geoinformation for Assessing Potential Impacts of Urbanization on Climate in Abuja City, Nigeria. *Remote Sensing* 8(220). Retrieved from http://www.mdpi.com/2072-4292/8/3/220/html

Manteghi, G., Bin Limit, H., & Remaz, D. (2015). Water bodies an urban microclimate: A review. *Modern Applied Science*, *9*(6), 1–12. https://doi.org/10.5539/mas.v9n6p1

McFeeters, S. K. (1996). The use of the Normalized Difference Water Index (NDWI) in the delineation of open water features. *International Journal of Remote Sensing*, *17*(7), 1425–1432. https://doi.org/10.1080/01431169608948714

McNairn, H., Champagne, C., Shang, J., Holmstrom, D., & Reichert, G. (2009). Integration of optical and Synthetic Aperture Radar (SAR) imagery for delivering operational annual crop inventories. *ISPRS Journal of Photogrammetry and Remote Sensing*, 64(5), 434–449. https://doi.org/10.1016/j.isprsjprs.2008.07.006

Mfondoum, A. H. N., Joachim, E., Nongsi, B. K., Mvogo Moto, F. A., Deussieu, F. G. N. (2016). Assessment of land degradation status and its impact in arid and semi-arid areas by correlating spectral and principal component. International journal of advance remote sensing and GIS, 5(2), 1539–1560.

Morris, C. J. G., Simmonds, I., & Plummer, N. (2001). Quantification of the Influences of Wind and Cloud on the Nocturnal Urban Heat Island of a Large City. *American Meteorological Society*, *1*(1), 1–14. https://doi.org/10.1175/1520-0450(2001)040<0169:QOTIOW>2.0.CO;2

Mukhtar, I. (2011). *A Comparative Analysis of Water Quality in the Kano River and the New Tamburawa Treatment Plant in Kano, Nigeria* (Doctoral dissertation). Ahmadu Bello University Zaria. Retrieved from http://kubanni.abu.edu.ng:8080/jspui/bitstream/123456789/2287/1/A COMPARATIVE ANALYSIS OF WATER QUALITY IN THE KANO RIVER AND.pdf

Mukhtar, S. (2016). Land Use Land Cover Change Detection through Remote Sensing Approach in Kano State Nigeria. *Pyrex Journal of Geography and Regional Planning*, *2*(2), 16–28. Retrieved from http://www.pyrexjournals.org/pjgrp

NASA (National Aeronautics and Space Administration, 2004). Urban heat islands make cities greener. In Gretchen, CA., Krishna R., and Ann, M. M. Retrieved March 30, 2017, from https://www.nasa.gov/centers/goddard/news/topstory/2004/0801uhigreen.html

NBS (National Bureau of Statistics, 2012). Annual Abstract of Statisitics 2012: Federal Republic of Nigeria. Garki Abuja, Nigeria:. Retrieved from http://www.nigerianstat.gov.ng/pdfuploads/annual_abstract_2012.pdf

Ouedraogo, I., Tigabu, M., Savadogo, P., Compaoré, H., Odén, P. C., & Ouadba, J. M. (2010). Land cover change and its relation with population dynamics in Burkina Faso, West Africa. *Land Degradation and Development*, *21*(5), 453–462. https://doi.org/10.1002/ldr.981

Oke, T. R. (1982). The energetic basis of the urban heat island. *Royal Meteorological Society*, *108*(455), 1–24. Retrieved from https://doi.org/10.1002/qj.49710845502

Oke, T. R. (1988). STreet Design and Urban Canopy Layer Cliamte. *Energuy and Buildings*, *11*, 103–113. Retrieved from https://doi.org/10.1016/0378-7788(88)90026-6

Olorunfemi, S. (2014). Determinants of Urbanization in Nigeria : Implication for Sustainable Development. *International Journal of Technical Research and Applications*, *2*(4), 50–57. Retrieved from www.ijtra.com

Pal, S. & Ziaul, S. (2016). Detection of land use and land cover change and land surface temperature in English Bazar urban centre. *The Egyptian Journal of Remote Sensing and Space Sciences*. https://doi.org/10.1016/j.ejrs.2016.11.003

Patz, A. J., Campbell-Lendrum, D., Holloway, T., & Foley, J. A. (2005). Impact of regional climate change on human health. *Nature*, *438*(7066), 310–317. https://doi.org/10.1038/nature04188

Pebesma E., Bivand R., Rowlingson B., Gomez-Rubio V., Hijmans R., Sumner M., MacQueen D., Lemon J., O'Brien J. (2017). sp: Classes and Methods for Spatial Data. R package version 1.2-5. Retrieved from *https://cran.r-project.org/web/packages/sp/index.html*

Peterson, T. C. (2003). Assessment of urban versus rural in situ surface temperatures in the contiguous United States: No difference found. *Journal of Climate*, *16*(18), 2941–2959. Retrieved from https://doi.org/10.1175/1520-0442(2003)016<2941:AOUVRI>2.0.CO;2

R Development Core Team (2011). R: A Language and Environment for Statistical Computing. R Foundation for Statistical Computing, Vienna, Austria. ISBN 3-900051-07-0. Retrieved from *http: //www.R-project.org/*.

Rosenzweig, C., Solecki, W. D., Parshall, L., Lynn, B., Cox, J., Goldberg, R., Watson, M. (2009). Mitigating new york city's heat island integrating stakeholder perspectives and scientific evaluation. *Bulletin of the American Meteorological Society*, *90*(9), 1297–1312. Retrieved from https://doi.org/10.1175/2009BAMS2308.1

Sailor, D. J. (2011). A review of methods for estimating anthropogenic heat and moisture emissions in the urban environment. *International Journal of Climatology*, *31*(2), 189–199. Retrieved from https://doi.org/10.1002/joc.2106

Shishegar, N. (2013). Street Design and Urban Microclimate: Analyzing the Effects of Street Geometry and Orientation on Airflowand Solar Access in Urban Canyons.

Journal of Clean Energy Technologies, *1*(1), 52–56. https://doi.org/10.7763/JOCET.2013.V1.13

Shishegar, N. (2014). The Impacts of Green Areas on Mitigating Urban Heat Island Effect: A Review. *The International Journal of Environmental Sustainability*, *9*(1), 119–130. Retrieved from https://www.researchgate.net/publication/271206461_The_Impacts_of_Green_Areas_on_Mitigating_Urban_Heat_Island_Effect_A_Review_Published_in_2014

Sinha, P., Kumar, L., & Reid, N. (2011). Seasonal land use / land cover mapping: Accuracy comparison of various band combinations. *ISPRS International Journal of Geo-Information*, (Icl), 3–6. Retrieved from http://www.isprs.org/proceedings/2011/ISRSE-34/211104015Final00280.pdf

Sims, D. A., & Gamon, J. A. (2002). Relationship between leaf pigment con- tent and spectral reflectance across a wide range species, leaf structures and development stages. *Remote Sensing of Environment*, *81*, 337–354. https://doi.org/10.1016/S0034-4257(02)00010-X

Sobrino, J. A., Jiménez-Muñoz, J. C., & Paolini, L. (2004). Land surface temperature retrieval from Landsat TM 5. *Remote Sensing of Environment*, *90*(4), 434–440. https://doi.org/10.1016/j.rse.2004.02.003

Sobrino, J. A., Jiménez-Muñoz, J. C., Sòria, G., Romaguera, M., Guanter, L., Moreno, J., … Martínez, P. (2008). Land surface emissivity retrieval from different VNIR and TIR sensors. *IEEE Transactions on Geoscience and Remote Sensing*, *46*(2), 316–327. https://doi.org/10.1109/TGRS.2007.904834

Solberg, A. H. S., Jain, A. K., & Taxt, T. (1994). Multisource classification of remotely sensed data: fusion of Landsat TM and SAR images. *IEEE Transactions on Geoscience and Remote Sensing*, 32(4), 768–778. https://doi.org/10.1109/36.298006

Solecki, W. D., Rosenzweig, C., Pope, G., Parshall, L., & Wiencke, M. (2003). *The Current and Future Urban Heat Island Effect and Potential Mitigation Strategies in the Greater Newark, New Jersey Region*. Research Gate. Retrieved from https://www.researchgate.net/publication/237722565

Solecki, D. W., C., R., Parshall, L., Pope, G., Clark, M., Cox, J., & Wiencke, M. (2005). Mitigation of the heat island effect in urban New Jersey. *Environmental Harzard, Elsevier*, *6*, 39–49. https://doi.org/10.1016/j.hazards.2004.12.002

Tayyebi, A. (2013). *Simulating Land Use Land Cover Change Using Data Mining and Machine Learning Algorithms*. Purdue University, West Lafayette, Indiana. Retrieved from http://docs.lib.purdue.edu/open_access_dissertations/1/

Thenkabail, P.S. and Wu, Z., 2012. An Automated Cropland Classification Algorithm (ACCA) for Tajikistan by Combining Landsat, MODIS, and Secondary Data. *Remote Sensing*, 4 (10), 2890– 2918. Retrieved from http://www.mdpi.com/2072-4292/4/10/2890

United Nations-Habitat. (2016). *Structural Transformation in Developing Countries: Cross Regional Analysis*. Nairobi, Kenya. Retrieved from

https://unhabitat.org/wp-content/uploads/2016/04/Structural-Transformation-in-Developing-Countries-FINAL.pdf

United Nations. (2007). *World Population Prospects: The 2006 Revision*. *Department of Economic and Social Affairs, Population Division*. New York, United Nations. Retrieved from http://www.un.org/esa/population/publications/wpp2006/WPP2006_Highlights_rev.pdf

United Nations. (2014). *World Urbanization Prospects: The 2014 Revision, Highlights (ST/ESA/SER.A/352)*. *New York, United*. New York, United Nations. https://doi.org/10.4054/DemRes.2005.12.9

USGS (United State Geological Survey). (2016). Landsat 8 (L8) Data Users Handbook. *USGS Science for Changing the World*. Sioux Falls, South Dakota: Earth Resources Obeservation and Science. Retrieved from https://landsat.usgs.gov/landsat-8-l8-data-users-handbook-section-2

Wang, F., Qin, Z., Song, C., Tu, L., Karnieli, A., & Zhao, S. (2015). An Improved Mono-Window Algorithm for Land Surface Temperature Retrieval from Landsat 8 Thermal Infrared Sensor Data. *Remote Sensing*, *7*(4), 4268–4289. https://doi.org/10.3390/rs70404268

Watts, J. D., Powell, S. L., Lawrence, R. L., & Hilker, T. (2011). Improved classification of conservation tillage adoption using high temporal and synthetic satellite imagery. *Remote Sensing of Environment*, 115(1), 66–75. https://doi.org/10.1016/j.rse.2010.08.005

Wegmann, M., Leutner, B. and Dech, S. (2016). Remote Sensing and GIS for Ecologist: Using Open Source Software. Exeter: Pelagic Publishing, UK.

Weng, Q. (2001). A remote sensing – GIS evaluation of urban expansion and its impact on surface temperature in the Zhujiang Delta , China. *International Journal of Remote Sensing*, *22*(10), 1999–2014. https://doi.org/10.1080/713860788

Weng, Q., Lu, D., & Schubring, J. (2004). Estimation of land surface temperature – vegetation abundance relationship for urban heat island studies. *Remote Sensing of Environment*, 89(4), 467–483. https://doi.org/10.1016/j.rse.2003.11.005

Weng, Q., Liu, H., & Lu, D. (2007). Assessing the effects of land use and land cover patterns on thermal conditions using landscape metrics in city of Indianapolis, United States. *Urban Ecosystems*, *10*(2), 203–219. https://doi.org/10.1007/s11252-007-0020-0

WMO. (2016). World Weather Information Service - Kano. Retrieved March 26, 2017, from http://worldweather.wmo.int/en/city.html?cityId=2050

Wu, Z., Thenkabail, P. S., & Verdin, J. P. (2014). Automated Cropland Classification Algorithm (ACCA) for California Using Multi-sensor Remote Sensing. *Photogrammetric Engineering & Remote Sensing*, 80(1), 81–90. https://doi.org/10.14358/PERS.80.1.81

Yang, B., Meng, F., Ke, X., & Ma, C. (2015). The Impact Analysis of Water Body Landscape Pattern on Urban Heat Island : A Case Study of Wuhan City.

Advances in Meteorology, 1–7. Retrieved from http://dx.doi.org/10.1155/2015/416728

Zemba, A. A., & Peter, E. D. (2014). Influence of sky view factor on temperature variability in urban Jimeta, Nigeria. *Asian Journal of Science and Technology*, *5*(12), 847–851. Retrieved from http://www.journalajst.com

Zhan, J., Huang, J., Zhao, T., Geng, X., & Xiong, Y. (2013). Modeling the impacts of urbanization on regional climate change: A case study in the beijing-tianjin-tangshan metropolitan area. *Advances in Meteorology*, *10*, 8. https://doi.org/10.1155/2013/849479

Zhang, F., Tiyip, T., Kung, H., Johnson, C. V., Maimaitiyiming, M., Zhou, M., & Wang, J. (2016). Dynamics of land surface temperature (LST) in response to the land use and land cover (LULC) changes in the Weigan and Kuqa river oasis, Xinjiang, China. *Arabian Journal of Geosciences*, *9*(499). https://doi.org/10.1007/s12517-016-2521-8

Zhou, G., & Lam, N. S. (2008). Reducing Edge Effects in the Classification of High Resolution Imagery. *Photogrammetric Engineering & Remote Sensing*, *74*(4), 431–441. Retrieved from http://www.rsgis.envs.lsu.edu/docs/Zhou-Lam-PERS-2008.pdf